UNIVERSITA' DEGLI STUDI DI MILANO

Scuola di Dottorato in Scienze Biomediche Cliniche e Sperimentali

Corso di Dottorato in Biotecnologie Applicate alle Scienze Mediche

ciclo XXIII

tesi di dottorato di ricerca

THE NOTCH LIGAND JAGGED1 REGULATES THYROID DEVELOPMENT IN ZEBRAFISH

Facoltà di Medicina e Chirurgia

Settore Scientifico Disciplinare Bio13

Coordinatore: Prof. Enrico GINELLI

Tutor: Prof. Luca PERSANI

Dottorando: Patrizia PORAZZI

Matricola n. R07847

Anno Accademico 2009-2010

Table of contents

ABSTRACT

Notch signaling is the result of the complex interaction of various Delta and Jagged ligands and their Notch receptors. This signal is known to have a relevant and expanding role in cell fate determination, survival and proliferation during embryonic development. Though Notch pathway is known to have a fundamental role in different endocrine systems (i.e. anterior pituitary and pancreatic cell specification), its possible involvement in thyroid development has never been studied. Our previous gene expression analysis in a thyroid cell line revealed the presence of several transcripts belonging to the Jagged1-Notch pathway, thus suggesting its potential role in thyroid development.

Then, we designed a series of experiments aimed at confirming these preliminary data *in vitro* and understand the role of Notch signaling in thyroid development. For this purpose, we took advantage of zebrafish, a versatile experimental model that has been shown to largely recapitulate the early events of mammalian thyroid gland organogenesis.

Gene expression analysis and experimental manipulations of zebrafish embryos were performed to identify the possible contribution of Jagged1 ligands to the thyroid development. Loss of Notch receptors activation in *mind bomb* (mib) mutants or DAPT-treated embryos led to an increased number of thyroid primordium cells. Conversely, Notch gain of function resulted in an impaired expression of the early thyroid marker genes (*nkx2.1a*; *tg*) *in vivo.*

Given that the entire pharyngeal architecture was seriously affected by these genetic conditions, the observed thyroid phenotypes could come from either cell-autonomous or non cell-autonomous activities of Notch signaling. In order to understand if Notch signaling plays a direct role in thyroid development, we then analyzed the co-expression pattern of the zebrafish *jag1a* and *jag1b*, orthologues of the mammalian Jagged1 ligand, and thyroid markers by double whole-mount

in situ hybridization. These experiments show the co-expression of these ligands in the thyroid region, at different times.

Next, to understand the biological role of these ligands, we took advantage of both morpholino knock-down strategy and specific zebrafish mutants. Thyroid development was impaired in several of these conditions, as shown by the altered expression of thyroid differentiation markers *tg* and *slc5a5* and T4 production at different time points.

As a consequence, a defective function of Jagged1 ligand might constitute a novel mechanism involved in the pathogenesis of congenital hypothyroidism.

1.Introduction

In this thesis I will examine the role of the Notch ligand Jagged1 in zebrafish thyroid development.

I will begin by discussing the events leading to the establishment, organization and functioning of thyroid follicular cells (TFCs), comparing data obtained from humans, mouse and zebrafish.

A deep comprehension of these processes is, first of all, fundamental in understanding the onset of congenital hypothyroidism (CH) and thyroid dysgenesis (TD) conditions. In the attempt to find new candidate genes involved in CH, in this work I will analyze the role of the Notch signaling pathway during thyroid development. To integrate and better comprehend our data, I will focus on the role of Notch pathway with specific attention to its function in other endoderm-derived organs and in the formation of the cardiac outflow tract.

As a rule, when referring to humans, the proteins and genes are named in capital letters (i.e., TG, thyroglobulin/protein; *TG,* gene*)*, referring to the mouse experimental model, the protein and genes are named in lowercase (Tg protein; *Tg* gene) and referring to zebrafish I will follow the nomenclature conventions of the zebrafish model organism database (www.zfin.org) (tg protein; *tg* gene). In order to avoid difficulties in understanding, in some particular cases of comparison between mouse and zebrafish, I will add the prefix **zf_** to zebrafish proteins and genes (i.e. zf_tg, protein; *zf_tg*, gene).

Thyroid development: a brief overview

The thyroid gland is an organ composed, in higher vertebrates, by the fusion of three primordia that develop from the anterior foregut: the endoderm-derived thyroid diverticulum and two neural crest derived bilateral structures, the ultimobranchial bodies (De Felice and Di Lauro, 2004; Elsalini et al., 2003; Fagman et al., 2006).

The diverticulum originates from the midline of the prospective pharynx, close to the tongue. This area, also called thyroid anlage, encloses a small group of endodermal cells, from which the thyroid follicular cells derive.

The ultimobranchial bodies (UBs) are a pair of transient embryonic structures derived from the fourth pharyngeal pouch, symmetrically located on the sides of the developing neck, containing the parafollicular calcitonin producing cells (C-cells).

The cells of the thyroid anlage and the ultimobranchial bodies migrate from their respective sites of origin and ultimately merge in the definitive thyroid gland. In the merging process, both the thyroid anlage and the ultimobranchial bodies disappear as individual structures, and the cells disperse in the adult compact thyroid gland (De Felice and Di Lauro, 2004). In general, the cells originating from the anlage will organize the thyroid follicles, whereas the C-cells will be scattered in the interfollicular space. Point of interest, in chicken and fish, the ultimobranchial structures remain distinct from the rest of the thyroid gland (Alt et al., 2006b; De Felice and Di Lauro, 2004; Varga et al., 2008).

The thyroid gland development is the result of a complex process that follows a sequence of morphogenetic steps, involving both cell autonomous and non-cell autonomous mechanisms.

Many significant questions on thyroid morphogenesis are still open: the signals responsible for the endoderm regional specification, the first events that recruit a group of cells to the thyroid fate as well as those responsible for the budding of

all of the organs originating from the gut, still remain elusive. Nevertheless, understanding these processes appears a fundamental step to clarify some aspects of CH.

Briefly, the foregut endoderm cells are specified to a thyroid fate and are first assembled as a placode in the pharyngeal floor. At the molecular level, these cells can be distinguished by the combined expression of a set of transcription factors: *Nkx2-1* (formerly known as TTF-1), *Pax8, Hhex* and *Foxe1* (formerly known as TTF-2) (Lazzaro et al., 1991; Plachov et al., 1990; Thomas et al., 1998; Zannini et al., 1996). These transcription factors play a fundamental role not only in the formation of the thyroid bud, but also in the functional differentiation of the gland in late development and postnatally (De Felice and Di Lauro, 2007; Parlato et al., 2004). The growing midline thyroid primordium buds off from the pharyngeal floor and moves caudally along the anterior neck region. Thereafter, following bilateral expansion of the embryonic thyroid tissue, it takes place the fusion with the UBs. Incorporation of the UBs designates early lobe formation, whereas the intermediate portion of the median primordium remains as the isthmus connecting the two thyroid lobes across the midline. By this process, the final shape of the gland is established, accompanied by folliculogenesis and terminal differentiation of progenitor cells to hormone-producing thyrocytes that express thyrotropin receptor (*TSHR*), sodium-iodide symporter (*NIS*) and thyroglobulin (*TG*) (Lazzaro et al., 1991; Postiglione et al., 2002). Notably, as evidenced by genetic deletion experiments, the thyroid-stimulating hormone (TSH), a fine regulator of thyroid function, does not participate in the early embryonic morphogenesis and growth of the gland (Postiglione et al., 2002).

We begin by discussing into details the multiple stages of thyroid development.

Endoderm origin of follicular thyroid cells: specification and commitment

The formation of the three primary germ layers (ectoderm, mesoderm and endoderm) takes place during early gastrulation of the vertebrate embryo. The inner layer, endoderm, contributes to organize the digestive tract and the associated organs: liver, pancreas, lung and thyroid. A precise control of endoderm patterning is required for proper organogenesis (Schier, 2001; Zorn and Wells, 2009).

The Nodal signaling pathway

The onset of endodermal layer development has been investigated in frog, chicken, zebrafish and mouse, revealing the presence of conserved molecular pathways, among which Nodal signaling plays a pivotal role (Schier, 2009).
During embryogenesis, the Nodal pathway is involved in the definition of mesoderm and endoderm from a common territory, the so called *mesendodermal* layer, as well as in positioning of the anterior–posterior axis, neural patterning and left–right axis specification. The *Nodal* gene was initially identified in mice, where it encodes an activin-like member of the transforming growth factor β (TGF-β) family (Zhou et al., 1993). Zebrafish possess two Nodal-related genes: *ndr1* (also known as *squint*) and *ndr2* (previously named *cyclops*) (Feldman et al., 1998). These ligands bind to a complex of the serine–threonine kinase receptors (*TARAM-A*) and the EGF-CTF co-receptor (*one-eyed pinhead*: *oep*) (Aoki et al., 2002; Whitman, 2001). The signaling process is then mediated by receptor-associated Smads (R-Smad) (Dick et al., 2000; Muller et al., 1999) that complex with nuclear transcription factors: i.e., the homeodomain protein Mixer *bonnie and clyde* (*bon*) (Kikuchi et al., 2000; Sirotkin et al., 2000). The latter, in turn, induces the expression of MIX-like (*bon*, *mezzo*) and GATA binding protein 5 (*gata5* or *fau*) transcription factors (Poulain and Lepage, 2002; Reiter et al., 2001). *Bon*, *mezzo* and *gata5* act in parallel, in a partially redundant manner,

upstream of *sox32* (previously named *casanova or cas*) transcription factor, to specify endodermal development (Aoki et al., 2002). *sox32* is in fact essential to activate the transcription of other endoderm-specific genes, i.e.: *sox17* and the forkhead homebox A2 (*foxa2*) (Alexander et al., 1999). The Nodal pathway acts in a long-range manner, due to the diffusion and stability of its ligands, and in a dose-dependent manner (Meno et al., 2001). An example of a dose-dependent response to the level of Nodal activity is the induction of endodermal *vs* mesodermal layer, where the dose of Nodal signals required for endoderm specification is higher than in the case of mesoderm (Rodaway et al., 1999). Different mechanisms can regulate the spatiotemporal features of Nodal signaling, varying from the control of ligand activity by proteolytic processing to the inhibitory effect of the soluble ligand antagonist *lefty (Meno et al., 2001; Thisse et al., 2000)*.

The Nodal signaling pathway and thyroid development

The thyroid gland derives from precursor cells located in the anterior primitive gut (Macchia, 2000). Fate-mapping experiments revealed the different fate of the cells that compose the endodermal layer and highlighted its regionalization, defined, for example, by the expression of specific transcription factors (Tremblay and Zaret, 2005; Warga and Nusslein-Volhard, 1999; Wells and Melton, 2000). As previously mentioned, the cells forming the thyroid placode in the anterior foregut endoderm co-express *Nkx2-1* (*zf_nkx2.1a*), *Foxe1 (zf_foxe1)*, *Pax8* (*zf_pax2a* and *zf_pax8*) and *Hhex (zf_hhex)*, defining the presumptive region where the primordium will develop (De Felice and Di Lauro, 2004; Fagman and Nilsson, 2009; Porazzi et al., 2009). Much of the role of Nodal signaling pathway in thyroid has been elucidated in the zebrafish model. Elsalini and Rohr showed the crucial role of Nodal signaling in specifying endoderm and in constituting the gut tube. In the Nodal co-receptor *one-eyed pinhead* mutant embryos (*oep*−/−), the loss of the endoderm is already evident during gastrulation, with an overall failure in the specification of mesendodermal cell

fates, leading to the absence of the thyroid primordium (Elsalini et al., 2003). Furthermore, the thyroid primordium has been analyzed in the nodal related gene *ndr2* mutant, *m294*−/−, a strain obtained by ENU-mutagenesis. In this circumstance, a strong reduction of pharyngeal endoderm is accompanied by the presence of a smaller thyroid primordium (reduced *nkx2.1a* and *hhex* expression from 26 hpf onward) and, eventually, by the reduction of the number of functional thyroid follicles, as evidenced by T4 immunostaining at 5 dpf (Elsalini et al., 2003). This suggests that the final thyroid size is constrained by the number of cells initially recruited to a thyroid fate. The thyroid phenotype is much more severe in the *ndr2* mutant *b16*−/−, where a gamma-ray-induced mutation caused the loss of the lower telomeric region of chromosome 12, encompassing not only *ndr2*, but also the *hhex* gene (Hatta et al., 1991). In this case, an initial reduction of *nkx2.1a* and *pax2a* expression was noticed in the thyroid primordium but, subsequently, both markers disappeared and no thyroid follicles were detectable by T4 immunostaining, confirming the evidence that both a correct endoderm specification and the expression of thyroid-specific transcription factors are required to complete thyroid development (Elsalini et al., 2003).

Finally, zebrafish mutants in the downstream effectors of Nodal signaling *bon*, *gata5* and *sox32* completely fail to develop the thyroid primordium, as a consequence of altered endoderm organization and of the loss of the direct inductive role that these factors play in specifying the thyroid primordium (Elsalini et al., 2003; Kikuchi et al., 2000; Reiter et al., 2001).

Timing of thyroid anlage specification and budding

The morphogenesis of the thyroid starts with the specification of anterior foregut cells to follow a thyroidal fate. This cellular domain is initially organized in an homogeneous layer, visible as a thickening of the endodermal epithelium in the foregut, which is referred as thyroid anlage (De Felice and Di Lauro, 2004).

The signals that induce the primary events in the origin of the thyroid primordium are not known. The ventral pharyngeal endoderm lies in close apposition to the heart mesoderm. An influence of the developing heart on thyroid organogenesis has been recently demonstrated (see paragraph: Interaction between endoderm and mesoderm in regulating thyroid development).

The thyroid primordium is first identified in zebrafish embryos at 24 hpf, while in mouse and human embryos at E8-8.5 and E20-22 respectively (see Table I for the timing of key thyroid morphogenetic events in different species) (Elsalini et al., 2003; Fagman and Nilsson, 2009). A conspicuous portion of the thyroid placode is very close to the aortic sac, a large vessel that communicates with the primitive heart outflow tract and from which the pharyngeal arch arteries develop (Alt et al., 2006a; Fagman et al., 2006).

The organization of thyroid progenitors in the pharyngeal endoderm is soon followed by budding. The earliest signs of thyroid budding become evident in late E9.5 (in zebrafish 32 hpf; in humans E24), when the dorsal portion of *Nkx2.1* positive placode is enlarged and then it shapes a hollow evagination of the endoderm. Throughout this process, the thyroid bud maintains a close association with the aortic sac (De Felice and Di Lauro, 2004). Budding probably occurs concomitantly with the recruitment of new progenitor cells to the growing anlage so that the simple epithelium of the thyroid turns into the pseudostratified and multilayered bud (Fagman et al., 2006).

Migration of midline thyroid primordium

During the developmental process, the thyroid of higher vertebrates undergoes a significant change in its position to reach the inferior neck at the level of the larynx and the proximal trachea (Fagman et al., 2006). A corresponding translocation takes place in zebrafish embryos, although the thyroid tissue does not assemble into an encapsulated organ (Alt et al., 2006a). This process is generally described as migration of the thyroid primordium.

During the relocalization, the thyroid bud forms a caudal cup-shaped evagination of the midline pharyngeal endoderm (E10.5) (Fagman et al., 2006). Eventually, the descending bud detaches from the overlying endoderm by gradual thinning of the thyroglossal duct, a transient embryonic structure (E11.5). Two days later, the thyroid primordium moves close to the trachea (E13.5) (zebrafish: 32-35 hpf; humans E25-50) (De Felice and Di Lauro, 2004). The molecular mechanisms involved in the translocation of the thyroid primordium have not been completely elucidated. Whether embryonic thyroid migration is an active process involving cell-autonomous mechanisms or it reflects the positional change and rearrangement of adjacent growing tissues is a matter of debate. To date there are evidence supporting both of the mechanisms. Of note, the active migration does not mutually preclude the possibility of a passive contribution and vice versa.

Analysis of mice deprived of the transcription factor Foxe1 demonstrates that the thyroid follicular precursors have an important role in the migration process. In absence of Foxe1 the thyroid bud is missing or remains a part of the pharyngeal endoderm (De Felice et al., 1998). On the contrary, knock-in of Foxe1 into the Nkx2-1 locus rescues the thyroid phenotype, underling the direct role of Foxe1, expressed by the follicular cells, in the detachment of the bud from the pharyngeal floor (Parlato et al., 2004).

In zebrafish, *foxe1* is expressed in thyroid, pharynx, and pharyngeal skeleton during development. *foxe1* loss of function embryos exhibit abnormal craniofacial development, but, unlike Foxe1-null mice, the thyroid development is unaffected. This suggests that Foxe1 might have acquired its role in mammalian thyroid morphogenesis during evolution or also that a zebrafish *foxe1* paralog and/or other *foxe* genes could compensate for *foxe1* in zebrafish thyroid development (Nakada et al., 2009).

However, active migration of thyroid cell precursors is questioned, considering that the follicular cells do not undergo an epithelial to mesenchymal transition (EMT) during migration (Fagman et al., 2006). EMT is a program of development characterized by the loss of cell adhesion, repression of E-cadherin expression, neo-expression of N-cadherin and increased cell mobility (Thiery et al., 2009).

An alternative mechanism to the active migration is that the thyroid primordium changes its position as a consequence of the adjacent tissue differential growth. A recent descriptive study based on a computational approach reconstructed and examined the thyroid gland formation in serially sectioned rat and human embryos. This strategy allowed to state that the positional changes of the thyroid primordium could be explained by differential growth (i.e., changes in the size and shape of the embryo and of its parts) (Gasser, 2006).

It is certain that the vascular system is an important factor in defining the correct localization and morphology of different organs. It is now well known that the human thyroid primordium get settled close to the aortic sac soon after budding and, during the relocalization process, it follows the development of carotid arteries, to end up with a bilobed gland located in front of the trachea (Fagman et al., 2006). The frequent association of congenital heart and thyroid malformations and the description of patients with intracardiac ectopic thyroid tissue confirm the close relationship between thyroid and vascular development (Casanova et al., 2000; Muzza et al., 2008; Olivieri et al., 2002). In zebrafish, the thyroid primordium expands and migrates posteriorly before dividing into scattered singular follicles along the pharyngeal midline (Alt et al., 2006b). Double *in situ* hybridization experiments show the close association among

thyroid primordium, ventral aorta and the first pair of branchial arteries at 55 hpf, and the development of the thyroid primordium along the extension of the ventral aorta at 120 hpf (Alt et al., 2006a). Zebrafish mutants or morphants, with alterations in the pharyngeal vessel architecture, display severe thyroid defects, such as abnormal lateral expansion and misalignment of thyroid follicles, pointing to a correlation between thyroid morphogenesis and vascular development (Alt et al., 2006a). The same consequences are highlighted by the Shh-deficient mouse, in which defective cardiac rotation and asymmetric carotid artery development lead to a single-lobed thyroid gland adjacent to the delocalized carotid arteries (Alt et al., 2006a; Fagman et al., 2006). Altogether, these data support the hypothesis that, despite species-specific anatomical variations, an intact pharyngeal vessel architecture acts as guide for follicular cell relocalization during thyroid development.

Growth of thyroid follicular cells and completion of the organogenesis process

In mammals, the next stages involve the thyroid tissue expansion and its division to eventually form two lobes connected by an isthmus in front of the trachea. The proliferating thyroid cells extend laterally along the third pharyngeal arch arteries originating from a bifurcation of the prospective aortic arch (Fagman et al., 2006). In the mouse model, at E13.5, the thyroid assumes its final shape, contacting and incorporating the UBs (Fagman et al., 2006). By E15.5, in mouse, the first evidence of follicular organization appears with many small follicles disseminated within the gland (De Felice and Di Lauro, 2004). With regard to zebrafish, the thyroid completes its development without assuming a glandular organization, with a raw of non-encapsulated thyroid follicles which get loosely distributed mainly within the sub-pharyngeal mesenchyme, along the ventral aorta (Alt et al., 2006b; Wendl et al., 2002). Moreover, in zebrafish, the onset of folliculogenesis takes place earlier than in mammals (T4 production assessed from 55 hpf) (Wendl et al., 2002). This is probably due to the fact that zebrafish

embryos demand to become independent from maternal thyroid hormone supply already in early development (Elsalini et al., 2003).

This phase, comprehending thyroid tissue proliferation and final anatomical organization (single follicles vs. compact lobular structure), establishes the major differences between zebrafish and mammalian thyroid gland. In fact, despite differences in the morphological organization and temporal progression of thyroid morphogenesis, the ontogeny of the thyroid follows the same pattern in all vertebrates and zebrafish, as previously described: the thyroid anlage always origins in the primitive pharynx and thyroid follicular cells migrate from the anlage to reach their definitive position and finally organize themselves into follicles in a specie-specific manner. Moreover, mammalian and zebrafish thyroid cells show the combined expression of a set of conserved transcription factors (Elsalini et al., 2003) (Fig. 1.1 and Table I).

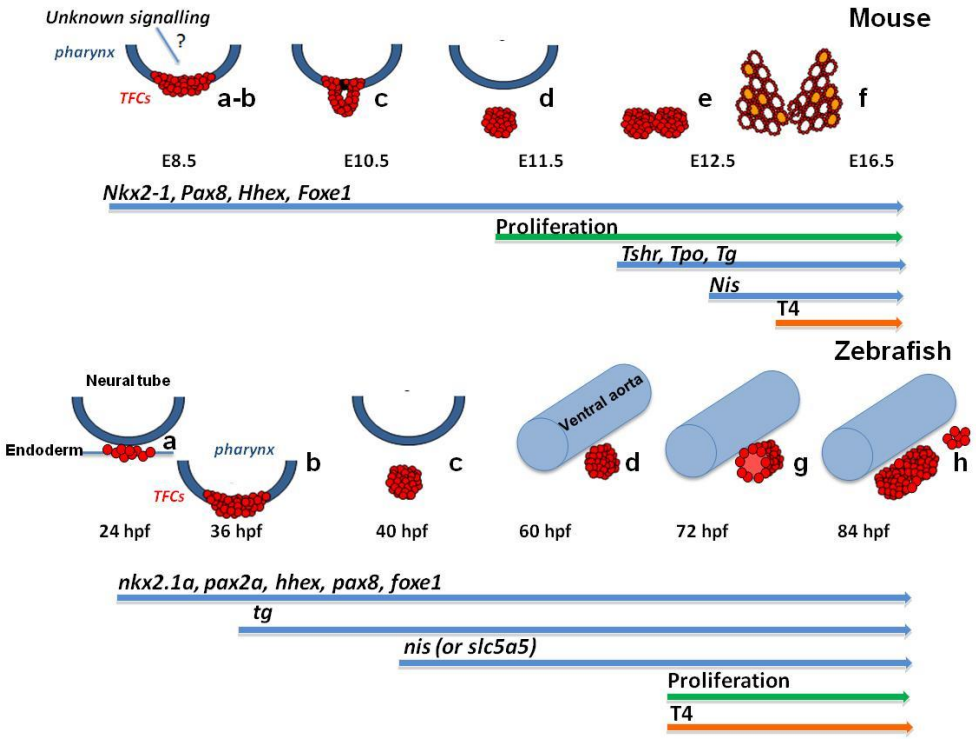

Figure 1.1: Comparison between thyroid development in mouse and zebrafish: schematic illustrations. The time of development is E (*embryonic day post-fertilization*) for mice and hpf (*hours post-fertilization*) for zebrafish. Red color indicates developing thyroid follicular tissue. (a) early marker gene expression in endoderm; (b) primordium at ventral midline of the pharynx; (c, d) evagination and re-localization; (e) bifurcation of primordium; (f) growth of thyroid follicular cells, surrounded by connective tissue; differentiation into many follicles at the same time; (g) differentiation into one first follicle; (h) growth of follicles. Blue arrows indicate the onset of early and differentiative marker gene expression. Green arrows indicate the onset of thyroid proliferation; orange arrows indicate the onset of thyroid function as judged by T4 production [Modified from (Alt et al., 2006b; Elsalini et al., 2003)].

Stage of morphogenesis	Embryonic hpf or days		
	zebrafish	mouse	humans
Thyroid early marker gene expression	24-26 hpf	E8–8.5	E20–22
Primordium at pharingeal ventral midline	32 hpf	E8–8.5	E20–22
Thyroid budding and migration	36 hpf to 45 hpf	E9.5 to E13.5	E24 to E45-50
Thyroid cells proliferation starts	72 hpf	E10.5	E24
Fusion with ultimobranchial bodies	/	E14	E45-E50
Onset of folliculogenesis	55 hpf (one first follicle)	E15.5 (many follicles)	E70 (many follilces)
Onset of T4 production	72 hpf	E15.5	E77

Table I: Comparison of thyroid development in zebrafish, mouse and humans. The key morphogenetic events are listed in the first column. The developmental stage is indicated as *hours post-fertilization* (hpf) in zebrafish, and *embryonic day post-fertilization* (E) in mouse and humans [Information is based on (De Felice and Di Lauro, 2004; Wendl et al., 2002)].

Genetic regulation of thyroid development

A set of transcriptional regulators, unique to the thyroid follicular cell type, has been identified as responsible for driving thyroid specific gene expression; it comprises the previously mentioned transcription factors Nkx2-1, Pax8, Hhex and Foxe1, each of which is also expressed in different cell types from the thyroid follicular cells. However, the combination of these factors is unique to the thyroid hormone producing cells, strongly suggesting that they play an important role in thyroid differentiation (Parlato et al., 2004). The four of them also play an important role in early thyroid development, at stages preceding the expression of the differentiated phenotype. Starting from E8.5 in mouse, and from 24 hpf in zebrafish, they are simultaneously expressed in the thyroid primordium (De Felice and Di Lauro, 2004; Fagman and Nilsson, 2009; Porazzi et al., 2009). The wide temporal expression, from the beginning of thyroid organogenesis to the adult state, suggests the continuous role of thyroid-specific transcription factors at distinct developmental stages.

Nkx2-1 or zf_nkx2.1a

Historically, the first transcription factor described in mouse and zebrafish developing thyroid gland was Nkx2-1 (Lazzaro et al., 1991; Rohr and Concha, 2000). Nkx2-1 is a member of the homeodomain transcription factor family, expressed in thyroid, lung and ventral forebrain of higher vertebrates (Lazzaro et al., 1991). In the primitive pharynx, Nkx2-1 is exclusively present in the thyroid anlage, and its appearance coincides with the specification of the anlage. *Nkx2-1* expression remains in the thyroid follicular cells during all stages of development and in adulthood (Lazzaro et al., 1991). Nkx2-1$^{-/-}$ mice are stillborn and lack the lung parenchyma and the thyroid gland. They show several alterations in the ventral forebrain (Kimura et al., 1996). Further investigations defined that, in Nkx2-1$^{-/-}$ mice, the thyroid rudiment is initially formed but then it disappears through apoptosis (Kimura et al., 1999; Parlato et al., 2004). These results

demonstrate that Nkx2.1 is not required for the initial specification of thyroid, but is absolutely essential for its development and morphogenesis. Coherently, in zebrafish, *nkx2.1a* morpholino knock-down results in failure of thyroid development at 5 dpf (absent T4 immunostaining). Morpholino-injected embryos show the early appearance of the thyroid primordium expressing *hhex* and *pax2a*, although the signal is weak and disappears by 60 hpf, thus resembling the phenotype of *Nkx2.1* knockout mice (Elsalini et al., 2003). Taken together, these data suggest that Nkx2-1 exhibits an evolutionary conserved role as cell-autonomous transcription factor in regulating thyroid development.

The paired box genes (mammalian Pax8 and zebrafish pax2a and pax8)

The *Pax* (paired box DNA-binding domain) gene family is divided into four groups: group II comprises the paralogous genes *Pax2/5/8* involved in vertebrate thyroid development (Plachov et al., 1990; Robson et al., 2006). In mammals, *Pax8* endodermic expression is only present in the thyroid anlage and it is detected in the developing thyroid from the time of specification (Plachov et al., 1990). The expression of *Pax8* is then maintained during all stages of development and in adulthood. *Pax8* knockout mice have a severe phenotype and die shortly after weaving. This is principally a result of thyroid defects, as other organs expressing *Pax8* have normal development, probably due to the redundant function of the paralogous genes *Pax2* and *Pax5* in these tissues. Hypothyroidism is the cause of death of the knockout animals: the administration of T4 to *Pax8*$^{-/-}$ mice allows the animals to survive (Friedrichsen et al., 2004). With regard to the thyroid gland, *Pax8* knockout mice initially develop a thyroid primordium, which disappears soon after evagination (E11.5–12.0), suggesting a role for *Pax8* in the maintenance and/or proliferation of thyroid precursor cells (Mansouri et al., 1998).

In zebrafish, both *pax8* and *pax2a* are expressed in the thyroid, and the latter certainly has an important role in thyroid development because thyroid follicles, and *pax8* expression, are absent in *pax2a* zebrafish mutant embryos (Wendl et al., 2002). The expression of *pax2a* in thyroid precursor cells starts at 24 hpf, as

for *nkx2.1a* and *hhex*, two hours before the appearance of *pax8*. *pax2a* expression is detectable until 7 dpf, completely overlapping the signal of *nkx2.1a*, *hhex* and *pax8* (Wendl et al., 2002). Zebrafish *pax2a* mutants develop the thyroid primordium and express *nkx2.1a* and *hhex* until 30 hpf, when the expression of these genes ceases. At 7 dpf T4 immunostaining is absent. Even in such circumstance, the expression pattern implies an initial thyroid primordium development in absence of *pax2a*. However, the functionality of this gene is fundamental for the proper development of thyroid follicles (Wendl et al., 2002). The finding that the phenotype of *pax2a* zebrafish mutants is similar to that of *Pax8* knockout mice is a further suggestion that zebrafish *pax2a* and mouse *Pax8* play a similar role during thyroid development (Mansouri et al., 1998).

Mouse Hhex and zebrafish hhex gene

Hhex is a critical transcription factor involved in many aspects of vertebrate development, such as the formation of endoderm-derived organs: thyroid, pancreas, liver, lung, thymus and gallbladder (Bogue et al., 2000). *Hhex* null mouse embryos exhibit defects in rostral forebrain and liver, as well as thyroid dysplasia. Thyroid primordium is aplastic or hypoplastic at E10.5, and no longer detectable at E13.5 (Martinez Barbera et al., 2000). These data suggest a very early function of *Hhex* in thyroid development. In zebrafish, the orthologous gene *hhex* is initially expressed in the anterior endoderm (Liao et al., 2000). Subsequently (from 22 hpf onward), *hhex* is present in thyroid precursor cells, colocalizing with the expression domain of *nkx2.1a* (Wendl et al., 2002). Similar to *nkx2.1a* morphants, the morpholino knock-down of *hhex* gene results in a lack of follicles and T4 immunostaining at 5 dpf. The early steps of thyroid primordium evagination and relocalization are not affected, as demonstrated by the initial presence of *nkx2.1a* and *pax2a* expression at the base of the lower jaw. However, the expression of this marker is lost at 60 hpf, similarly to *Hhex* knockout mice (Elsalini et al., 2003; Martinez Barbera et al., 2000). On the other hand, injecting zebrafish with *hhex* mRNA results in a gain of- function phenotype, characterized by an increase in the number of thyroid precursor cells

and precocious anterior-posterior expansion (Elsalini et al., 2003). Altogether, these studies emphasize the role that the *Hhex* gene plays after induction and evagination of the thyroid primordium, phase in which it appears to control not only thyroid differentiation, but also proliferation and growth.

Foxe1 or zf_foxe1

Rat *Foxe1* cDNA was cloned and characterized as a member of a winged helix/forkhead family of transcription factors (Zannini et al., 1997). *Foxe1* mRNA is detected at E8.5 in all the endodermal cells of the foregut floor, including the thyroid anlage. Expression of *Foxe1* in the thyroid cell precursors is maintained during development. *Foxe1* is also expressed in most of the craniopharyngeal ectoderm. Expression of *Foxe1* in thyroid cell precursors is down regulated after migration, suggesting that this factor is involved in the early steps of thyroid development (De Felice et al., 1998). *Hhex* null mutant mice exhibit cleft palate and either a sublingual or completely absent thyroid gland, emphasizing a role of Foxe1 in the migration of the thyroid primordium soon after budding (De Felice et al., 1998). In zebrafish, *foxe1* is expressed in thyroid, but the knock-down situation does not affect thyroid development (Nakada et al., 2009). The possibility of a compensatory role of another *foxe1* paralogue gene in zebrafish has to be considered.

Interaction between endoderm and mesoderm: tissue-tissue interaction during thyroid development

The specification of the gut region and the derived organs also depends on the cross-talk between the endoderm and the mesoderm. Recent studies highlight the importance of permissive signals sent from the mesoderm layer to promote endoderm organogenesis (i.e. during liver and pancreas development) (Gualdi et al., 1996; Jung et al., 1999; Kumar et al., 2003; Manfroid et al., 2007; Serls et al., 2005). As the thyroid primordium develops in close association with the visceral mesoderm that forms the secondary heart field and the outflow tract, it is conceivable that thyroid inductive signals may originate there. In mouse explants, direct contact of cardiac mesoderm with ventral endoderm is required to induce *in vitro*, via FGF, the expression of both transcription factors, such as *Nkx2-1*, and downstream lung and thyroid target genes (*Tg*) (Serls et al., 2005).
Some evidence of a role of FGF for proper thyroid primordium specification and development comes from zebrafish (Wendl et al., 2007). The study of zebrafish *hand2* mutants suggested that, even in the presence of a normal endodermal development, the lack of this transcription factor prevents thyroid specification in a non-cell-autonomous manner (Wendl et al., 2007). The *hand2* locus encodes a bHLH transcription factor, named *heart and neural crest derivatives expressed transcript 2*, which is expressed in fin buds, in pharyngeal arches and in the anterior lateral plate mesoderm. In particular, focusing on the area where the thyroid primordium originates, *hand2* is expressed in the heart tube, in the first pair of branchial arteries, in the neural crest mesenchyme of the pharyngeal arches and in the same pharyngeal endoderm, although at low levels (Wendl et al., 2007; Yelon et al., 2000). Zebrafish *hand2* mutants, *hand2s6* and *hand2c99*, besides defective heart, pharynx and fin development, lack a thyroid primordium (failed expression of *pax2a*, *hhex* and *nkx2.1a* at 24 hpf) and differentiated follicles (absent T4 immunostaining at 7 dpf). The thyroid phenotype is more severe in *hand2s6* mutants, which have a deletion of 100 kb around the *hand2* locus and show complete absence of the thyroid, than in *hand2c99* mutants, in

which the *hand2* gene undergoes an altered splicing, leading just to a reduction of thyroid size (Wendl et al., 2007; Yelon et al., 2000). Using a fate-mapping approach, Wendl and Adzic demonstrated that endodermal thyroid precursor cells originate close to the lateral plate mesoderm and maintain a position proximal to the *hand2*-expressing cardiac mesoderm from somitogenesis onwards (Wendl et al., 2007). It has been demonstrated that this transcription factor acts in a cell-autonomous manner in the tissues surrounding the thyroid primordium and, among them, cardiac mesoderm produces signaling factors responsible for thyroid development. The early association of the thyroid primordium with the aortic sac in the mouse, or the heart outflow tract in the zebrafish, allows endodermal thyroid precursors to receive permissive signals from the cardiac lateral plate mesoderm (Wendl et al., 2007). To date, the FGF signaling pathway is the principal mediator identified in both zebrafish and mouse models. In fact, zebrafish *fgf8a/ace* mutants show a small thyroid primordium with a reduced number of differentiated follicles and the same thyroid phenotype derives from the pharmacological inhibition of FGF signaling (Reifers et al., 2000; Wendl et al., 2007). Furthermore, beads soaked with recombinant FGF are able to reconstitute a proper thyroid gland in *hand2s6* mutants, proving that FGF has an action parallel to, or downstream of, *hand2* signaling (Wendl et al., 2007).

A link between the FGF signaling pathway and thyroid development has been demonstrated also in the mouse. Mice deficient for the *FGF receptor 2-IIIb* or *FGF10* lack an adult thyroid gland, even though an initial thyroid primordium develops (Ohuchi et al., 2000). In addition, Kameda et al. have recently confirmed the role of FGF in promoting the development of pharyngeal endoderm derivates (such as the thyroid, ultimobranchial bodies, thymus and parathyroid glands) in the mouse (Kameda et al., 2009). In FRS2$\alpha^{2F/2F}$ mouse mutant embryos, which lack the docking protein FRS2α that links FGF receptors to a variety of intracellular signaling pathways, thyroid development is severely affected and the gland, despite the formation of the thyroid diverticulum, is, in the end, absent or hypoplastic (Kameda et al., 2009).

Furthermore, a connection between thyroid and cardiac development is supported by the finding that infants with CH have an increased risk of additional congenital malformations (from about 1–2% to 8–10%), cardiac abnormalities representing at least half of them (Olivieri et al., 2002). Moreover, ectopic thyroid tissues can be found in the heart (Casanova et al., 2000). The frequent association of thyroid and heart abnormalities stresses the importance of physical and molecular contacts between the thyroid anlage and the aortic sac. Recently, the T-box transcription factor *Tbx1* emerged as an actor in this process. Tbx1 null mutations cause thyroid hemiagenesia (Fagman et al., 2007). Indeed, Tbx1 is required for normal development of the aortic arch and is expressed in the mesenchyme surrounding the thyroid, defining thyroid size and its final position by non-cell-autonomous mechanisms (Fagman et al., 2007). Tbx1, via interaction with *FGF* genes, has an important role in the development of the pharyngeal apparatus and the secondary heart field from which the cardiac outflow tract derives (Aggarwal et al., 2006; Nowotschin et al., 2006).

A murine model with *Tbx1* gene targeted deleted in the mesoderm, showed that proliferation in the foregut endoderm, and the number of cells in the thyroid placode, is reduced by mesoderm ablation of Tbx1 (Lania et al., 2009). These effects are largely mimicked by deletion of Fgf8 in the Tbx1 expression domain. Conversely, over-expression of Fgf8 from the Tbx1 locus, on a Tbx1 deficient background, rescues the hypoplastic thyroid condition of Tbx1 null embryos (Fagman et al., 2007). It is possible to conclude that an FGF8 signal, dependent on Tbx1, emanates from the mesoderm of the secondary heart field to the thyroid primordium at early developmental stages.

These recent findings may explain the increased risk of thyroid dysfunctions in patients affected with the Di George syndrome (Bassett et al., 2005), which is characterized by a number of phenotypic features including cardiovascular defects, and is caused by 22q11 deletions that encompass the Tbx1 gene (Lindsay et al., 2001; Merscher et al., 2001).

Taken together, studies in zebrafish and mice firmly establish that the cardiac mesoderm is a source of inductive and permissive signals for thyroid

development. Among these signals, the FGF pathway plays a crucial role (Lania et al., 2009; Wendl et al., 2007).

In zebrafish it has been demonstrated that fgf8 is required for the development of the heart precursors, particularly during the onset of the cardiac gene expression, sustaining the expression of *nkx2.5* and *gata4* (Reifers et al., 2000).

Nkx2.5, a homeodomain-containing transcription factor, has a conserved role also in mouse heart morphogenesis. In addition, on E8.5–9.5, the presence of *Nkx2.5* transcript has been detected in the precursors of thyroid cells in the pharyngeal floor (Lints et al., 1993). At later stages, *Nkx2.5* pharyngeal expression is limited to the area corresponding to the thyroid primordium and *Nkx2.5*$^{-/-}$ embryos display a reduced number of thyroid precursor cells compared to that in WT (Dentice et al., 2006; Lints et al., 1993).

This process led us to infer that the close spatial relationship between heart and thyroid during development could also be sustained by common patterning traits, and Nkx2.5 could be an example of this situation.

Another example of a developmentally important transcription factor expressed in both thyroid and heart progenitor cells is Isl1. Isl1 is active in both endoderm progenitors of the anterior foregut and of the adjacent cardiogenic mesoderm in early mouse embryos (Cai et al., 2003). Strikingly, Isl1 deficiency causes apoptosis in the pharyngeal endoderm together with the severe malformations of the heart and cardiac outflow tract that leads to embryonic lethality around E10.5 (Cai et al., 2003). It has been well demonstrated that Isl1 is widely expressed in the thyroid primordium that buds from the pharyngeal floor (Westerlund et al., 2008). During further development, the Isl1 expression is maintained in all thyroid progenitor cells, until the anlagen fuse at E13.5. Thereafter Isl1 is restricted to the C-cell precursors and down-regulated in the follicular cells (Westerlund et al., 2008). It is thus feasible to assume that Isl1, expressed from early thyroid development, may be important for the growth and the expansion of thyroid precursors during the budding stage and thereafter. This possibility is supported by the observation that the thyroid placode had a reduced size in the Isl1 knockout mice, compared to WT embryos (Westerlund et al., 2008).

Genes expressed during embryogenesis in thyroid and heart precursors are promising candidate genes to be investigated for their involvement in the pathogenesis of CH.

In addition to cardiac mesoderm, the possible involvement of embryonic vessels and endothelial cells as a source of inductive signals for endoderm-derived organs has to be considered. In distinct endocrine organs a role of the endothelial cells in inducing a specific fate is wildly recognized. The best example of this is found in pancreatic development. *In vitro* experiments with embryonic mouse tissues demonstrate that blood vessel endothelium induces insulin expression in isolated endoderm (Lammert et al., 2001). Moreover, removal of the dorsal aorta in *Xenopus laevis* embryos results in the failure of insulin expression *in vivo*. On the contrary, ectopic vascularization in the posterior foregut leads to ectopic insulin expression and islet hyperplasia, thus indicating that vessels provide not only metabolic sustenance, but also inductive signals for organ development (Lammert et al., 2001). Also in the liver, the vasculogenic endothelial cells and nascent vessels are critical for the earliest stages of organogenesis (Matsumoto et al., 2001).

Considering that the early thyroid primordium associates with the aortic sac endothelium, an involvement of endothelial instructive signals during thyroid development cannot be excluded (Fagman et al., 2006). At the moment some evidence comes from the zebrafish model where, however, a compromised endothelial development and organization does not influence the thyroid primordium specification. In fact, in presence of a disrupted endothelial patterning of the pharyngeal vessels, the thyroid precursor cells are correctly specified (Alt et al., 2006a). Notably, the zebrafish thyroid primordium is present also in a situation of complete lack of all vascular progenitors (Alt et al., 2006a). Considering all these data, a role of the endothelial cell in inducing the thyroid primordium fate can be excluded, at least in zebrafish.

Congenital hypothyroidism (CH)

Congenital hypothyroidism (CH) is the most common congenital endocrine disorder and screening programs report a rather constant incidence of primary CH of 1:3000 newborns in iodine-sufficient regions (De Felice and Di Lauro, 2004; Gruters and Krude, 2007). The aetiology of primary CH is, in most of the cases (75-85%), the result of a defective thyroid gland development: TD (thyroid dysgenesis). TD constitutes an heterogeneous group of affections that can occur for altered differentiation, migration or growth of the thyroid gland (Gruters et al., 2004).

Ectopic thyroid, resulting from a defect in the migration of the median thyroid anlage, accounts for 30-45% of CH cases. The ectopic thyroid is frequently located in a sublingual position and, in most of the cases, the tissue is hypoplastic with lack of the normal lateral expanded bilobed structure (Gillam and Kopp, 2001; Gruters et al., 2004). The second most common variant of thyroid dysgenesis is the complete absence of thyroid follicular cells, commonly named athyreosis, which is observed in 35-40% of the cases. Finally, hypoplasia of the bilobed thyroid gland accounts for at most 5% of cases of CH (Gillam and Kopp, 2001; Gruters et al., 2004). Because the thyroxine hormone (T4), produced by the thyroid gland, is essential for neural development, CH condition represents, if not recognized, the most common cause of mental retardation (Gruters and Krude, 2007).

The pathogenesis of TD is largely unknown. Most cases of CH with TD occur as a sporadic disease; however accumulating evidences indicate that genetic factors are involved in the pathogenesis of TD (Castanet et al., 2010).

The frequent observation of discordant monozygous twins rules against a genetic origin (Perry et al., 2002), nevertheless a linkage and mutational analysis of familial TD has demonstrated the high frequency of morphological alterations in 1st- and 2nd-degree relatives of CH patients (Castanet et al., 2005). Several evidences suggest the presence of a strong genetic component at the origin of

CH: a mouse model by Amendola et al. has demonstrated a multigenic origin of TD in mice, strongly suggesting that a similar pathogenetic mechanism might be observed in humans (Amendola et al., 2005). Moreover, CH patients have an 8- to 15-fold higher risk of presenting associated congenital abnormalities of heart, eye, intestine, bone or other organ or apparatus (Olivieri et al., 2002). The evidence that mutations in genes involved in thyroid development cause TD in animal models and that mutations in the same genes are associated with TD in humans confirms that TD can be a genetic and inheritable condition (De Felice and Di Lauro, 2007). The current data suggest that there is a spectrum of TD ranging from monogenic to multifactorial genetic etiologies and that environmental and epigenetic modifiers are likely to be contributing factors (Vassart and Dumont, 2005).

PAX8 mutations

Different cohorts of TD have been screened for *PAX8* mutations and, in all the reported studies, the mutation rate is very low (Congdon et al., 2001; Esperante et al., 2008; Macchia et al., 1998; Tonacchera et al., 2007; Vilain et al., 2001). In humans, heterozygous *PAX8* mutations are rarely identified in TD patients with variable thyroid phenotypes, mostly characterized by hypoplastic gland. Most patients with a *PAX8* mutation have a thyroid of reduced size, suggesting that PAX8 also plays an important role in the proliferation and survival of differentiated thyroid cell (Montanelli and Tonacchera, 2010).

In an initial SSCP screening for *PAX8* mutations among 145 Italian patients with TD, Macchia et al. reported mutations in two sporadic patients and one familial case. All three point mutations are located in the paired domain of PAX8, reducing the ability of this transcription factor to bind DNA (Macchia et al., 1998). Contrary to the mouse model, in which the phenotype is present in the homozygous state, the identified affected human subjects are heterozygous for the mutation and, in the familial cases, the transmission is autosomal dominant. The autosomal dominant transmission has been further proved with the description of a mutation of *PAX8* causing thyroid hypoplasia (Vilain et al., 2001).

The mutation consists of the substitution of a tyrosine for cysteine in the paired domain of PAX8 resulting in a mutant allele unable to exert its normal transactivation effect on *TPO* transcription (Vilain et al., 2001). To date, only ten inactivating mutations in the *PAX8* gene have been identified in sporadic and familial cases of CH with TD, demonstrating that an heterozygous mutation of *PAX8* is sufficient to produce a phenotype, without evidence for a dominant negative effect of the mutants; the phenotype is highly variable, suggesting the concomitant alteration of modifier genes, which, together with *PAX8,* control morphogenesis (Congdon et al., 2001; Esperante et al., 2008; Tonacchera et al., 2007).

NKX2-1

Early studies searching for *NKX2-1* mutations in CH humans with TD did not reveal any variants. Focusing on children with CH associated with respiratory problems or with pleiotropic neurological dysfunction, Pohlenz and Krude independently identified heterozygous *NKX2-1* point mutations in a total of five individuals (Krude et al., 2002; Pohlenz et al., 2002). The hypothyroid condition in these patients was highly variable, with either normal or hypoplastic thyroid gland. To date it is known that, in humans, *NKX2-1* haploinsufficiency gives rise to a syndrome characterized by thyroid hypoplasia, choreoathetosis and pulmonary disease (OMIM: #610978) (Krude et al., 2002; Pohlenz et al., 2002). The neurological symptoms cannot be rescued by thyroxin, illustrating the importance of *NKX2-1* transcriptional activity in the basal ganglia formation and diencephalic development. Of interest, the thyroid phenotype of *NKX2-1* haploinsufficiency depends on the genetic background. The mechanism by which heterozygous mutations cause the phenotype is most likely haploinsufficiency. Although the heterozygous *NKX2.1* mice have been previously reported to be unaffected, Pohlenz study describes abnormalities of thyroid function and neurological development also in the heterozygous mice (Pohlenz et al., 2002).

FOXE1

In humans, three homozygous *FOXE1* loss-of-function mutations have been reported in five patients with Bamforth syndrome (OMIM: #241850) (Bamforth et al., 1989; Baris et al., 2006; Castanet et al., 2002). This syndrome is a rare inherited condition whose main features are TD, usually athyreosis, cleft palate, and spiky hair, with or without choanal atresia and bifid epiglottis.

In the affected individuals *FOXE1* mutations were typically inherited from heterozygous carrier parents who were usually consanguineous. *In vitro* studies documented a significant decrease in DNA binding activity of the mutated FOXE1 protein and loss of transcriptional activity (Castanet et al., 2002). Nevertheless, *FOXE1* mutations have been identified only in a minority of the affected patients. Recent data suggest that the transcription factor encoded by *FOXE1* may act as a susceptibility factor for thyroid dysgenesis and variations in FOXE1 polyalanine tract length may modulate the risk of thyroid dysgenesis (Carre et al., 2007).

NKX2-5

NKX2–5 mutational screening was carried out by Dentice et al. in a group of 241 patients with TD, allowing the identification of three distinct heterozygous missense mutations in four subjects with very mild or absent cardiac phenotype (Dentice et al., 2006). Functional characterization of the identified mutations showed a reduction in DNA binding and/or trans-activation ability. These data suggest a possible pathogenic role for *NKX2–5* mutations in TD. The variable thyroid phenotypes (ectopic thyroid with or without hypothyroidism and athyreosis) in patients with *NKX2–5* loss of function mutations suggest that other factors/genes may play a role in modulating penetrance and expressivity at both cardiac and thyroidal levels (Dentice et al., 2006).

Notch signaling

Notch is a high conserved, local cell signaling mechanism that participates in a variety of cellular processes and is involved in many aspects of development and disease. Notch signaling governs cell fate differentiation and critical cell fate decisions during development i.e. segmentation in lower organism, somitogenesis in vertebrates, neurogenesis, vasculogenesis and cardiogenesis (Artavanis-Tsakonas et al., 1999; Lai, 2004).

One important function of Notch signaling is to mediate lateral inhibition, a process in which one cell prevents neighboring cells from adopting similar fates by activating Notch. In the lateral inhibition process, equivalent cells take up different fates as the result of signaling between them (Cabrera, 1990; Lai, 2004). At the beginning, each of the cells in the group has the means to send and receive the signal, but, with time, a single one becomes the signaling cell and the surrounding ones become receiving cells. This relies on a feedback mechanism within each cell where the activation of the receptor leads to down-regulation of the ligand in the same cell. The net result of lateral signaling is to obtain neighboring cells adopting alternative fates: this gives rise to a 'salt and pepper' pattern of differentiation. Such a situation takes place, for example, among the neural precursors in the development of both vertebrates and invertebrates (Lai, 2004).

Mammals have four Notch proteins (Notch 1–4) that are membrane-bound type I receptors (with a single-pass transmembrane domain), harboring a large extracellular domain involved in ligand binding, and a cytoplasmatic Notch intracellular domain (NICD) involved in signal transduction (Fig. 1.2, A and B). The extracellular domain contains a variable number of epidermal growth factor (EGF)-like repeats, which are critical for ligand-receptor interactions. The EGF-like repeats are followed by three cysteine rich LIN12/Notch repeats (LNR), that prevent signaling in the absence of the ligand. The NICD contains a RAM23 domain and six ankyrin/cdc10 repeats involved in protein-protein interactions,

two nuclear localization signals (N1 and N2), a transcriptional activation domain (TAD) that differs among the four receptors, and a PEST sequence that mediates the proteolytic degradation of the protein (Fiuza and Arias, 2007).

In mammals, Notch receptors interact with different ligands, belonging to Delta-like and Jagged families (Fig 1.2, A and B). Like their receptors, Notch ligands are EGF-containing transmembrane proteins, and they are, respectively, orthologs of invertebrate Delta and Serrate/Lag-2 proteins. Collectively, the ligands contain an N-terminal extracellular DSL motif that mediates the binding to the receptor and a variable number of EGF-like repeats (eight in mammalian Delta-like and 15–16 in Jagged ligands) (Bray, 2006). Jagged ligands have an extra cysteine-rich domain highly homologous to the von Willebrand factor in proximity to the transmembrane region (Fig. 1.2,B). The ligand intracellular domain contains a conserved C-terminal PDZ-binding motif. This motif seems to be important for the activation of Jagged target genes in a bi-directional signaling model (Ascano et al., 2003).

Binding and ubiquitination of ligands by the E3 ubiquitin ligases Neuralized (Neur) and Mind bomb (Mib) are essential for ligand activation (Le Borgne et al., 2005; Le Borgne and Schweisguth, 2003). This ubiquitination and the activity of the endocytic ubiquitin-binding protein are requirements for ligand internalization from the cell surface and Notch signaling (Chitnis, 2006; Le Borgne et al., 2005).

The binding of the ligand to the Notch receptor results in two proteolytic cleavages of the receptor (Fig. 1.2, C), mediated by the activity of the ADAM10 or TACE (TNF-α-converting enzyme; also known as ADAM17) metalloprotease, and by the γ-secretase complex (Weinmaster, 2000). Following this proteolytic process, the NICD is released and it enters into the nucleus where it interacts with the DNA-binding CSL (CBF1, Su(H) and LAG-1) protein. The co-activator Mastermind (Mam) and other transcription factors are recruited to the CSL complex, whereas co-repressors (Co-R) are released (Lai, 2002). This process triggers the transcription of Notch target genes such as the basic helix–loop–helix (bHLH) proteins Hairy/Enhancer of Split (Hes) and Hes-related proteins

(Hey), which, in turn, act as transcriptional regulators of further downstream genes (Iso et al., 2003).

A

Core components	*D. melanogaster*	*Danio rerio*	*Mammals*
Receptors	**Notch**	**notch1a**	**Notch1**
		notch1b	**Notch2**
		notch2	**Notch3**
		notch3	**Notch4**
Ligands	**Delta**	**deltaA**	**Delta-like 1 (DLL-1)**
		deltaB	**Delta-like 3 (DLL-3)**
		deltaC	**Delta-like 4 (DLL-4)**
		deltaD	
	Serrate	**jagged 1a**	**Jagged 1 (JAG1)**
		jagged 1b	**Jagged 2 (JAG2)**
		jagged 2	

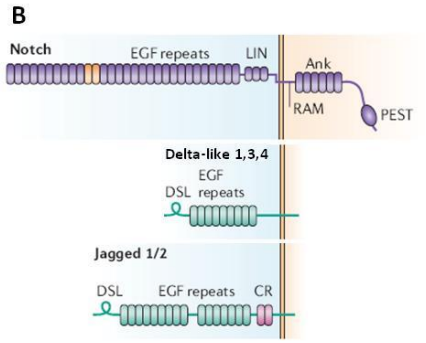

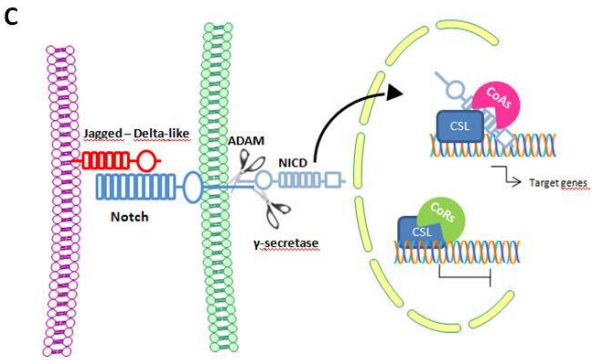

Figure 1.2: Schematic overview of the components of the Notch signaling pathway. A) Names of core components of Notch signaling (receptors and ligands) in different species; all metazoan organisms studied to date contain one or more orthologs of each of the proteins summarized in table; B) Structure of Notch receptors and ligands: the Notch protein consists of an extracellular domain with 36 EGF domains, three LIN repeats, and a heterodimer domain followed by a transmembrane domain, ankyrin repeats (Ank), and a PEST motif. Both the Delta-like and Jagged ligands have a DSL domain and EGF repeats. In addition, Jagged proteins have a cysteine-rich domain (CR); C) basic operations of the Notch signaling: activation of Notch by its ligand triggers two proteolytic cleavages of Notch (ADAM and γ-secretase). γ-secretase cleavage releases the Notch intracellular domain (NICD), which translocates into the nucleus. NICD activates CSL. The CSL co-repressor complex is displaced by a co-activator complex containing NICD (CoAs, pink icon), which mediates Notch target gene activation. In the absence of nuclear NICD, CSL associates with a co-repressor complex (CoRs, green icon), which actively represses the transcription of Notch target genes [Modified from (Bray, 2006)].

Notch signaling and thyroid

The role of the Notch signaling pathway during thyroid development has never been clarified. Nor embryonic expression of Notch receptors or ligands have been documented in the thyroid primordium and in the subsequent phases of thyroid follicular cell development. Moreover, information on the thyroid phenotypes in the numerous Notch mutant mouse models are not available, in most of the cases as a consequence of the early embryonic lethality of these conditions; the effects of increased Notch activity in thyrocytes have not been elucidated. A recent study by Ferretti et al. provided the first evidence of the expression of components of the Notch pathway in postnatal murine thyroid tissue, in a follicular thyroid cell line (FRTL-5) and in adult human thyroid samples (Ferretti et al., 2008). The expression of Notch receptors (Noch1,2,3) and the downstream transcription factor Hes1 has been detected in both FRTL-5 and in adult human thyroid samples by real time PCR. In both samples, the analyzed mRNAs were up-regulated by the presence of TSH, thus demonstrating that TSH is able to induce the expression of Notch pathway components in parallel with the expression of specific markers of thyroid differentiation (i.e. the sodium-iodine symporter, *Nis*). Moreover, the study demonstrates a direct ability of Notch1 in promoting the expression of *Nis*, documenting the presence of Hes1 responsive elements in rat and human *Nis* promoter. Eventually, Ferretti highlighted that some elements of the Notch signaling are variably expressed in thyroid tumor tissues (follicular, papillary and anaplastic thyroid tumors) and the activity of this pathway is clearly down-regulated in these pathological situations. The overexpression of Notch1 in thyroid cancer cell lines (ARO and WRO) restored normal expression levels of several markers of thyrocytes differentiation and reduces the growth rate of these cells (Ferretti et al., 2008).

A role of the Notch pathway is better defined in thyroid C-cells. The Notch pathway plays an important role in the normal development of neuroendocrine cells, including the calcitonin producing C-cells. This effect is mediated through modulation of the downstream basic Helix-Loop-Helix transcription factor ASCL1 (achaete-scute complex-like 1 or ASH1, achaete-scute homolog-1) (Lanigan et al.,

1998). Studies on the embryonic development of C-cells have shown that C-cells highly express ASCL1 and its expression strongly decreases by the time these cells reach maturity (adult C-cells don't express ASCL1). An *ASCL1* knockout mouse shows a reduced number of C-cells, visualized by staining for serotonin and calcitonin. This suggests that ASCL1 is important for the growth and differentiation of C-cells, supporting the survival of the embryonic precursors and inhibiting apoptosis (Kameda et al., 2007; Lanigan et al., 1998).

Jagged1-Notch signaling and thyroid

In search for novel candidate genes implicated in thyroid organogenesis, circumstantial evidence suggests that the Notch signaling and the ligand Jagged1 may be of particular interest.

- CH patients have a 8- to 15-fold higher risk of presenting associated congenital abnormalities of the heart, eye, gastro-intestinal system, bone or other organ or apparatus; the Notch signaling pathway actively regulates many developmental steps in this context (Bolos et al., 2007; Olivieri et al., 2002).
- Strikingly, *JAG1* deficiency causes the human disorder Alagille syndrome (ALGS, OMIM: 118450), an autosomal dominant disorder that has traditionally been defined by a paucity of intrahepatic bile ducts, in association with three of the five main clinical abnormalities: cholestasis, cardiac disease, skeletal abnormalities, ocular abnormalities, and a characteristic facial phenotype (Li et al., 1997; Oda et al., 1997). More recently, mutations in *NOTCH2* have been identified in two affected families (McDaniell et al., 2006). Congenital heart disease has been reported in up to 90% of patients with ALGS. Patients have a large range of congenital heart defects, the most common affecting the cardiac outflow tract. These include right-sided obstructive lesions such as pulmonary artery stenosis and tetralogy of Fallot (TOF), as well as

ventricular septal defects (McElhinney et al., 2002). Of particular interest, mutations in *JAG1* have also been implicated in isolated non-syndromic cases of congenital heart disease, including pulmonary artery stenosis and tetralogy of Fallot, underlining that the precise outcome of *Jagged1* inactivation is often sensitive to cellular context, developing timing, and concomitant presence of other susceptibility alleles (Eldadah et al., 2001; Krantz et al., 1999). Moreover, long term follow-up of less severe Alagille patients reported associated problems: hypothyroidism, glaucoma, haepatocellular carcinoma and pancreatic insufficiency (Dufour and Pratt, 2001; Hoffenberg et al., 1995).

- Recently, a genome-wide analysis of over 100 TOF patients and unaffected parents revealed 11 de novo copy number variations (CNVs) and ten unique loci were identified, including those at the *NOTCH1* and *JAGGED1* loci, providing a first evidence that also the *NOTCH1 receptor* mutations can be associated with human TOF (Greenway et al., 2009).
- *Jag1* knockout mice show vascular defects that result in embryonic lethality before E11.5, precluding their use in studying thyroid and cardiac outflow tract remodeling (Xue et al., 1999). A detailed analysis of thyroid follicular cell proliferation and differentiation in *Jag1* knockout mice has never been conducted yet. *Jag1* heterozygous mice are viable and have no cardiovascular defects, but develop mild ocular defects suggestive of ALGS (Xue et al., 1999). Combined haploinsufficiency of *Jag1* and *Notch2* results in mice with multisystem defects that strongly resemble those seen in patients with Alagille syndrome, including pulmonary artery stenosis and ventricular septal defects (McCright et al., 2002). This result, together with the findings of heterozygous *JAG1* or *NOTCH2* mutations in humans with Alagille syndrome, strongly implicates this ligand–receptor pair in development of the cardiac outflow tract, despite the fact that gene-dosage sensitivity seems to be different when comparing mice with humans.

- A recent work of High and colleagues dissected the role of *Jag1* in the second heart field, by crossing *Islet1*^{Cre} mice with mice harboring a conditional allele of *Jag1* (*Jag1*^{flox}). *Islet1*$^{Cre/+}$*;Jag1*$^{flox/flox}$ mutants died in the neonatal, displaying severe cardiac and aortic arch defects (i.e. persistent truncus arteriosus, double outlet right ventricle, ventricular septal defects, atrial septal defects, and aortic arch defects such as right-sided aortic arch and interrupted aortic arch) (High et al., 2009).
- Multiple *jagged* and *notch* genes are expressed during development in zebrafish (Zecchin et al., 2005). Knockdown of zebrafish *jagged* genes, alone or in combination with *notch* genes, perturbs zebrafish biliary, pancreatic, cardiac, kidney and craniofacial development in a manner compatible with an ALGS phenocopy (Lorent et al., 2004). These data confirm an evolutionarily conserved role for Notch signaling in vertebrate development, and, considering the redundancy of *jagged* and *notch* gene function during zebrafish development, they stress again the importance of the dosage of the Notch signal for development.
- The Notch signaling pathway is required for proper development of other endocrine cells: pancreatic, gut, and bone endocrine tissues. Enforced activation of Notch signaling in pancreatic progenitors impairs their differentiation into the various pancreatic cell lineages, whereas inactivation of Notch signaling leads to premature differentiation of endocrine pancreas: the developing pancreatic epithelium expresses Notch ligands of the Jagged family (Apelqvist et al., 1999; Jensen et al., 2000; Murtaugh et al., 2003). Knockdown studies using zebrafish embryos showed that the loss of specific Jagged ligands causes ectopic islet-cell differentiation. Notch/Jagged pathway is necessary for the differentiation of endocrine cells in the developing pancreas, limiting the number of differentiating precursors in zebrafish (Zecchin et al., 2007).
- The expression pattern of *Jag1* suggests that it is a candidate to act as an important Notch ligand in the thyroid. At E10.5 and E11.5, *Jag1* is expressed in the pharyngeal endoderm, pharyngeal mesenchyme, and

the OFT of the heart. In addition, it is expressed in the endothelium and smooth muscle of the aortic arch arteries (Crosnier et al., 2000; High et al., 2009).

Considering the close spatio-temporal relationship between the thyroid and the outflow tract development, the strong influence of the signals emanating from the cardiac mesoderm on thyroid development and the deep involvement of the Notch-Jagged signaling in cardiac development and disease, this pathway is a strong candidate to have a direct role, which deserves to be unraveled, during thyroid development.

GENE NAME	MUTANT MOUSE MODEL(S)	STAGE OF LETALITY	CARDIAC PHENOTYPE	VASCULAR PHENOTYPE	OTHER SIGNIFICAT PHENOTYPES	HUMAN DISEASE	CARDIOVASCULAR MANIFESTATIONS
NOTCH1	NOTCH1-/-	E9.5 to E10.5	hypocellular endocardial cushons, impaired ventricular trabeculation	yolk sac and ambryonic vascular defects	neural and somite defects	Aoric valve disease	Bicuspid aortic valve, aortic valve calcification
NOTCH2	NOTCH2-/-	E10.5 to E11.5	not reported	not reported	widespread cell death	Alagille syndrome	Pulmonary artery stenosis, Tetralogy of FIlot
	NOTCH2del1/del1	E11.5 to birth	pericardial effusion, thinned myocardium	haemorrhage, oedema	kidney and eye defects		
JAG1	JAG1-/-	E10.5 to E11.5	pericardial oedema	yolk sac vascular defects, abnormal head vessels, haemorrhage	not reported	Alagille syndrome and Isolated congenital heart disease	Pulmonary artery stenosis, Tetralogy of FIlot, ventricular septal defects, vascular anomalies
NOTCH2 and JAG1	JAG1+/-;NOTCH2+/del1	postnatal to birth	pulmonary artery stenosis, ventricular septal defects, atrial septal defects	not reported	bile duct defects, jaudice, kidney defects, eye defects		

Table II: Notch mutant mouse models that have a cardiovascular defects related to the outflow-tract development; human cardiovascular diseases associated with mutations in Notch signaling components. Modified from High, 2008.

2.Materials and Methods

Abbreviations

BCIP: 5-bromo-4-chloro-3-indolyl phosphate, toluidine salt

BSA: albumin from bovine serum

DIG: digoxigenin

dpf: days post fertilization

EDTA: ethylenediaminetetraacetic acid

FLUO: fluorescein

HM: hybridization mix

hpf: hours post fertilization

INT: 2-4-iodophenyl-3-4-nitrophenyl-5-phenyltetrazolium chloride

LB: Luria-Bertani Broth medium

NBT: 4-Nitro blue tetrazolium chloride

NTP: ribonucleotides triphosphate

O/N: over night

PBS: phosphate buffered saline

PBT: phosphate buffered tween

PFA: paraformaldehyde

PTU: 1-phenyl-2-thiourea

RT: room temperature

SSC: saline standard citrate

cDNA: complementary DNA

TAE: Tris-acetated buffer-EDTA

Tris: Tris base (2-amino-2-hydroxymethyl-propane-1,3-diol)

TE: Tris-ETDA

WT: wild type

Recipes and Buffers:

FISH WATER 1X:

100 ml SALINE STOCK SOLUTION 50X

50 µl Methylen Blue 1000X

dH_2O up to 5 lt.

SALINE STOCK SOLUTION 50X:

25 mM NaH_2PO_4 (3.43 g)

25 mM Na_2HPO_4 (4.45 g)

75 g ISTANT OCEAN

ddH_2O up to 5 lt.

RINGER'S SOLUTION (normal):

116 mM NaCl

2.9 mM KCl

1.8 mM CaCl2

5 mM HEPES, pH 7.2.

PTU:

0.003% PTU (1-phenyl-2-thiourea) in fish water.

TRICAINE:

(3-amino benzoic acid ethyl ester also called ethyl 3-aminobenzoate) comes in a powdered form from Sigma. Make tricaine solution for anesthetizing fish by combining the following in a glass bottle with a screw cap.

Stock solution 25X:

400 mg tricaine powder

97.9 ml dH_2O water

~2.1 ml 1 M Tris (pH 9).

Adjust pH to ~7. Store this solution in the fridge.

To use tricaine as an anesthetic combine the following in a 50 ml beaker: 2 ml tricaine solution ~48 ml clean fish water.

DANIEAU SOLUTION (1X):

58 mM NaCl

0.7 mM KCl

0.4 mM $MgSO_4$

0.6 mM $Ca(NO_3)_2$

5 mM HEPES pH 7.6

LB MEDIUM:

5 g tryptone

2.5 g yeast extract

5 g NaCl

ddH_2O up to 500 ml and autoclave to sterilize.

LB AGAR:

2 g tryptone

1 g yeast extract

2 g NaCl

3 g agar

ddH_2O up to 200 ml and autoclave to sterilize.

DEPC WATER (Nuclease-free water):

1 ml DEPC (Diethyl pyrocarbonate) in 1lt ddH_2O. Shake for 1h to O/N. DEPC must then be completely destroyed by autoclaving.

TAE (50X) ELECTROPHORESIS RUNNING BUFFER

Tris base	240 g
Glacial acetic acid	57.1 ml

0.5 M EDTA	100 ml
ddH_2O	to 1 lt.

Methods for keeping and raising zebrafish

The zebrafish, *Danio rerio*, is a tropical freshwater fish belonging to the minnow family (Cyprinidae) of order Cypriniformes.

Zebrafish are kept and raised, with the suitable adaptation to laboratory conditions, according to methods described in two main texts, the Zebrafish Book and Zebrafish: a Practical Approach (Nusslein-Volhard and Dahm, 2002; Westerfield, 1995).

Zebrafish laboratory strains are maintained in large-scale aquaria systems ("Aquarienbau Schwarz, ZebTech, TECNIPLAST and Müller-Pfleger). Recirculation systems with biological filters and a reverse osmosis supply are used to provide high-quality water and a regular water exchange rate. These large-scale recirculation systems allow raising and maintaining very large numbers of fish located in hundreds of tanks serviced by a common filter unit. High-quality water is sterilized by UV radiation before distribution to the tanks to reduce the risk of disease spreading.

Zebrafish are maintained in overflow containers according to the number of individuals, 1-liter plastic boxes for keeping single individuals, 5 or 10-litre glass or plastic boxes for 2 up to 30 fish. Fish tanks are placed in rows on to rimmed plastic or glass shelves in several suitable aquaria racks provided with constantly water recirculation from reservoirs located above the racks. Water enters into each container through a little outlet and exits through an overflow on to the shelf, from where it is drained to the filter. In racks where mouse cages are used as tanks, these are equipped with an outflow at the top margin where a hole of 3,5 cm diameter is covered by grids of different mesh size, depending on the age of the fish, in order to prevent fish to escape through the overflow. For 1-liter tanks a 2 cm long slit of a 2 mm width is cut into the top edge in the front side of the box. The water enters into the tanks via a series of outlets tubes made of

silicone equipped, at their end, with a cut-off Eppendorf pipette tip so that tanks are provided with overflow water.

Healthy and fecund fish need to be maintained in constant saline, temperature and pH conditions. Fish re-circulating water is provided with a suitable saline salt supply and maintained at a pH of about 7 and a conductibility between 200 and 400 µS at a temperature of 28.5°C.

Adult fish are fed with a dietary suitable to keep them in good breeding conditions. Fish are fed once with dry food flakes (TetraMin) and twice with live food composed of *Artemia salina* nauplia. Artemia, a species of small shrimps, is bought as cysts from suppliers and then raised to nauplia stage into appropriate hatcheries. These hatcheries are made of inverted plastic cones of about 15 liters with cut-off bottoms provided with an outlet and lighted with a neon lamp. Each cone contains 8 liters of tap water added with 192 gr of sea salt (NaCl) and 80 ml of shrimp cysts. Air pump with a bubbling stone has to be inserted into the cone to ensure vigorous mixing and to keep Artemia live. After two days the shrimps are completely hatched and reach the nauplia stage, stage at which they have the suitable nutritional value, and they can be harvested. To harvest Artemia nauplia, aeration has to be stopped so that shrimps can sink to the bottom of the plastic cone, while the cysts' shells are floating on the water. Then, the nauplia are collected through the outlet at the bottom of the cone, filtered and washed to remove excess of salt. Artemia nauplia are resuspended in fresh tap water and fed with a laboratory squirt bottle.

Zebrafish larvae are fed twice a day from 6 dpf with powder made of dry Artemia (Novo Tom, JBL).

Zebrafish are usually kept on a 12-hour light - 12-hour dark cycle regulated with appropriate timers.

Fish are bred according to the Zebrafish Book, and mating crosses are set up in late afternoon using suitable mating boxes (Westerfield, 1995). These boxes consist essentially of plastic tanks with a removable inner container that fit tightly with the external one. The inner container holds the paired fish and its base is made of a grid through which the eggs fall into the outer container so

that they are protected from being eaten by their parents. Sometimes a small bundle of green plastic grass is added in the inner containers as a way to reduce fish aggression.

Zebrafish mate and spawn when the light turns on in the morning. Fish eggs hold in the outer box of the mating tanks are collected by pouring the water from this outer container through a fine tea net. Eggs are then transferred from the tea net to a Petri dish in embryo medium (Fish Water). Laid eggs are then observed under a dissection microscope and unfertilized eggs or dead embryos have to be regularly removed because they are a substrate for growth of bacteria and moulds. Embryos are incubated at a temperature range between 25°C to 33°C and then fixed at suitable stages for in situ hybridization or immunohystochemistry protocols. Alternatively embryos can be raised to adulthood: at 6 dpf larvae are transferred in 1-liter tanks (about 50-80 larvae per tank) and maintained in an incubator at 28.5°C until they reach 1 month of age when they are moved to the ZebTech, TECNIPLAST aquarium. Tanks of this system are equipped with mesh that does not allow young fish to escape so that they can grow to adulthood.

Immunofluorescence staining of Jagged1 and Notch (1-4) on murine thyroid tissue

Adult thyroid glands were obtained from 2-month-old mice, immediately embedded in OCT compound (BDH), cryostat sectioned (10-µm), absorbed on super-frost microscope slides and stored at – 80°C until use.

Immunofluorescence staining protocol:

- Fix the sample with frozen acetone, 10-15 min;
- Air dry the slides, 30 min, RT;

- Encircle the samples with the PAP-pen. This provides an hydrophobic barrier around the specimen on a slide in order to keep the staining reagents localized on the tissue sections;

- Rehydrating the sections: 3 x 5 min, 1X PBS;

- Permeabilization: 1X PBS, 1% BSA, 0,2% Triton®X (Sigma); filter the solution, 10 min at RT;

- Wash steps: 3 x 5 min, 1X PBS;

- Blocking: 1X PBS, 1% BSA, 2% Donkey Serum (Invitrogen); filter the solution, 1h at RT;

- Primary antibody incubation: 1:100 anti-Jagged1 in 1X PBS, 1% BSA, 4°C, O/N (Jagged1, H-114, Santa Cruz Biotechnology, Inc.: a rabbit polyclonal antibody raised against animo-acids 1110-1223 of Jagged1 of human origin); or 1:100 anti Notch1 (C-20, Santa Cruz Biotechnology, Inc.), Notch2 (M-20, Santa Cruz Biotechnology, Inc.), Notch3 (M-20, Santa Cruz Biotechnology, Inc.), Notch4 (M-18, Santa Cruz Biotechnology, Inc.) in 1X PBS, 1% BSA, 4°C, O/N; the Notch primary antibodies are goat polyclonal, raised against the C-terminal end;

- Wash step: 3 x 5 min, 1X PBS;

- Blocking: 1X PBS, 1% BSA, 2% Donkey Serum (Invitrogen); filter the solution, 20 min at RT;

- Secondary antibody incubation: 1:400 Alexa Fluor 488-donkey Anti-Rabbit IgG (Invitrogen) or 1:400 Alexa Fluor 555-donkey Anti-Goat IgG (Invitrogen) diluted in 1X PBS, 1% BSA, 2% Donkey Serum (Invitrogen); filter the solution, 1h at RT in the dark;

- Wash step: 5 x 5 min, 1X PBS, protected from light;

- Mounting medium: 30% glycerol and 1:20 DAPI stock solution (1 µg/ml) in 1X PBS;

- Store the slides at 4°C until microscope observations.

Cloning of zebrafish thyroid markers

nkx2.1a

To produce the antisense probe for *nkx2.1a* a portion of the exon2 (702 bp) has been cloned in pCRII-TOPO. This fragment has been generated by PCR reaction, starting from a sample of zebrafish genomic DNA.

The primer sequences for *nkx2.1a* are as follows:

zf_nkx2.1a_fw: 5'-GGAATGGACGCCAGTAAATC-3'

zf_nkx2.1a_rv: 5'-CACAAATCCGTATACAATTCACG-3'

The polymerase chain reaction product was cloned into the pCRII-TOPO plasmid (Invitrogen).

pax2a

A clone containing the full cDNA of zebrafish *pax2a* was already present in the laboratory: pGEM-3zf(+)_*pax2a*. A portion of zebrafish *pax2a* gene (926 bp) has been produced by PCR.

The primer sequences for the *pax2a* are as follows:

zf_pax2a_fw: 5'-ATCCCATTCTTGAAGAGAGG-3'

zf_pax2a_rv: 5'-GAAAGGCTGCTGAACTTTGG-3'

The polymerase chain reaction product was cloned into the pCRII-TOPO plasmid (Invitrogen).

slc5a5 (previously named nis)

A clone containing the full zebrafish *slc5a5* open reading frame (ORF) has been obtained from RZPD (Berlin, Germany); a portion of zebrafish *slc5a5* gene (1105 bp) has been produced by PCR.

The primer sequences for the *slc5a5* are as follows:

zf_slc5a5_fw: 5'-ATGGCTATGGACTCTGACAGACCAC-3'

zf_slc5a5_rv: 5’-CCTCCATAGTGACAGCAGCC-3’

The polymerase chain reaction product was cloned into the pCRII-TOPO plasmid (Invitrogen).

tg

To produce the zebrafish *tg* probe, a PCR fragment (860 bp) has been generated from a pool of cDNAs. These cDNAs were obtained by retro-transcription of different embryonic stages RNAs (48-120 hpf). The retro-transcription has been conducted in presence of random hexamers and a specific zf_tg_rv primer.

The primer sequences for amplification of *tg* are as follows:

zf_tg_fw: 5’-TGGGAGGCTCAGTGTTTTCT-3’

zf_tg_rv: 5’-TCCACCTACATGAGGCATGA-3’

The key feature of TOPO® cloning is the enzyme DNA topoisomerase I, which functions both as a restriction enzyme and as a ligase. Its biological role is to cleave and rejoin DNA during replication. TOPO® vectors are provided linearized with topoisomerase I covalently bound to each 3´ phosphate. This enables the vectors to readily ligate DNA sequences with compatible ends (i.e., PCR product) (Figures 2.1). The ligation is complete in only 5 minutes at room temperature.

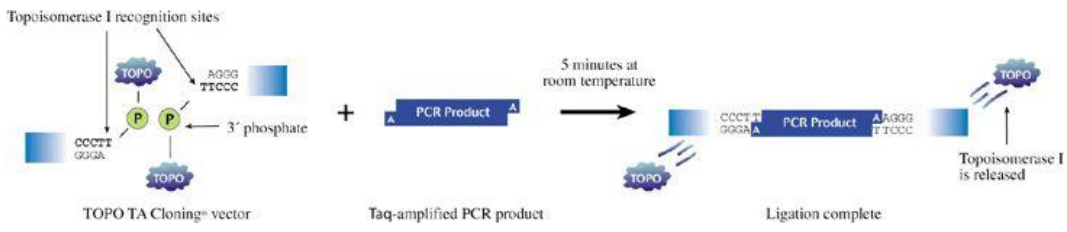

Figure 2.1: Principle of TOPO cloning reaction. Invitrogen provides linearized plasmids with covalently attached TOPOisomerase I for the fast insertion of any PCR product. The standard protocol uses the 3' A overhang PCR product produced by Taq (high-fidelity polymerases). The reaction takes 5 min at RT**.**

As the TOPO cloning system (Invitrogen) allow the desired PCR fragment to be inserted in the backbone without a preferential orientation, all the clones have been sequenced with both T7 and SP6 primers.

Transformation of *E. coli*

Bacterial transformation allows obtaining large plasmids copy number. Vectors containing part of the DNA/cDNA of interest were introduced in bacterial *E. coli* cells (One Shot® TOP10 Chemically Competent E. coli, Invitrogen). Vectors confer to the bacterial cells antibiotic resistance as a selectable marker for plasmid-containing cells.

Chemically competent *E. coli* stored at -80°C were placed on ice; a small amount of plasmid DNA (10-50 ng) is added to the bacteria cells that were left on ice for 30 minutes before performing heat shock. A 30-second long heat shock at 42°C allows the *E. coli* cells to take up vector DNA. Transformed cells are re-placed on ice for 2 min, adding 200 µl of nutrient S.O.C medium (Invitrogen™) and then incubated for about 45 min in a shaker at 37°C. This incubation allows antibiotic resistance to be expressed so that cells can be plated on agar containing ampicillin or kanamycin. Plates are incubated over night and plasmid-containing colonies can grow on solid medium. Positive colonies are then selected and singles clones are cultured in Luria-Bertani medium with the suitable antibiotics to improve selection of vector-containing clones. Liquid cultures provide massive bacterial growth in order to obtain a large plasmid copy number after extraction and purification.

Purification of plasmid DNA

Extraction and purification of plasmid DNA were performed using commercial kits provided by Qiagen (QIAprep Spin Miniprep kit), based on the alkaline lysis of bacterial cells in order to release plasmid DNA. These kits are provided with special silica matrix columns that bind plasmid DNA with high affinity in the

presence of high salt (Vogelstein and Gillespie, 1979). Then two washes with suitable buffers are performed to remove excess of salts and improve DNA recovery.

High-quality plasmid DNA is then eluted from the column with 50–100 µl of nuclease-free water pre-heated at 65-70°C in order to increase elution efficiency.

Anti-sense probe synthesis

An improving possibility to study the expression of genes of interest is to generate an epitope-tagged antisense RNA probe directed against the targeted gene/mRNA. To construct digoxigenin or fluorescein-labeled antisense RNA probes, the partial cDNA of the gene of interest is cloned into a plasmid vector such it is under the control of a phage promoter. These phage promoters are recognized by the RNA polymerases encoded by phages as T3, T7 or SP6 and they allow large amounts of RNA to be produced *in vitro*. To set up the anti-sense probe synthesis the plasmid is linearized, using a suitable restriction enzyme, at the 5' end of the inserted gene of interest (Table 2.I). This step is necessary as polymerases will fall off the end of the linearized plasmid after transcription and the enzyme can start a new transcription, in a process called run off synthesis.

Linearization reaction is performed in a 50 µl total volume with approximately 5 µg of plasmid to be digested, and using 1.2 µl of the suitable restriction enzyme coupled with its buffer and BSA when requested to enhance the endonuclease performance:

- ddH_2O up to 50 µl
- plasmid DNA of interest 5 µg
- 10X buffer 2 µl
- BSA 100x (if needed) 0.5 µl
- restriction enzyme 1.2 µl

Linearization reaction goes from 2 h to O/N at 37°C (or at a temperature suitable to the enzyme activity).

The linearized plasmid is then purified and precipitated over night at -80°C.
The purification of the vector after linearization is carried out using Phase Lock gel tubes (Eppendorf):

- centrifuge column tubes 1 minute at max speed to pack the gel at the bottom of the tube;
- add nuclease free water to 100 µl to the sample of linearized DNA, and transfer the volume on the top of the gel of Phase Lock column;
- add 50 µl phenol and 50 µl chloroform;
- centrifuge 5 min max speed;
- the Phase Lock gel separates solvents with saline buffers and enzymes of the linearization reaction from the aqueous phase containing the DNA;
- add 100 µl chloroform and centrifuge 5 min max speed;
- collect the aqueous phase containing purified linearized DNA (approx. 100 µl) that is on the top of the gel, and transfer it in a new 1,5 ml tube.

Then add to the purified DNA a final concentration of 0.2M NaCl, 2.5 volumes of Ethanol absolute and 2 µl of glycogen; mix well and precipitate at least 2 h or over night at -80°C.

- After precipitating the linearized DNA, centrifuge 15 min at max speed;
- remove the surnatant being careful not to touch the pellet;
- wash the pellet 3 times with 200 µl 70% ethanol centrifuging 2 min max speed each time and removing surnatant;
- dry the pellet from ethanol residuals and the re-suspend it in the desired volume of nuclease-free water (usually 15-20 µl).

Then run an electrophoresis on 1.5% agarose gel, loading 1 µl of purified linearized plasmid DNA in order to control the quality of the digestion.
If the linearization was successfully carried out, the antisense RNA probe can be transcribed starting from a phage promoter (T7, T3 or SP6) flanking the 3' end of the inserted gene of interest. The nucleotide mix contains a part of digoxigenin-

or fluorescein-labelled UTP, which will be incorporated by RNA polymerases to obtain a labeled antisense probe.

Synthesis of mRNA probes were performed in a 20 µl reaction volumes at a temperature of 37°C from 2 hours to 6 hours, depending on probe length:

- linearized plasmid DNA (1 µg) X µl
- 10X transcription buffer (Roche) 2 µl
- DIG- or FLUO-RNA Labeling Mix (Roche) 2 µl
- RNAsin® Ribonuclease Inhibitor (Promega) 1 µl
- (T7, T3 or SP6) RNA Polymerase (Roche) 2 µl

After the transcription, a step is required to digest template plasmid DNA with 2 µl of DNAse (RNAse-Free DNAse, Promega) at 37°C for 20 min. This allows to purify a high quality RNA probe.

The purification of antisense RNA probes is performed using a commercial kit (MEGAclear™ provided by Ambion®). Once purified, the RNA probe can be stored at -80°C. Then an electrophoresis is performed on 1.5% agarose gel, loading 1 µl of purified probe, in order to control and quantify the transcription. Prior to being loaded on gel, the probes have to be denatured at 65°C for at least 5 min.

Table 2.I: Vectors containing part of the genes of interest to synthesize the anti-sense RNA probes, each one with the suitable restriction enzyme and RNA polymerase.

Plasmid name	Endonuclease	RNA polymerase
pCRII_TOPO_*jag1a*	*Apa*I	Sp6
pCRII_TOPO_*jag1b*	*EcoR*V	Sp6
pCRII_TOPO_*nkx2.1a*	*Xho*I	Sp6
pCRII_TOPO_*pax2a*	*Xho*I	Sp6
pCRII_TOPO_*tg*	*Xho*I	Sp6
pCRII_TOPO_*slc5a5*	*Xho*I	Sp6

Whole mount *in situ* hybridization (WISH)

Whole mount *in situ* hybridization is a technique largely used to study gene expression patterns.

The improvement of this method allows the detection of weak signals and the visualization of one or more mRNAs in the same embryo. This permit a finer dissection of the spatial and temporal relationship between the expression of genes, even to the level of been able to show simultaneous expression of two genes within one cell. The method uses RNA complementarity to the endogenous RNA to generate an "antisense-RNA" labeled with a particular antigenic group, as previously described. These probes are hybridized to the embryo and visualized using anti-digoxygenin or anti-fluorescein antibodies conjugated to alkaline phosphatase. Various chromogenic substrates for alkaline phosphatase are commercially available and we routinely use NBT/BCIP (blue precipitate), INT/BCIP (violet/brown precipitate) or FastRed (Roche) (red precipitate).

The method used for *in situ* hybridization involved fixing the embryos, digesting with low amount of proteinase to partially free the target mRNA from proteins, pre-hybridizing to block non specific binding of probe to the fixed material, hybridizing with the probe and detect the probe enzymatically.

Solutions

HYBRIDIZATION MIX (HM):

60% formamide

4.6 µM citric acid pH 6

SSC 5X

50 µg/ml heparin

500 µg/ml torula yeast total RNA (tRNA)

0.1% Tween-20

dH_2O up to 100 ml

WASHING MIX (HM WASH):

HM without tRNA and heparin

PBS 1X:

150 mM NaCl

10 mM Na_2HPO_4

ddH_2O up to volume

PBT 1X:

1X PBS

0.1% Tween-20

PFA:

4% paraformaldehyde in PBS 1X

ANTIBODIES ANTI DIGOXIGENIN/FLUORESCEIN:

Antibodies used for whole mount *in situ* hybridization are provided by Roche; they are diluted 1:1000 in a PBT 1X/2% sheep serum/200 mg:ml BSA solution and pre-adsorbed using a variable number of embryos (usually 100-200) at different developmental stages. After 2 h at RT, the antibody solution is diluted to 1:3000 and filtered. Then NaN_3 is added for better storage at 4°C.

NBT/BCIP STAINING BUFFER:

100 mM Tris-HCl pH 9.5

50 mM MgCl2

100 mM NaCl

0.1% Tween20

ddH_2O

NBT/BCIP STAINING SOLUTION:

NBT/BCIP (Roche) stock solution: use 20 µl/ml in staining buffer.

Alternatively use separate components:

- 7.5 µl/ml NBT (Nitro Blue Tetrazolium provided by Sigma) 50 mg/ml (50 mg NBT dissolved in 0.7 ml anhydrous dimethylformamyde and 0.3 ml H2O). Store in the dark at –20°C.
- 3.5 µl/ml BCIP (5-Bromo 4-Chloro 3-Indolyl Phosphate, provided by Sigma) 50 mg/ml (50 mg dissolved in 1 ml anhydrous dimethylformamyde). Store in the dark at –20°C.

BENZYL BENZOATE-BENZYL ALCOHOL

Benzyl-benzoate:benzyl alcohol 2:1.

Method

Preparation of the embryos

1. Sort the embryos at the stages required for the experiment. Staging according to Kimmel et al. (Kimmel et al., 1995);
2. Remove chorions manually;
3. Fix the embryos in 4% paraformaldehyde (PFA) in 1xPBS overnight at 4°C;
4. Rinse with PBS several times; transfer the embryos into 100% Methanol (MeOH) and store them at -20°C until use.

Single probe in situ hybridization (protocol 1)

Progressive rehydratation of the embryos:

- 75% MeOH / 25% PBS for 5 minutes
- 50% MeOH / 50% PBS for 5 minutes
- 25% MeOH / 75% PBS for 5 minutes
- 100% PBT (PBS/Tween20 0.1%) 4x 5 minutes

Digestion with proteinase k (10 mg/ml)

Stage of the embryos	***Incubation time (min)***
24 hpf	7
48 hpf	25
72 hpf	40
120 hpf	55

* zebrafish embryos younger than 24hpf can skip the permeabilization step;

Brief wash with PBT

Post-fixation step

Post-fix the digested embryos with PFA 4% in PBS for 20 min at RT. Then wash four times with PBT (5' each).

Hybridization

Prehybridize the embryos in HM for 3 hours at 65°C.

Incubate with HM containing ~100-200 ng/mL of antisense DIG-RNA probe O.N. at 60-65°C. The hybridization temperature depends on the required stringency (in most of the cases 65°C is satisfactory). The day after, remove the probe. Most of the probes can be reused up to three times. Probes in HM are stable for at least 6 months at – 20°C.

Post-hybridization washes:

- 100% HM WASH at 65°C for 15 minutes
- 75% HM WASH / 25% 2x SSCT 1x at 65°C for 15 minutes
- 50% HM WASH / 50% 2x SSCT 1x at 65°C for 15 minutes
- 25% HM WASH / 75% 2x SSCT 1x at 65°C for 15 minutes
- 2x SSCT 1x at 65°C for 15 minutes
- 0.2x SSCT 2x at 65°C for 15 minutes

  *Note: all the solutions should be pre-warmed in order to ensure that the required temperatures are reached quickly during the washing procedure.

- 75% 0.2x SSCT /25% PBT 1x at RT for 15 minutes
- 50% 0.2x SSCT /50% PBT 1x at RT for 15 minutes
- 25% 0.2x SSCT /75% PBT 1x at RT for 15 minutes
- PBT 2x at RT for 15 minutes

Blocking:

- Blocking solution: PBT-2% sheep serum-2mg/ml BSA at RT for at least 2 hours

Antibody incubation:

Incubate with anti-DIG Fab-alkaline phosphatase at 1:3000 dilution in blocking solution and rock gently overnight at 4°C.

Post-antibody washes:

6x 15 minutes with PBT at RT.

Staining:

- Wash 3x 15 minutes with NBT/BCIP staining buffer at RT.
- Incubate embryos in staining solution (7.5 µl NBT 50 mg/ml; 3.5 µl BCIP 50 mg/ml per ml added) at RT in the dark.
- Monitor the staining reaction with a stereo-microscope.
- Stop the reaction with 4% PFA when the desired signal is come up.

Double probes in situ hybridization (protocol 2)

In many cases is very useful to be able to compare the expression patterns of two different genes in the same specimen. This task is facilitated by using two different epitopes to label the respective probes, allowing detection of the expression domains in different colors.

Follow the previous protocol up to the hybridization step.

Hybridization

Prehybridize the embryos in HM for 3 hours at 65°C.

In this case, it is necessary to prepare HM adding an appropriate amount (~100-200 ng/mL) of both probes and incubate overnight the embryos at 60-65°C.

Post-hybridization washes:

See and follow protocol 1.

Blocking:

- See and follow protocol 1.

Anti-fluorescein antibody incubation:

Incubate with anti-fluorescein Fab-alkaline phosphatase at 1:3000 dilution in blocking solution and rock gently overnight at 4°C.

Post-antibody washes:

6x 15 minutes with PBT at RT.

Staining:

- Wash 3x15 minutes with INT/BCIP or FastRed staining buffer at RT.
- Develop the red staining solution in the dark. Stop the staining by washing with large volumes of PBT.

Anti-fluorescein antibody stripping:

- Wash 3 x 5’ with a stripping solution made of 100 mM glycine pH 2.2-0,1% Tween20. This efficiently destroys any enzymatic activity from the alkaline phosphatase bound to the fluorescein-labelled probe. Then wash in PBT 3x5 min each.
- *Blocking:*

Repeat the blocking step with PBT-2% sheep serum-2mg/ml BSA at RT for at least 2 hours.

Anti-digoxygenin antibody incubation:

Incubate with anti-DIG Fab-alkaline phosphatase at 1:3000 diluition in blocking solution and rock gently overnight at 4°C.

Post-antibody washes:

6x 15 minutes with PBT at RT.

Staining:

- Wash 3x 15 minutes with NBT/BCIP staining buffer at RT.

- Develop the blue staining solution in the dark. Stop the staining by washing extensively in PBT.
- Analyze and document as soon as possible in case of FastRed staining since this precipitate is not as stable as the NBT-BCIP precipitate.

RNA isolation from zebrafish embryos

Several methods work well to isolate high quality RNA from zebrafish embryos. This protocol is based on the TRIzol® method and is a quick way of isolating good RNA from multiple samples. It is possible to follow this protocol to obtain RNA from embryos at different developmental stages, with or without the chorion.

Homogenization

1. Homogenize a maximum of 50-60 embryos in 1 ml of Trizol Reagent using a bead-based homogenizer for an efficient and complete lysis and homogenization of the biological sample. The sample volume should not exceed 10% of the volume of Trizol used for homogenization.

Phase separation

2. Incubate the homogenized samples for 5 minutes at RT to allow the complete dissociation of nucleoprotein complexes. Add 0.2 ml of chloroform per 1 ml of Trizol and briefly vortex. Centrifuge the samples at no more than 12,000 x g for 15 minutes at 4°C. Following centrifugation, the mixture separates into a lower red, phenol-chloroform phase, an interphase, and a colorless upper aqueous phase. RNA remains exclusively in the aqueous phase. The volume of the aqueous phase is about 60% of the volume of Trizol used for homogenization.

RNA precipitation

3. Transfer the aqueous phase to a fresh nuclease-free tube. Precipitate the RNA from the aqueous phase by mixing with 1 µl of glycogen and 0.5 ml of isopropyl alcohol per 1 ml of Trizol used for the initial homogenization. Incubate samples O/N at - 80°C and then centrifuge at no more than 12,000 x g for 30 minutes at

4°C. The RNA precipitation forms a gel-like pellet on the side and bottom of the tube.

RNA wash

4. Remove the supernatant. Wash the RNA pellet once with 75% ethanol, adding at least 1 ml of 75% ethanol per 1 ml of Trizol used for the initial homogenization. Centrifuge at no more than 7,500 × g for 5 minutes at 4°C.

Redissolving the RNA

5. At the end of the procedure, briefly dry the RNA pellet (air-dry for approximately 5 minutes). It is important not to let the RNA pellet dry completely as this will greatly decrease its solubility (partially dissolved RNA samples have an A260/280 ratio <1.6). Dissolve RNA in RNase-free water and incubating for 10 minutes at 55-60°C. Store RNA at -80°C until use.

Reverse transcription of total RNA

Reverse transcription of total RNA was performed using the ImProm-II™ Reverse Transcription System (Promega). This kit includes a reverse transcriptase for synthesis of first-strand cDNA in preparation for PCR amplification.

Briefly, 1 µg of the total RNA purified are digested with DNase I before starting the reverse transcription protocol.

Mix1: DNase I digestion

1 µg total RNA

1 µl Dnase I (Promega)

0.8 µl DNase Buffer (10X)

Up to a final volume of 8 µl with nuclease-free water

Place the samples at 37°C for 30 min.;

Inactivate the reaction: add 1 µl EDTA and incubate at 65°C for 15 min, then place on ice.

Mix2: primers/template mix

The RNA sample s combined with the primers (random examers);

Add 1 µl of random examers to the RNA samples.

The primer/template mix is thermally denatured at 70°C for 5 min and chilled on ice.

Mix3: reverse transcription reaction mix

- nuclease-Free Water (to a final volume of 10µl) 1.8 µl
- ImProm-II™ 5X Reaction Buffer 4.0 µl
- $MgCl_2$ (final concentration 1.5mM) 1.2 µl
- dNTP Mix (final concentration 0.5mM each dNTP) 1.0 µl
- Recombinant RNasin® Ribonuclease Inhibitor 20u 1.0 µl
- ImProm-II™ Reverse Transcriptase 1.0 µl

Add 10 µl of mix3 to each sample.

Anneal: Place the tubes in a controlled-temperature heat block at 25°C, and incubate for 5 min.

Extend: Incubate the tubes in a controlled-temperature heat block at 42°C for up to one hour.

Inactivate Reverse Transcriptase: Incubate the reaction tubes in a controlled-temperature heat block at 70°C for 15 min.

RNaseH digestion*:

Add 1 µl of DNAse-free RNAse

Incubate the reaction tubes at 37°C for 30 min.

(*cDNA yield and amplification sensitivity can be increased by removing or degrading the RNA prior to PCR).

cDNA were amplified and analyzed using the following primers for the genes of interest:

- *beta-actin* (housekeeping gene, internal control):

beta-actinF primer: 5′-TGTTTTCCCCTCCATTGTTGG-3′

beta-actinR primer: 5′-TTCTCCTTGATGTCACGGAC-3′

annealing temperature: 59°C

- *jagged1a* (RT-PCR on embryos injected with *jag1a*^{spli}MO):

jagged1aF primer (exon1): 5'-GACAGACAAACCGGGATGAT-3'

jagged1aR primer (exon4): 5'- CATTGACGGTTTGGGTTGAT-3'

annealing temperature: 56°C

- *jagged1b* (RT-PCR on embryos injected with *jag1b*^{spli}MO):

jagged1bF primer: 5'- TATCAATCGCGAGTTTCCTC -3'

jagged1bR primer: 5'- GTCACCCGGATTTGGTACTC -3'

annealing temperature: 59°C

Example of PCR conditions (25 µl reaction volume):

GoTaq® Green Master Mix, 2X*	12.5 µl
upstream primer, 10 pmol/µl	0.75 µl
downstream primer, 10 pmol/µl	0.75 µl
cDNA template	0.5-2µl
Nuclease-Free Water	to 25µl

*GoTaq® Green Master Mix, 2X**:** GoTaq® DNA Polymerase is supplied in 2X Green GoTaq® Reaction Buffer (pH 8.5) containing 400µM dATP, 400µM dGTP, 400µM dCTP, 400µM dTTP and 3mM MgCl2.

Genomic DNA isolation for PCR analysis

Anesthetization of zebrafish and tail fin clipping

1) Set up small fish tanks (approximately 1 L each) and fill them with system water;

2) Fill 50 ml beaker with 48 ml fish water containing 2 ml of 25X Tricaine;

3) Place up to 2-3 fish to be genotyped in the Tricaine/fish water solution and wait for the fish to stop moving. Quickly remove each fish with a plastic spoon and place it on a clean 35 mm-petri dish filled with some fresh fish water. Once the fish is placed cut 1/3 of the tail fin with the surgical scissors and transfer it to a 1.5 ml clean tube. Then place the fish into a numbered isolation tank and label the fin clip-containing tube with the same number;

4) Repeat as necessary until all fish are genotyped.

Genomic DNA isolation

1) To each fin clip-containing tube, add 100 µl of adult zebrafish lysis buffer (10 mM Tris pH 8.2; 10 mM EDTA; 200 mM NaCl; 0,5% SDS). Make sure the fin is submerged;

2) Vortex tube for 30 seconds;

3) Add 10 µl proteinase K solution (10 mg/ml) to each tube. Incubate at 55 °C O/N;

5) Optional: incubate at 98 °C for 10 min. to inactivate proteinase K;

6) Add an equal volume of Tris buffer-saturated phenol;

7) Vortex tube for 5 seconds;

8) Centrifuge tube at 14,000 rpm for 15 minutes;

9) Transfer top (aqueous) layer to new tube, being careful not to include the water/phenol interface;

10) Repeat steps 6-9 on aqueous layer;

11) Extract remaining phenol in aqueous layer with an equal volume of chloroform;

12) Vortex tube for 5 seconds;

13) Centrifuge tube at 14,000 rpm for 5 min.;

14) Transfer genomic DNA-containing aqueous layer to new tube;

15) Add and 1 µL glycogen (20 mg/mL) and 2.5 volumes of isopropyl alcohol and mix by inverting;

16) Precipitate genomic DNA overnight at – 20 °C (or at least 2 hours);

17) Centrifuge at 14,000 rpm for 15 min. at 4 °C;

18) Discard supernatant and wash pellet with cold 70% ethanol;

19) Remove 70% ethanol and air-dry the pellet;

20) Resuspend genomic DNA in MilliQ water (50 µl/fin clip).

Genomic DNA isolation post in situ hybridization

- wash the embryo 2 x 10 min. in PBT;
- remove the PBT and transfer the embryo in a clean 1.5 ml tube;
- add 50 µl of embryo lysis buffer (100 mM Tris-HCl pH 8; 50 mM KCl; 0.3% Tween-20);
- heat 10 min. at 98°C;
- add 2.5 µl of proteinase K (20 mg/ml);
- incubate O/N at 55°C;
- vortex well;
- heat 10 min. at 98°C to inactivate the proteinase K.

Genotyping the embryos

jag1b^{b1105} zebrafish mutant strain

The *jag1b*^{b1105} allele was identified in an ENU mutagenesis screen in which parthenogenic diploid progeny was analyzed for skeletal defects (Zuniga et al., 2010). These mutants have a G-to-A transition that converts tryptophan 223 to a premature stop codon, truncating the Jag1b protein within the extracellular DSL domain required for Notch binding (Fig. 2.2).

For *jag1b*^{b1105} genotyping, we amplified a PCR product, encompassing the mutation site, using the following primers:

Jag1b-fw: 5'-GTACCAAATCCGGGTGACCT-3'

Jag1b-rv: 5'-GTGGCTTTTTGGGTCATTATCA-3'

Annealing temperature: 60°C

The generated PCR products (206 bp) were then digested with *Bsge*I at 55°C (at least 2 hours); the resulting digestion pattern allow to discriminate between *jag1b* ^{b1105} homozygous mutants, heterozygous or wt fish:

jag1b ^{b1105}*/ jag1b* ^{b1105} (mutants): 206 bp fragment;

jag1b ^{b1105}*/jag1b* (heterozygous): 206/134/72 bp fragments;

jag1b/jag1b (wt homozygous): 134/72 bp fragments.

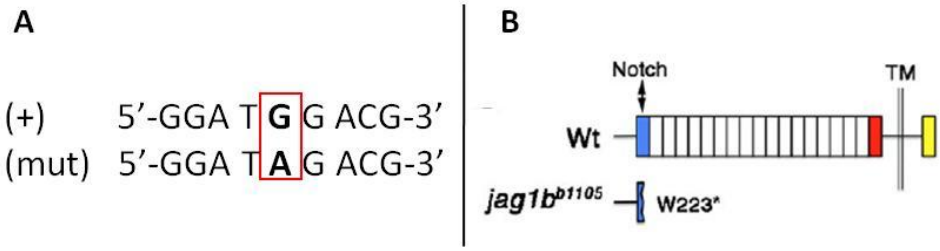

Figure 2.2: Characterization of *jag1b*^{b1105} mutation site. (A) Sequence surrounding the G-to-A transition that creates a premature stop codon in *jag1b*^{b1105} mutants (B) Schematic of Jag1b protein showing DSL (blue), EGF-like (white), cysteine-rich (red), transmembrane (TM) and intracellular (yellow) domains. The *jag1b*^{b1105} lesion is a nonsense mutation (W223*) that truncates Jag1b in the DSL domain required for Notch binding.

Tg(UAS:N^{icd}) zebrafish genotyping:

The following PCR conditions have been followed in order to:

- genotype adult fish, heterozygous for the cassette *Tg*(UAS:N^{icd});
- confirm the presence of the transgenic cassette UAS:N^{icd} in half of the embryos generated from the mating pairs of homozygous Hsp70:Gal4 with heterozygous *Tg*(UAS:N^{icd}), after the heat shock experiments and *in situ* hybridization analysis.

UASNIC-fw: 5′-CATCGCGTCTCAGCCTCAC-3′

UASNIC-rv: 5′-CGGAATCGTTTATTGGTGTCG-3′

Annealing temperature: 62°C

Amplification program:

1.	Initial denaturation	95°C - 3min
2.	Denaturation	95°C – 1 min
3.	Annealing	62°C – 1 min
4.	Extension	72°C – 1 min 15 sec (go to step 2 x 3 cycles)
5.	Denaturation	95°C – 1 min
6.	Annealing	62°C – 45 sec
7.	Extension	72°C – 45 sec (go to step 5 x 35 cycles)
8.	Final extension	72°C – 5 min
9.	Hold	4°C - ∞

Heat shock experiments

For Notch gain-of-function analyses, embryos were obtained from mating between homozygous carriers of the Hsp70:Gal4 and heterozygous carriers of *Tg*(UAS:N^{icd}) (Scheer and Campos-Ortega, 1999). Notch1a intracellular domain (N^{icd}) overexpression was induced by transferring embryos to 40°C medium for 30 min.

Following heat shock, embryos were incubated at 28.5°C until fixation. When the fixation was planned later than 12 h after the heat shock, one or more intermediate heat shocks were performed at intervals of 10–12 h in order to guarantee a continuous expression of N^{icd}. After *in situ* hybridization and documentation, embryos were digested by proteinase K and genotyped (see *Tg*(UAS:N^{icd}) zebrafish genotyping paragraph).

T4 whole mount immunohistochemistry

Larvae at 5 dpf are fixed in 4% PFA at 4°C overnight, washed briefly in PBT, and stored in methanol at –20°C.

To visualize larval T4 production, proceed as follows:

- Progressively rehydrate the embryos with series of decreasing MetOH/ increasing PBT;
- Bleaching and blocking endogenous peroxidase activity: 10% H_2O_2 in PBS, 30 min, RT;
- Washing step: 2 X 5 min, PBT;
- Digestion with proteinase-k (10 µg/ml, final concentration) in PBS, 40 min, RT;
- Post-fixation: 4% PFA, 40 min, RT;
- Washing step: 4 X 5 min, PBT;
- Blocking: 3% normal goat serum (NGS, S-1000, Vector Laboratories) in PBS;
- Primary antibody incubation: 1:2500 rabbit anti-thyroxin BSA serum (ICN Biochemicals), diluted in blocking medium, O/N at 4°C;
- Washing step: 3 X 10 min, 4 x 30 min, PBT;
- Secondary antibody incubation: 1:200 biotinylated anti-rabbit IgG in PBS (Vectastatin ABC Kit PK-4001), RT, 2 hours;
- Washing step: 3 X 10 min., 2 x 30 min, PBT;
- Preparation of Vectastatin ABC reagent: add 10 µl of reagent A + 10 µl of reagent B each ml of PBS, mix immediately; let the Vectastatin ABC reagent to stand for about 30 min. in the dark before use;
- Incubate the embryos for 30 min. with Vectastatin ABC reagent;
- Washing step: 1 brief wash and 1 X 10 min., PBS;
- Transfer the embryos in a 24 multi-well plate;
- Add 30 µl of ImmPACT DAB Chromogen concentrate to 1 ml ImmPACT Diluent, mix well and incubate the embryos in this peroxidase substrate until desired stain intensity develops (ImmPACT DAB peroxidase Substate, SK-4105, Vector Laboratories);
- Rinse larvae in PBT;
- (For detailed analysis, larvae are post-fixed in 4% PFA, washed in PBT and gradually transferred to 80% glycerol).

Morpholino knockdown experiments

In order to generate a loss-of-function phenotype for a known zebrafish gene during development it is possible to transiently inhibit the protein function by injecting antisense-oligos, so called morpholinos, into fertilized eggs (Nasevicius and Ekker, 2000). The morpholinos are 20-25 bases chemical modified oligos that bind specifically to the 5' UTR region or early coding sequences of a given mRNA and block the translation. Morpholinos can also be designed to overlap splice sites and to block splicing (Draper et al., 2001; Nasevicius and Ekker, 2000). Morpholinos are highly specific, since it is sufficient to alter 4 bases within a given sequence to abolish their inhibitory function. Stability and thus functionality of a specific morpholino can be quite different, but a decrease in the efficiency to block translation usually cannot be observed before 4 dpf.

Morpholinos used during this work were directed against zebrafish *jagged 1a* (GenBank accession number: NM_131861) and zebrafish *jagged 1b* (GenBank accession number: NM_131863). MO oligos were designed and synthesized by Gene Tools, Philomath, USA (www.gene-tools.com).

The sequences of MOs used in this work (mismatches in lowercase) are as follows:

*jag1a*_MO-ATG: 5'-CGGTTTGTCTGTCTGTGTGTCTGTC-3';

*jag1a*_MO-spl_E2i2: 5'-AAACAGCCTCTGAAACTCACCGGCC-3';

*jag1a*_mmMO: 5'-CTgAgATACgTGcAACAAAATAcAC-3';

*jag1b*_MO-spl_E3i3: 5′-AATCCTGCTACTCACTTTCACTGGC-3′;

*jag1b*_mmMO: 5′-ATAgTGAAgTCCcTCGCAcAATgAT-3′;

Morpholino oligos were delivered as a prequantitated, sterile, salt-free, lyophilized powder in a glass vial. The stock solution (8 mg/ml) was prepared with nuclease-free water, as advised by Genetool's protocols, and kept at RT. Morpholino working solutions were prepared by diluting stock solutions in Danieau Buffer 1X (58 Mm NaCl; 0.7 mM KCl; 0.4 mM MgSO4, 0.6 mM (CaNO3)2, 5 mM HEPES, pH 7.6), adding 0.5 % Phenol Red (Sigma, Milan, Italy), to make the

solutions visible during microinjection, and 0.5% rhodamin-dextran. Rhodamin-dextran enables the selection of the embryos efficiently injected that can be scored for red fluorescence during gastrulation. Embryos without rhodamin-dextran fluorescence during gastrulation were not considered any further. Different MO concentrations were tested in a range between 0.5 and 3 µg/ml.

mRNA rescue experiment

Full length human JAGGED1 cDNA was cloned into pcDNA3.2/V5-DEST (Invitrogen) between the T7 promoter sequence and the TK polyadenilation signal. One positive clone, after complete sequencing to check for nucleotide changes that could alter the amino acid sequence or interrupt the translation reading frame, was linearized with *NsiI*. Efficiency of linearization was checked on agarose gel electrophoresis and the linearized plasmid DNA was purified using the phenol/chloroform extraction. Full length mRNA was *in vitro* transcribed and 5'-capped using the mMessanger mMachine kit, according to the manufacturer's protocol (Ambion, Inc.)

The reaction was as follows:

2X NTP/CAP	10 µl
10 X Reaction Buffer	2 µl
Linear template (1 µg)	(X)µl
Enzyme-mix	2 µl
Nuclease-Free Water	up tp 20 µl

The reaction was incubated at 37°C, 2h. The template DNA was digested at the end of the reaction with DNAse I, RNAse-free. The RNA was then purified using the MEGAclear kit, to obtain a highly purified RNA. The RNA concentration was determined through gel electorphoresis using a marker designed for nucleic acids quantification. The mRNA was stored at -80°C. For rescue experiments, the mRNA was injected at concentrations ranging from 0,75 to 15 pg/embryo.

Needle preparation and microinjection procedure

Injection needles were pulled from 1.2 mm thin walled glass capillaries (World Precision Instruments, WPI, Germany) with a pipette puller (Flaming/Brown p-97 Micropipette Puller, Sutter Instruments, Crisel Instruments, Rome Italy) and the parameters were set as follows: heat = 395, velocity = 60, time = 50, pull = 60. Before injection, embryos were collected and placed aligned along the border of a clean glass slide, in the lid of a Petri dish. Injections were performed under a dissecting microscope using a micromanipulator attached to a microinjector (Leica Microsystems, Milan, Italy) controlled by a pedal to inject the desired amount of reagent. The samples (MOs, expression vectors or mRNAs) were loaded with GELoader tips 0.5-20 µl (Eppendorf, Milan, Italy) into the injection needles. Then, the tip of injection needles was broken with dissection forceps. The samples were injected into the yolk sac of 1 or 2-cell stage embryos. After injection, embryos were incubated in 1X fish water and kept at 28.5°C in an incubator. Morpholino- and/or plasmid- mRNA-injected-embryos were raised to the desired stages for observations or collected for further analysis.

Visualization of cell death with acridine orange

A stock of acridine orange is prepared at 1 mg/ml (100X) in milliQ water and stored at 4°C (light protected). In order to visualize cell death proceed as follows:

- Dilute the stock solution in fish water 1:100;
- Incubate the dechorionated alive embryos (usually at 24 hpf) into the acridine orange solution at 28.5°C for 30 mi in the dark;
- Wash 3 x 10 min with fresh fish water;
- Anesthetize embryos with tricaine;
- Visualize dead cells under a dissecting microscope with a green fluorescent filter.

Cartilage staining with Alcian Blue

Staining solution:

Prepare 100 ml of staining solution, filter the solution before use:

70 % EtOH

1% hydrochloric acid (HCl 37%)

0.1% Alcian blue

- Fix the larvae at 5 dpf with 4% PFA (2 hours at RT or O/N at 4°C);
- Transfer the larvae into 100% MetOH and store them at -20°C until use;
- Rehydrate the larvae in a series of MetOH / PBT;
- Wash the larvae: 3 x 5 min., PBT;
- Incubate the larvae in the Alcian Blue solution, O/N at RT, gently shaking;
- Bleach: H_2O_2 3%, KOH 1% (3 x 5 min. or until the eyes are completely transparent);
- Wash: 2x10 min with PBT; rinse bleach out well.

Mounting and imaging

Labeled embryos are mounted in 100% glycerol. Embryos at early developmental stages are observed in glycerol on depression slides. Whole mount pictures were acquired with a Nikon SMZ 1500 Microscope provided with a digital camera. Embryos starting from 20-somite stage were manually de-yolked using dissection needles and then flat mounted on slides. Slides were provided with small chambers cut into several layers of adhesive tape (1 layer until 24 hpf, 2 layers for 48 hpf and so on); the embryos are then placed, in the desirable position, in glycerol into the chamber and then flattened using a cover slip. Flat mount pictures were acquired with a Leica DMR Microscope. Digitalized pictures are saved as TIFF files, then adjusted for contrast, brightness and color balance using a Photoshop CS2 software.

3.RESULTS

Expression of Jagged1 ligand and Notch receptors in murine thyroid follicular cells.

The Notch pathway is a highly conserved intercellular signaling mechanism relevant for development, differentiation and homeostasis of many organs and systems, but its function has been only partially defined in thyroid (Ferretti et al., 2008).

Rat FRTL5 cells are a widely used model of well-differentiated thyroid cells that require TSH for growth and retain many of the functional properties of thyrocytes. A global gene expression profiling of TSH-stimulation on FRTL5 cells allowed us to identify new signal transduction pathways, transcription factors and effectors that are regulated by TSH (Calebiro et al., 2006). Among these, particular interest was raised by the expression of several elements of the Notch pathway, such as the ligand Jagged1 (Jag1), and their down regulation after TSH stimulation.

As a first step, we confirmed these data by Real-Time PCR on FRTL5 (Fig. 3.1, A-B). The expression of *Jag1* ligand was analyzed in FRTL-5 cells. Under basal conditions, FRTL5 have a detectable level of *Jag1* mRNA. The expression of *Jag1* was significantly down-regulated by TSH at different time points (30 min. and 17 h; One-way ANOVA, $F_{(2,6)}$= 402,9, p< 0,001) (Fig. 3.1, A). Moreover, we confirmed the down-regulation of other genes, important for the activation of the Notch signaling (*Presenilin, DRAL*) upon TSH stimulation (Fig. 3.1, B).

We have been able to verify the expression of *Jagged1* in adult mouse thyroid tissues *ex-vivo* by immunofluorescence (Fig. 3.2, A-B).

We have then analyzed the expression of the Notch receptors (Notch1, Notch 2, Notch3 and Notch4) in parallel sections of mouse thyroid tissues (Fig. 3.2, C-G).

In general, immunofluorescence staining has been performed with anti-Jagged1 or anti-Notch antibodies raised against a segment mapping near the C-terminus

intracellular domain; these antibodies are able to detect both the full-length proteins, present in the plasma membrane, or the cleaved intracellular domain (Jag intracellular domain, JICD, or Notch intracellular domain, NICD), that translocate into the nucleus to promote the expression of downstream target genes.

Immunofluorescence analysis of Jagged1 expression in murine thyroid tissue revealed a positive staining at both plasma membrane and nuclear level (Fig. 3.2, A). The same pattern of expression was observed in case of Notch1 (Fig. 3.2, C). Notch2 and Notch3 are also expressed, but the receptors are detectable only in the follicular plasma membrane (Fig. 3.2, D and E). Notch4 has a more exclusive nuclear localization (Fig. 3.2, F).

We have then performed a double immunofluorescence staining to visualize the combined expression of Jagged1 and the different Notch receptors (Fig. 3.3). In this case we revealed three different situations: Jagged1-Notch1 (Fig. 3.3: A, E and I) are both present in the membranes and into the nuclei of the cells, revealed by the overlapping signals. It is also noteworthy the exclusive Jagged1 expression in the inter-follicular vessels (Fig. 3.3: I and L, arrows); Jagged1 and Notch2/Notch3 have distinct follicular localization, as Notch2 and Notch3 are present at the cell membrane level (Fig 3.3.: B-C; F-G; J-K). Jagged1-Notch4 are both detected into the nuclear compartment but, in some cases, we can visualize neighboring cells expressing either Jagged1 or Notch4 (Fig. 3.3: L, arrowheads).

In summary, these data reveal the expression of some elements of the Notch signaling pathway (Jagged1 ligand and the four Notch receptors) in murine adult thyroid follicular cells. Moreover, the ability of TSH, a fine regulator of thyroid cell proliferation and differentiation, to down-regulate Jagged1 expression, suggests a cross-talk between these pathways in thyroid. This evidence led us to suppose that, in the presence of such a specific differentiative stimulus (TSH), the thyroid cells down regulate Notch signaling. On the other hand, this pathway could be important in maintaining the homeostasis of adult thyroid tissue at

basal level and/or, during development, in early phases of thyroid primordium development, a period of time known to be independent from TSH action.

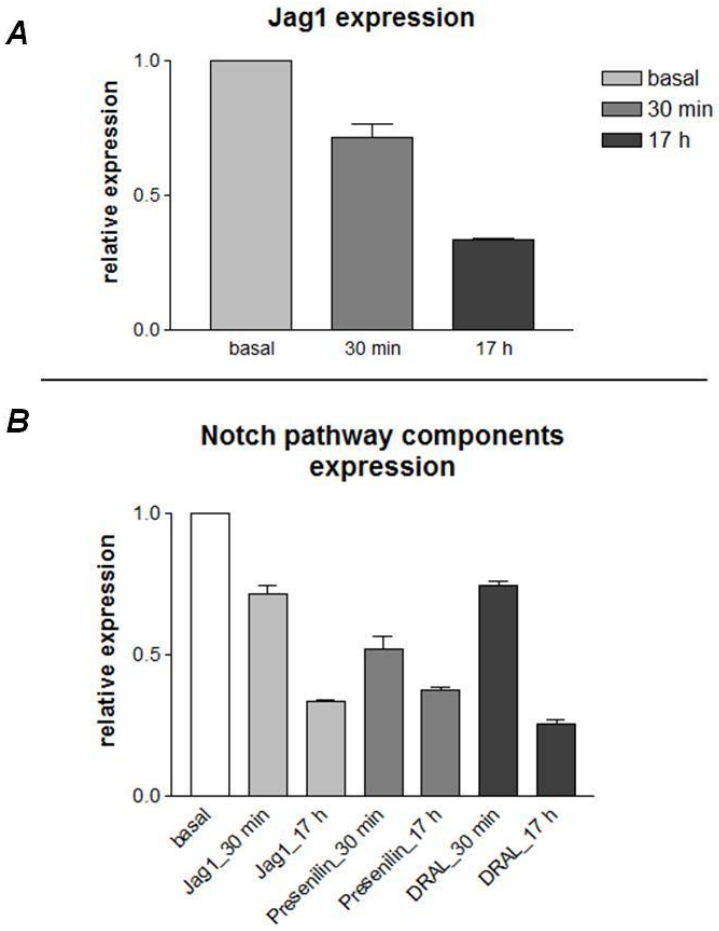

Figure 3.1: Expression of components of the Notch signaling pathway in FRTL5. Validation by real-time PCR. (A) The modulation of the expression level of Jag1 gene was evaluated by real-time PCR after stimulation with bTSH (0.1 U/L) at 30 min. and 17h. mRNA levels are expressed relative to basal condition (time 0); values are expressed as mean ± SEM. (B) The Notch pathway components Jag1, Presenilin, and DRAL are downregulated by bTSH in a time-dependent manner; (Presenilin and DRAL are important elements for Notch receptors cleavage and activation). mRNA levels are expressed relative to basal condition (time 0); values are expressed as mean ± SEM.

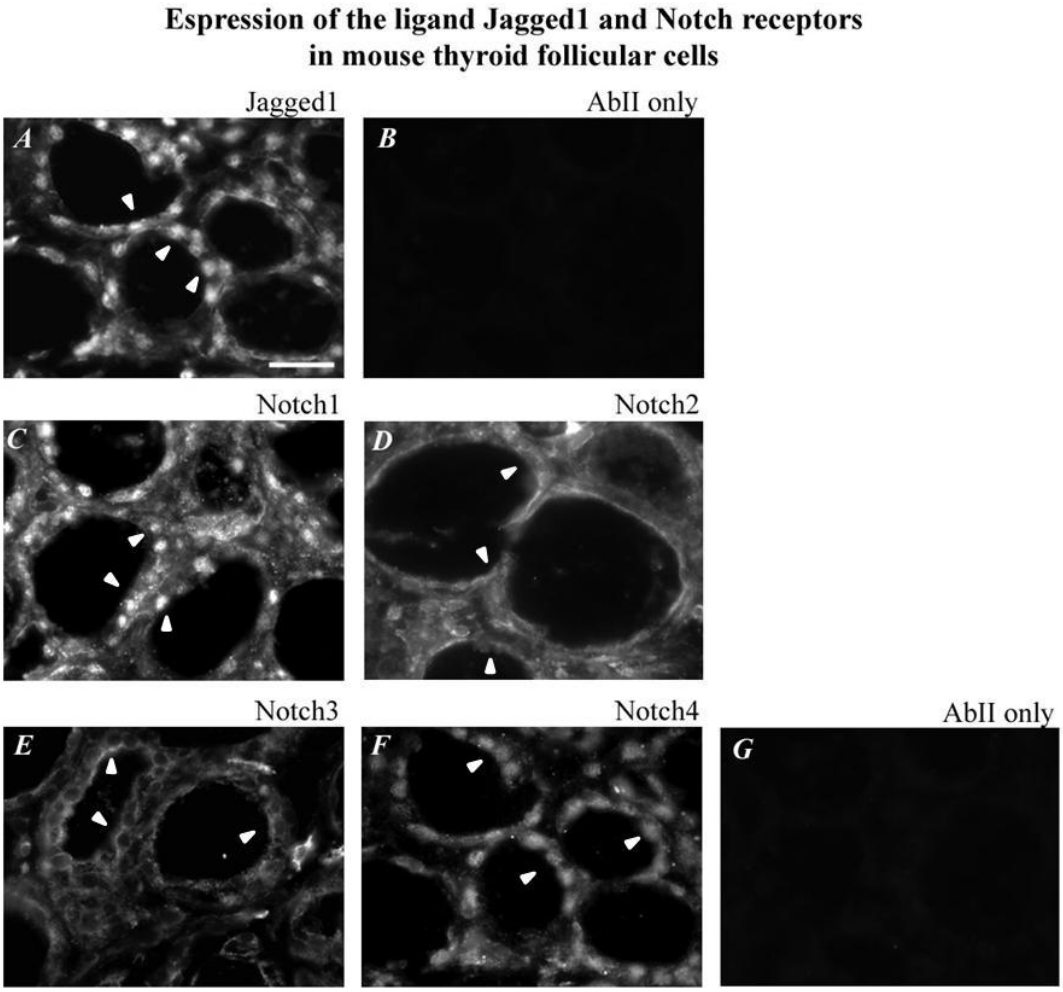

Figure 3.2: Expression of Jagged1, Notch1, Notch2, Notch3 and Notch4 proteins in normal murine thyroid tissues.

Immunofluorescence staining for Jagged1 (A), Notch1, Notch2, Notch3 and Notch4 (C-F) in age-matched tissue samples collected from 3 month-old mice. A nuclear positive signal is detectable for Jagged1, Notch1 and Notch4; Notch2 and Notch3 exhibit a membrane localization. Arrowheads indicate positive staining. (B, G): negative control (AbII only). Scale bar: 100 µm.

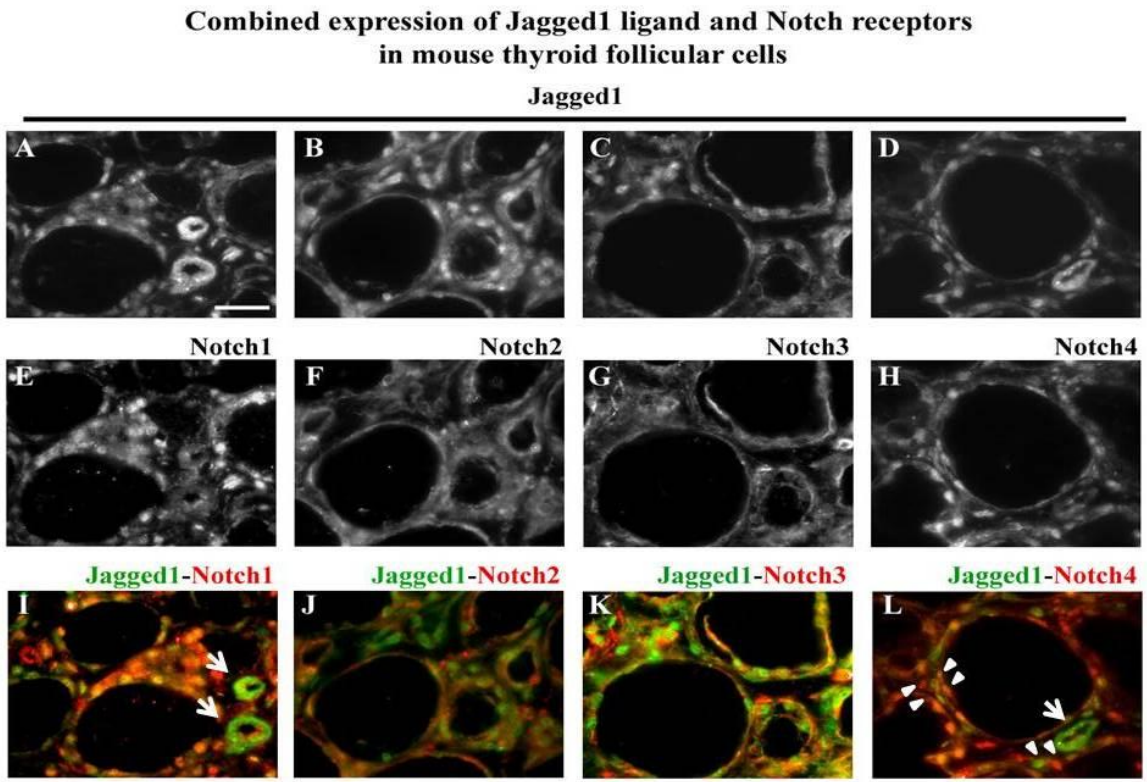

Figure 3.3: Combined expression of Jagged1 ligand and Notch1, Notch2, Notch3 and Notch4 receptors in thyroid follicular cells.

(A-D) Jagged1 positive staining at the membranes and nuclei of thyroid follicular cells; (E-H) Notch1, Notch2, Notch3 and Notch4 expression in thyroid follicular cells. (I) Jagged1 expression co-localizes with Notch1 in the follicular cell nuclei; arrows: Jagged1 positive thyroid follicular vessels. (J-K) Jagged1 nuclear expression and Notch2/Notch3 membrane expression. (L) Jagged1-Notch4 co-expression reveals not only some nuclei with overlapping signals, but also neighboring cells expressing either Jagged1 or Notch4 (arrowheads). Arrows: thyroid follicular vessels. Scale bar: 100 μm.

Zebrafish thyroid gland origin and differentiation

To define the role of the ligand Jagged1 and, more in general, of Notch signaling pathway during thyroid development, we took advantage of zebrafish, a powerful animal model for developmental biology studies. In zebrafish, the orthologs of *Jagged1* and *Notch* genes have been functionally characterized, confirming the evolutionary conserved role of Notch signaling in vertebrate organ development.

Despite the lack of a compact thyroid gland, the zebrafish thyroid tissue originates from the pharyngeal endoderm and the main genes involved in its patterning and early development are conserved between zebrafish and mammals (Alt et al., 2006b; Wendl et al., 2002).

Developmental expression pattern of thyroid-related transcription factors (e.g.: *nkx2.1a* and *pax2a*) and differentiative markers (e.g.: *tg* and *slc5a5*) has been well characterized in zebrafish (Alt et al., 2006b; Wendl et al., 2002). On the basis of published data, we amplified part of *nkx2.1a*, *pax2a*, *tg* and *slc5a5* coding sequences and cloned them into appropriate expression vectors to produce antisense probes and visualize, by whole mount *in situ* hybridization (WISH), zebrafish thyroid development and differentiation.

The starting point of this study aimed to confirm the thyroid expression of these genes and analyze their temporal expression (Fig. 3.4 and Fig. 3.5). Our analysis showed that, in zebrafish, thyroid specification occurs at 24 hpf, with the combined onset of *nkx2.1a* and *pax2a* expression in the pharyngeal endoderm (Fig. 3.4, A-B). Thyroid differentiation occurs early during development, as *tg* expression is observed even before the thyroid primordium has evaginated from the pharyngeal epithelium (Fig. 3.4, C). In zebrafish, *tg* expression is first observed exclusively in the thyroid primordium, at approximately 36 hpf (Fig. 3.4, C), with *slc5a5* expression initiating later, at around 48 hpf (Fig. 3.4:, D).

A time course analysis of *nkx2.1a* and *pax2a* expression revealed that these transcription factors appear at 24 hpf in thyroid primordium and their expression

is detectable until 72-96 hpf (Fig. 3.5, A-H). *nkx2.1a* and *pax2a* are undetectable by 120 hpf (Fig. 3.5, D and H), indicating that their expression strongly decreases after early thyroid specification and differentiation. We suppose that these transcription factors, known to be essential not only for thyroid development, but also in the maintenance of the follicular cells, could be still expressed, but their levels decrease and become undetectable by WISH during late thyroid development.

tg and *slc5a5* maintain detectable high levels of expression from their onset to the following stages of thyroid development (Fig. 3.5, I-N).

The thyroid hormone (T4) can be detected in the thyroid follicles of wild-type zebrafish larvae from 72 hpf, when the first thyroid follicle has differentiated. In this study we used an antibody against thyroid hormone (T4) in order to monitor the thyroid gland functionality in developing zebrafish larvae (Elsalini and Rohr, 2003; Wendl et al., 2002). In whole mounts of wild-type larvae, a growing number of thyroid follicles is detectable at 120 hpf in the pharyngeal area, dispersed along the ventral aorta (Fig. 3.5, O).

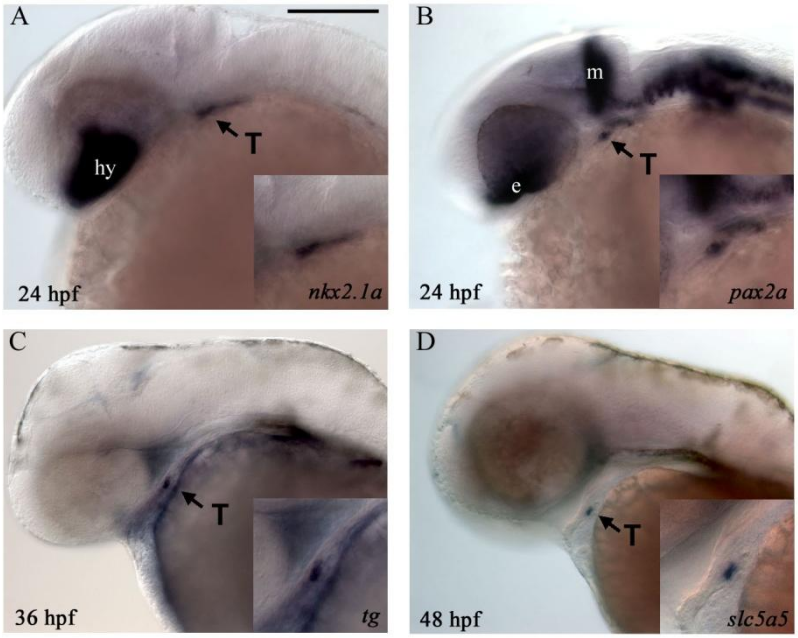

Figure 3.4: Expression of zebrafish thyroid markers. Examples of thyroid-related genes expressed in zebrafish. (A-B) *In situ* hybridization with antisense probes specific for *nkx2.1a* (A) and *pax2a* (B) in 24 hpf zebrafish embryos. (C) *In situ* hybridization for *tg* in a 36 hpf embryo. (D) *In situ* hybridization for *slc5a5* in a 48 hpf embryo. All images are lateral views, with anterior to the left. Bottom-right inserts display enlargements of the thyroid region. Abbreviations: T, thyroid; e, eye; mhb, midbrain–hindbrain boundary; hy, hypothalamus. Stage: bottom left. Scale bar: 100 µm.

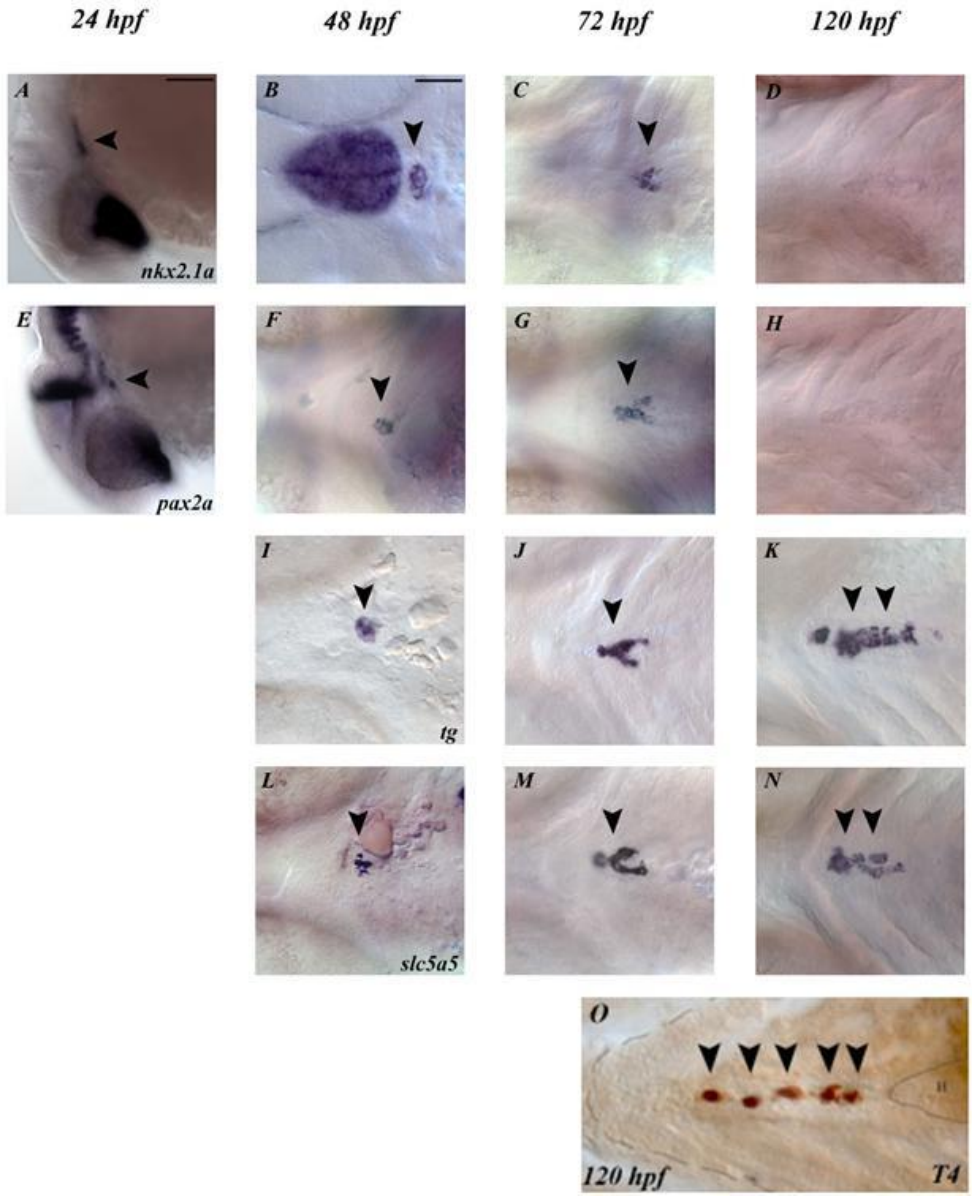

Figure 3.5: Developmental expression of thyroid early and differentiative markers. (A-H) *nkx2.1a* and *pax2a* start to be expressed in the zebrafish thyroid primordium at 24 hpf and their expression is detectable until 72 hpf (arrowheads); (I-N) *tg* and *slc5a5* are expressed from 48 hpf, in a compact globular group of cells. This primordium then elongates along the midline (J-K, M-N) following the development of the ventral aorta. (O) T4 antibody labels the thyroid hormone in the follicles (brown staining) of a zebrafish larva (A and E) lateral view, anterior to the left; (B-D and F-O) ventral views, always anterior to the left. The stages are shown in the upper part of the panel, the probe/staining bottom right. Abbreviations: h, heart. Arrowheads: thyroid cells expressing early and differentiative markers or T4. Scale bar: 100 µm.

Thyroid differentiation is controlled by Notch signaling

To test whether Notch signaling plays a role in zebrafish thyroid primordium formation, we over activated and blocked Notch signaling and analyzed expression of thyroid marker genes by mRNA *in situ* hybridization.

Notch gain of function and thyroid development

To produce a Notch gain of function situation we took advantage of transgenic embryos containing a heat shock-inducible hsp70:Gal4 transgene, in combination with a Gal4-responsive UAS:Notch1a-intracellular-domain (NICD) allele (Scheer and Campos-Ortega, 1999). Embryos were heat shocked at 20 hpf, slightly before thyroid cell specification, and maintained until 24, 48 or 65 hpf at 28.5 °C, fixed, and hybridized with RNA antisense probes for *nkx2.1a* and *tg*. When the fixation was planned later than 12 h after the heat shock, more intermediate heat shocks were performed at intervals of 12 h in order to guarantee a continuous expression of NICD transgene. The induction of NICD expression at 20 hpf is sufficient to abolish the expression of *nkx2.1a* in the thyroid primordium, analyzed at different time points (24 hpf, 48 hpf and 65 hpf) (Fig. 3.6); the hypothalamic expression of *nkx2.1a* was only slightly reduced. Moreover, the number of cells expressing *tg* was lost or strongly reduced at 48 and 65 hpf (Fig. 3.7). Due to the high mortality of embryos repeatedly heat shocked to maintain an overexpression of NICD, it was not possible to conduct analysis after 65 hpf. After *in situ* hybridization, we flat mounted the embryos and counted the number of cells expressing *tg*. The difference between the number of wt and NICD *tg* expressing cells was calculated by dividing the area of positive staining by the average area of a single cell. The number of *tg* expressing cells is significantly different between wt and NICD expressing embryos both at 48 (WT: 45,2 ±2,6; NICD: 8 ± 2,4; $P<0,001$ by Student's t-test) and 65 hpf (WT: 64,45 ± 4,3; NICD: 7,8 ± 1,3; $P< 0,001$, by Student's t-test) (Fig 3.7, B-C).

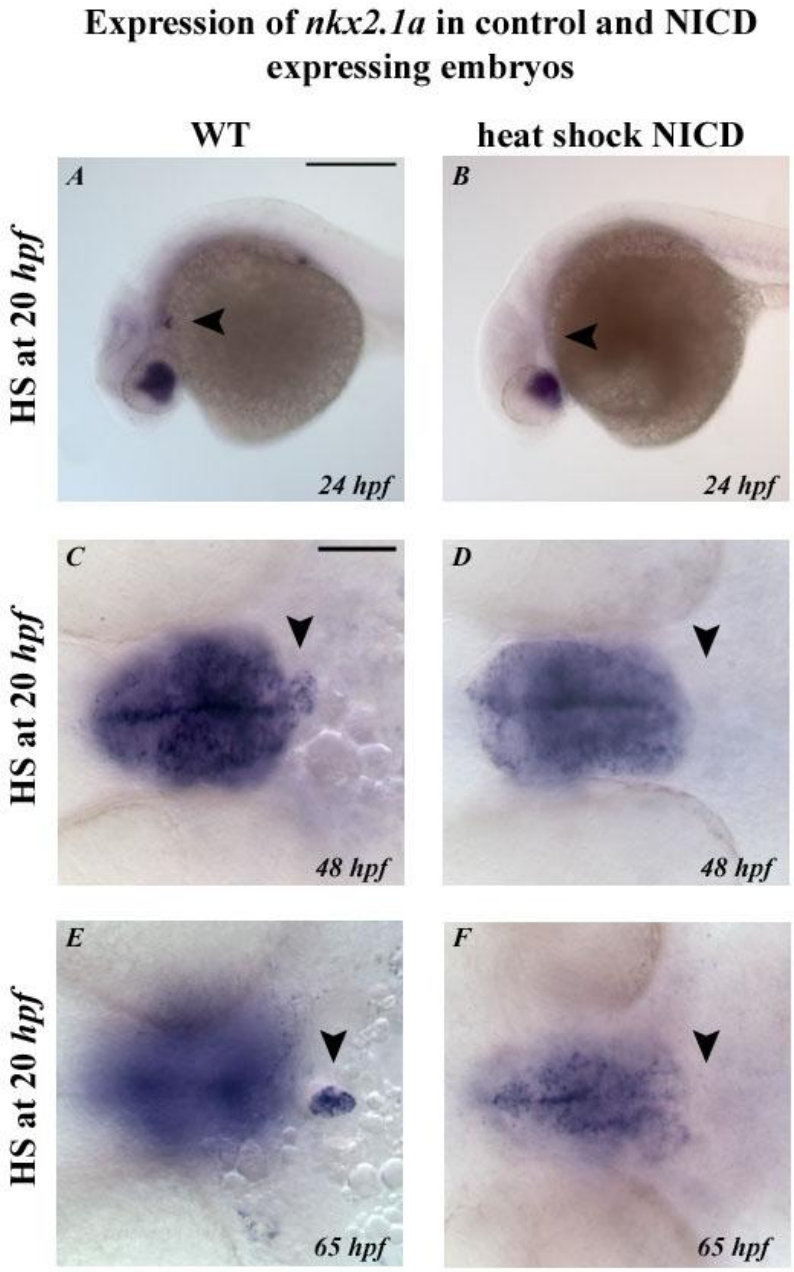

Figure 3.6: Expression of *nkx2.1a* in NICD over-expressing embryos. Whole mount *in situ* hybridization showing *nkx2.1a* expression. (A-C-E) Wild-type control embryos reveal normal distribution of *nkx2.1a* cells at 24, 48 and 65 hpf; *nkx2.1a* is detectable in the hypothalamus and thyroid cells (arrowheads). (B-D-F) transgenic embryos, in which NICD was induced at 20 hpf, lost *nkx2.1a* expression in the thyroid region at 24, 48 and 65 hpf (arrowheads). *nkx2.1a* is only reduced in the hypothalamus. Individual embryos were genotyped by PCR for presence or absence of each transgene. (A-B) Lateral views; (C-F) ventral views, anterior to the left. The stage is indicated bottom right. Scale bar A-B: 250 µm; C-F 100 µm.

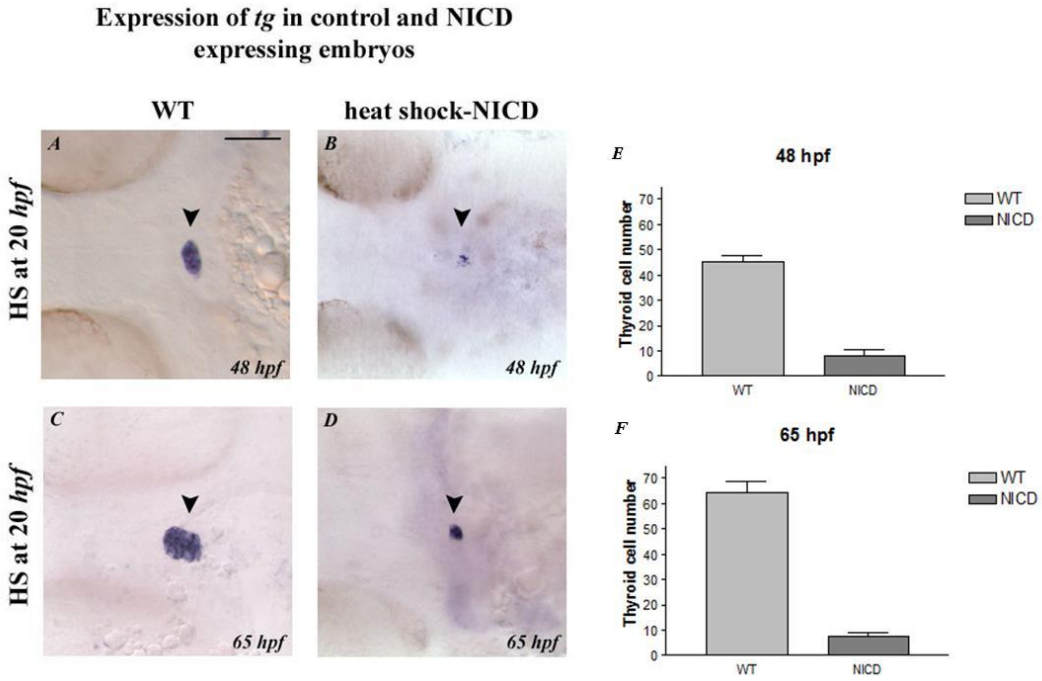

Figure 3.7: Expression of *tg* in NICD over-expressing embryos. (A-C) Wild-type control embryos reveal the normal distribution of *tg* expressing cells (tg^+) at 48 and 65 hpf; *tg* is exclusively expressed by thyroid differentiating cells (arrowheads). (B-D) transgenic embryos, in which NICD was induced at 20 hpf, display a severe reduction in *tg* expression at 48 and 65 hpf (arrowheads). Individual embryos were genotyped by PCR for presence or absence of each transgene. Ventral views, anterior to the left. The stage is indicated botton right. Scale bar: 100 µm. (E) quantification of tg^+ cells, at 48 hpf, in the wild-type (WT) and NICD group of embryos. Bars indicate the average number of tg^+ cells per embryo. Data were obtained from 15 WT and 15 NICD embryos at 48 hpf: WT embryos have an average number of 45.24 ± 2.5 *tg* positive cells; NICD embryos have an average number of 8.029 ± 2.4 tg positive cells; the two groups significantly differ in the average number of cells expressing *tg:* 37.21 ± 3.5; t test, t(26)= 10,4 P<0,0001. (F) Quantification of *tg* expressing cells at 65 hpf in the WT and NICD group of embryos. Bars indicate the average number of tg^+ cells per embryo. Data were obtained from 10 WT and 10 NICD embryos at 65 hpf: WT embryos have an average number of 64.45 ± 4.3 *tg* positive cells; NICD embryos have an average number of 7.860 ± 1.3 *tg* positive cells; the two groups significantly differ in the number of cells expressing *tg*: 56.59 ± 4.5, t test, t(18)= 12,4, P<0,0001.

Notch loss of function and thyroid development

To further investigate the role of Notch signaling in thyroid cell differentiation, we analyzed *tg* expression in 48 and 72 hpf zebrafish *mib* mutants (Fig. 3.8, E-F), DAPT-treated (Fig. 3.8, G-H), and wild-type sibling embryos (Fig. 3.8, A-D). *mib* mutants lack an ubiquitin ligase essential for the activation of Notch signaling after ligand-receptor binding, resulting in the failure to release NICD (Itoh et al., 2003). DAPT treatment prevents the release of NICD by inhibiting the gamma-secretase activation. DAPT phenocopies some aspects of the *mib* phenotype such as fused somites, increased neurogenesis and lack of pigmentation (Geling et al., 2002). Embryos have been treated continuously with 100 µM DAPT from 20 hpf and analyzed, by *in situ* hybridization, at 48 and 72 hpf; control embryos of the same clutch were treated with DMSO only.

By *in situ* hybridization we found that *mib* mutants displayed an excess of thyroglobulin expressing cells along with a disorganized shape of the compact globular primordium when compared with the sibling (*sib*) counterpart (Fig. 3.8, A-B; E-F). The increased number of thyroglobulin expressing cells is evident at both 48 and 72 hpf (Fig. 3.8, A-B; E-F). DAPT treated embryos had a similar expansion of thyroglobulin expression domain (Fig. 3.8, C-D; G-H), overlapping the thyroid phenotype of *mib* mutants. In *mib* and DAPT treated embryos thyroid tissue is not limited to the midline and often expands laterally in an irregular fashion. We analyzed the number of thyroglobulin producing cells in *mib* mutants and compared these data with the number of thyroglobulin positive cells in the sibling embryos; we used the same approach employed to evaluate the reduction of *tg* expressing cells in embryos over-expressing NICD. After *in situ* hybridization, we flat mounted the embryos and computationally estimated the number of cells expressing thyroglobulin. The number of *tg* expressing cells is significantly different between *sib* and *mib* embryos both at 48 (*sib*: 55.64 ± 4.5; *mib*: 77.13 ± 8.2; P<0,05, by Student's t-test) and at 72 hpf (*sib*: 77.50 ± 4.2; *mib*: 114.5 ± 11.6; P< 0,05, by Student's t-test) (Fig. 3.8, I-J).

Moreover we observed a parallel increased expression of *nkx2.1a* and *slc5a5* in *mib* mutants at 72 hpf, thus indicating that thyroid precursor cells maintain a

correct identity although a global morphological disorganization of the primordium (Fig. 3.9).

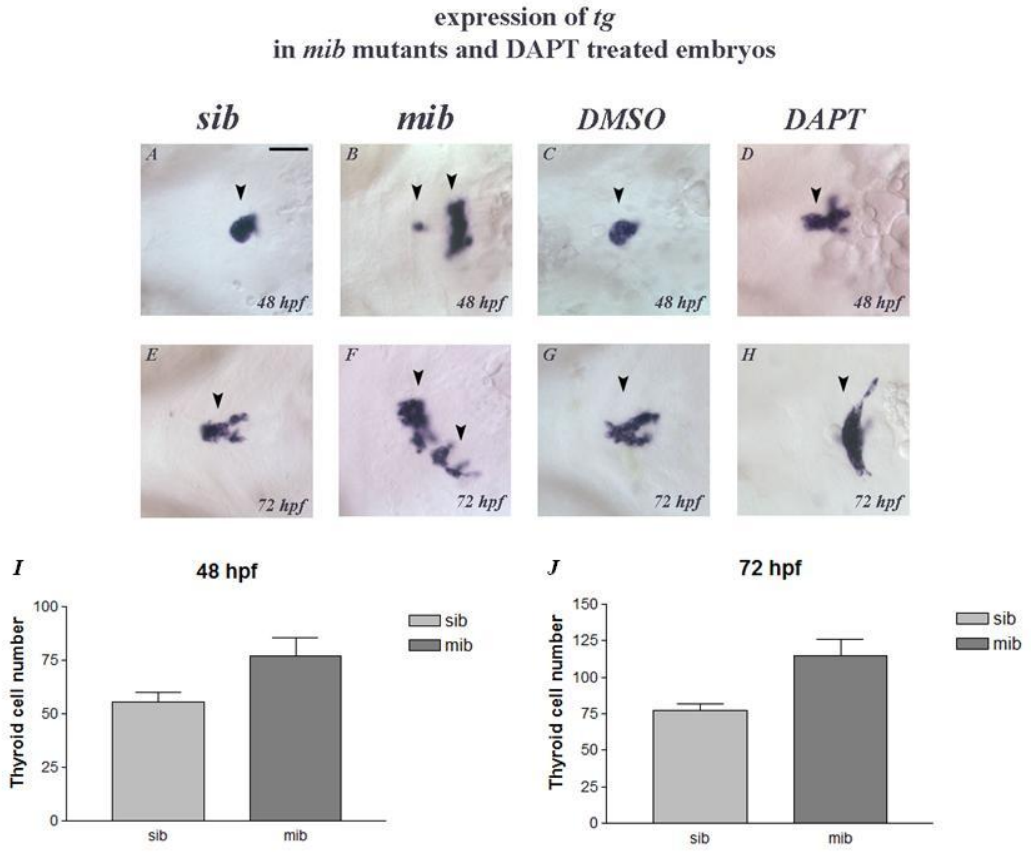

Figure 3.8: Expression of *tg* in *mib* mutants and DAPT treated embryos. Inhibition of Notch signaling increases differentiation of tg^+ cells. *In situ* hybridizations showing *tg* expression in *mib* mutants (B, F) and DAPT-treated embryos (D, H) at 48 and 72 hpf. (B, F) *tg* expression is strongly increased in *mib* mutants, with an overall disorganized primordium and the presence of ectopic cells compared to the controls (A, E). (D, H) DAPT treatment affects thyroid differentiation in the same way as in *mib* embryos, when compared to the controls (C, G). Arrowheads: *tg* expressing cells. Embryos are presented in a ventral view with anterior to the left. The stage is indicated bottom right. Scale bar: 100 µm. (I) Quantification of tg^+ cells at 48 hpf in sibling embryos (*sib*) and *mib* mutants. Bars indicate the average number of tg^+ cells per embryo. Data were obtained from 10 sib and 10 *mib* embryos. Sib embryos have an average number of 55.64 ± 4.5 *tg* positive cells; *mib* embryos have an average number of 77.13 ± 8.2 *tg* positive cells; the two groups significantly differ in the number of cell expressing *tg*: -21.49 ± 9.4 (Student's *t* test, t(18)= 2,28; P<0,035); (J) quantification of *tg* expressing cells at 65 hpf in sib and *mib* mutants. Bars

indicate the average number of *tg*$^{+}$ cells per embryo. Data were obtained from 10 sibs and 6 *mib* embryos at 72 hpf: sib embryos have an average number of 77.50 ± 4.2 *tg* positive cells; *mib* embryos have an average number of 114.5 ±11.6 *tg* positive cells; the two groups significantly differ in the number of cells expressing *tg*: -37.02 ± 10.35 (Student's t test, t(14)= 3,57; P<0,003).

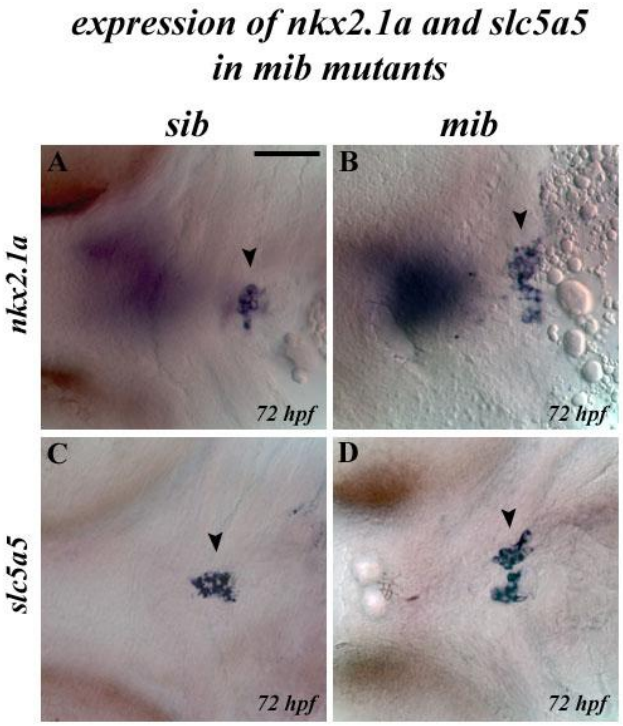

Figure 3.9: Expression of *nkx2.1a* and *slc5a5* in *mib* mutants. Loss of functional Notch signaling in *mib* mutants lead to expansion of *nkx2.1a* and *slc5a5* positive cells. (A-B) Expression domain of *nkx2.1a* in sib and *mib* embryos, the latter showing and increased number of *nkx2.1a* expressing cells, and a planar expanded thyroid primordium (arrowheads). (C-D) Expression of *slc5a5* in sib and *mib* embryos; *mib* mutants have an increased number of cells expressing *slc5a5*, not well organized along the antero-posterior axis (arrowheads). Ventral views, anterior to the left; all embryos at 72 hpf (bottom right); Scale bar: 100 µm.

The thyroid follicular cells develop in close association with the outflow tract, the ventral aorta and the first pair of branchial arteries, which physically contact the thyroid and maintain the primordium at the midline (Alt et al., 2006a). It is well known that perturbed pharyngeal vessel architecture leads to thyroid defects in zebrafish, affecting the anteroposterior elongation of the thyroid primordium (Alt et al., 2006a). The presence of ectopic thyroid tissue expanded laterally in irregular fashion prompted us to investigate the relationship between the thyroid and the pharyngeal vessels in *mib*. In zebrafish, *Kdrl* (previously known as *Flk1*) is an endothelial specific Vegf receptor, required for vasculogenesis (Covassin et al., 2006; Habeck et al., 2002). By double whole mount *in situ* hybridization, using this endothelial marker, we were able to visualize the thyroid primordium and the adjacent pharyngeal vessels at 48 and 72 hpf (Fig. 3.10). At 48 hpf the thyroid primordium starts to develop from a correct midline position between the first pair of branchial arteries in both sib and *mib* embryos (Fig 3.10, A-B). Subsequently, in *mib* mutants, the thyroid fails to elongate from this position along the AP axis. In sib embryos, the thyroid is correctly surrounded by the hypobranchial artery (HA), the mandibular arch arteries (AA1) and the opercular artery (ORA) (Fig 3.10, C). In *mib* mutants the thyroid tissue loses the correct contacts with the pharyngeal vessel architecture and the *tg* positive cells constitute a not well organized and irregular group (Fig 3.10, D).

These experiments lead us to the conclusion that perturbing Notch signaling has significant impact on thyroid development. An excess of Notch signaling is sufficient to prevent the correct thyroid primordium specification, while Notch inhibition allows extra cells adopting a thyroid cell fate. Given that the pharyngeal vascular structure is seriously affected by these treatments, the observed thyroid phenotypes could result from both cell-autonomous and non cell-autonomous activities of Notch signaling. In order to define if Notch signaling plays a direct role in thyroid early development, we tested the co-expression of thyroid markers with Jagged1 Notch ligand at various stages of zebrafish development.

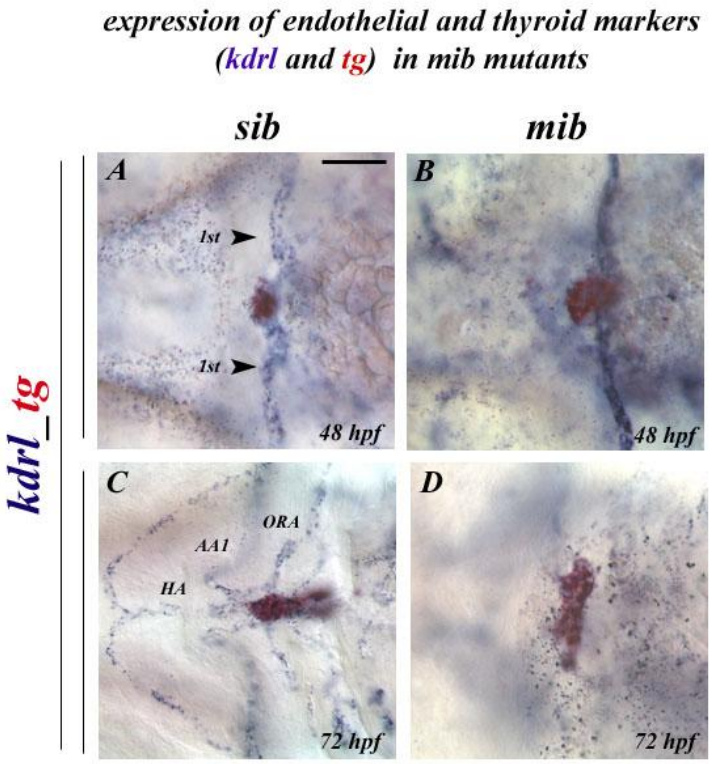

Figure 3.10: Expression of endothelial and thyroid markers in *mib* mutants. A double whole mount *in situ* hybridization allows the visualization of the thyroglobulin expressing cells (red) and the endothelial marker *kdrl* (blue). (A-B) the thyroid primordium originates at the midline, surrounded by the first pair of branchial arteries (arrowheads) both in sib and *mib* mutants at 48 hpf. The endothelial marker *kdrl* is expressed in pharyngeal vessels around the thyroid (arrowheads). (C-D) at 72 hpf the primordium elongates along the AP axis in sib embryos, but loses the contacts with the surrounding pharyngeal vessels in *mib* mutants; this causes the planar expansion of the thyroglobulin expressing cells. Ventral views, anterior to the left; stage: bottom right; abbreviations: 1st: first pair of branchial arteries; HA: hypobranchial artery; AA1: mandibular arch artery; ORA: opercular artery. Scale bar: 100 µm.

Two zebrafish *jagged1* homologues are expressed in the developing thyroid.

Two homologues of *Jagged1* (*jag1a* and *jag1b*) have been identified in zebrafish (Zecchin et al., 2005). To explore the function of Jag1 activity *in vivo*, we next examined the expression of *jag1a* and *jag1b* genes in zebrafish embryos. These genes are expressed from somitogenesis and dynamically regulated in a spatio-temporally specific manner. We found that *jag1a* and *jag1b* were expressed in the thyroid in similar, but not identical patterns (Fig. 3.11 and Fig. 3.12).

jag1a is not expressed in the pharyngeal endoderm expressing *nkx2.1a* at 24 hpf (Fig. 3.11, A, D). By double whole mount *in situ* hybridization we were then able to analyze the expression of *tg* and *jag1a* at 48 and 72 hpf. *jag1a* staining is not overlapping the *tg* expressing cells at 48 hpf (Fig. 3.11, B, E). At 48 hpf *jag1a* expression is detectable in the hyoid arch cartilage, a structure adjacent to the thyroid cells. By 72 hpf *jag1a* expression appeared in the most anterior domain of thyroid primordium, co-localizing with the cells that constitute the first active and differentiated thyroid follicle (Fig. 3.11, C, F).

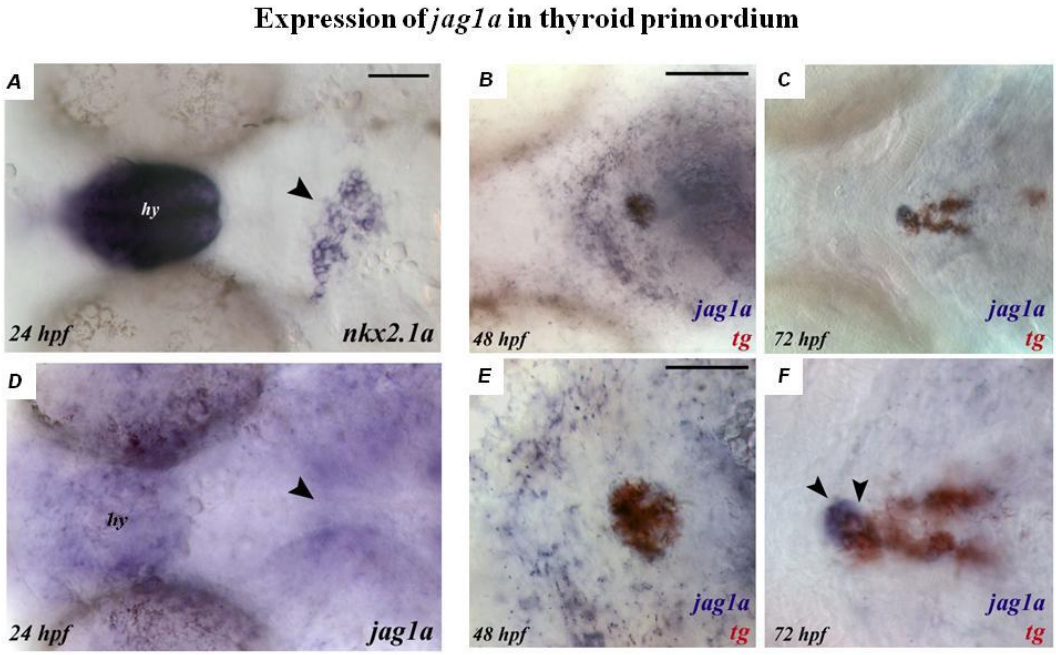

Figure 3.11: Expression of *jag1a* in thyroid primordium. (A) Thyroid precursor cells expressing *nkx2.1a* constitute part of the pharyngeal endoderm epithelium at 24 hpf (arrowhead); the hypothalamus (hy) is positive for *nkx2.1a* expression; (D) the pharyngeal floor is negative for the expression of *jag1a* (arrowhead) at 24 hpf. (B-C, E-F) double whole mount *in situ* hybridization showing *tg* positive cells, labeled in red color, and *jag1a* positive cells, labeled in blue. (B, E) minor and major magnification; the *tg* positive cells don't express *jag1a,* that is detectable in the hyoid cartilage region, anterior to the thyroid at 48 hpf; (C, F) minor and major magnification, the thyroid primordium co-expresses *tg* and *jag1a* in a group of cells of the most anterior part (arrowheads) at 72 hpf. Ventral views, anterior to the left; stage bottom left; abbreviations: hy, hypothalamus. Scale bar: A-D: 50 µm; E-F: 20 µm.

We have then analyzed *jag1b* expression pattern between 24 and 72 hpf. We have found that *jag1b* is expressed in a "salt and pepper" manner, a characteristic pattern of Notch signaling activity, in the portion of the pharyngeal endoderm comparable to that expressing *nkx2.1a* at 24 hpf (Fig 3.12, A, D). Moreover, at 48 hpf and 72 hpf, *tg* positive cells co-express *jag1b (*Fig. 3.12 B-C; E-F).

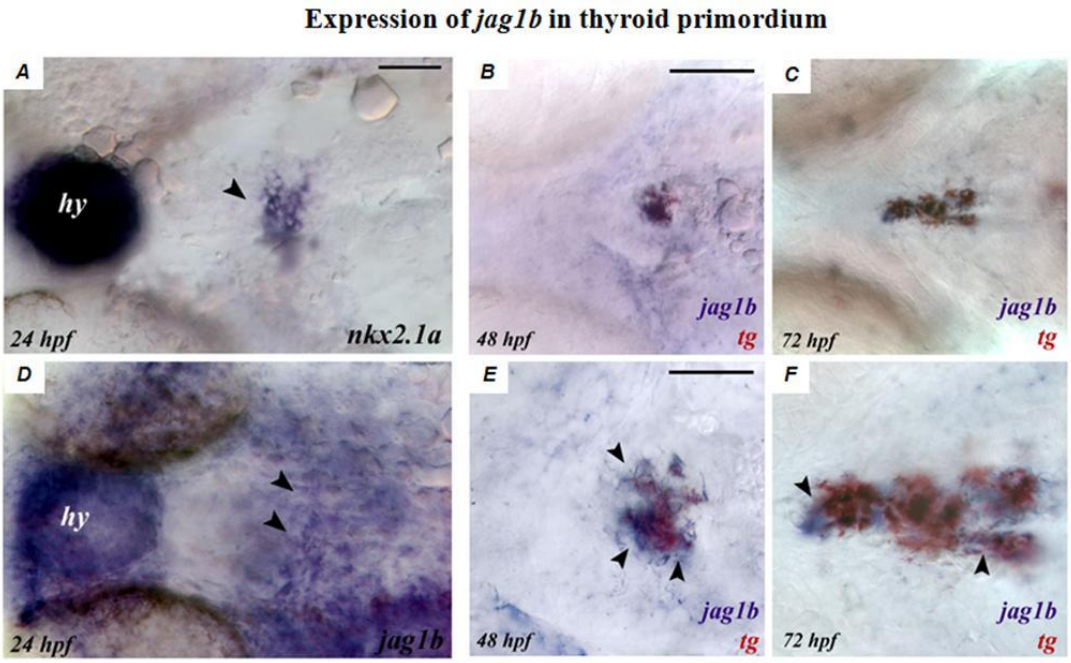

Figure 3.12: Expression of *jag1b* in thyroid primordium. (A): *nkx2.1a* expression in the pharyngeal endoderm of an embryo at 24 hpf. The thyroid primordium is indicated with a black arrowhead; (D): expression of *jag1b* reveals a characteristic "salt and pepper" pattern in the pharyngeal endoderm of an embryo at 24 hpf (arrowheads); (B-C, E-F): double whole mount *in situ* hybridization reveals the expression of *tg* (red) and *jag1b* (blue) in the thyroid primordium at 48 and 72 hpf. The co-localization signals are indicated with black arrowheads. Stages: bottom left. Abbreviations: "hy" indicates the hypothalamus; embryos are in ventral views with anterior to the left. Scale bar: A-D: 50 µm; E-F: 20 µm.

Jag1-Notch signaling defects cause impaired thyroid function

Loss of function experiments with jag1a and jag1b morpholino antisense oligos

To define the function of *jag1a* and *jag1b* during thyroid development, we used antisense morpholino oligos (MOs) to knock down Jag1a and Jag1b protein levels.

jag1a and *jag1b* MOs were designed to target, respectively, the splice donor sites of the second and third exon-intron boundary (splMOs, see diagrams in Fig. 3.13, A and C). The injection of either *jag1a* or *jag1b* splMOs caused a strong reduction in the wild-type transcript and the production of short transcript forms (see Fig. 3.13, B, D); DNA sequencing of these transcripts revealed that these splice-blocking MOs activated cryptic splice donor sites and potentially produced premature truncated Jag1a and Jag1b proteins. We also used a second *jag1a* morpholino (*jag1a* atgMO) to block the translation of *jag1a*. *jag1a* atgMO was already published (Lorent et al., 2004) and, in our experimental conditions, produces a similar phenotype to that obtained with the morpholino targeting the splice donor site.

Moreover, we analyzed the thyroid function in a *jag1b* mutant line: *jag1b*^{b1105}. This mutation converts tryptophan 223 to a premature stop codon, truncating the Jag1b protein within the extracellular DSL domain required for Notch binding and probably resulting in the production of a short soluble N-terminus peptide (Zuniga et al., 2010).

Figure 3.13: Morpholino-mediated knockdown of the *jag1* genes in zebrafish.

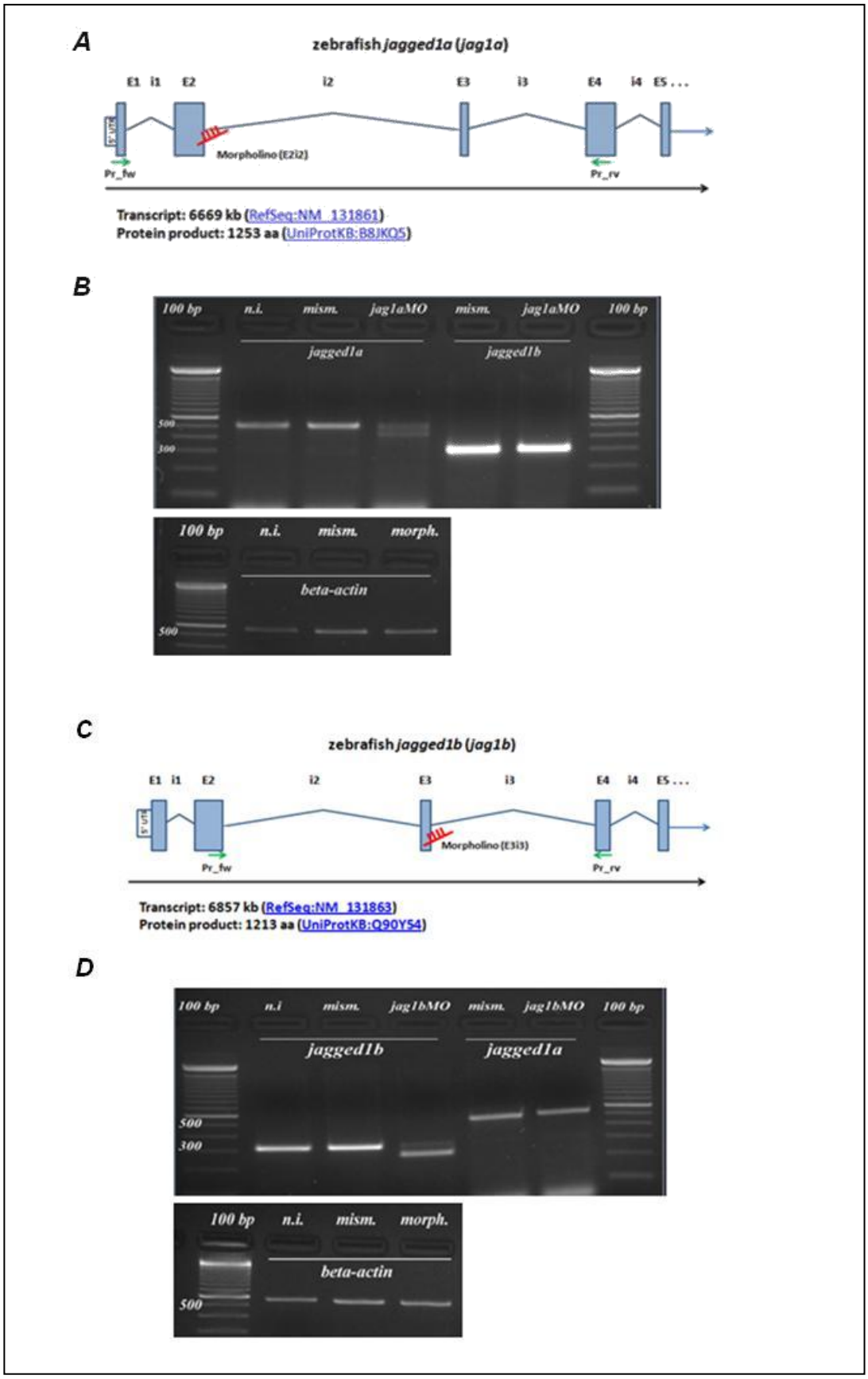

Figure 3.13: Morpholino-mediated knockdown of the *jag1* genes in zebrafish. (A**)** *jag1a* gene structure: the squared boxes correspond to the exons, the blue lines correspond to the introns. *jag1a* splMO (*jag1aMO*) is targeted to the splice donor site between exon 2 and intron 2 (E2i2). The position of the primers used to analyze the altered splicing is indicated in green. (B) RT-PCR analysis of *jag1* genes expression in *jag1a*MO: *jag1aMO* alters the E2i2 splicing donor sites. Not injected and mismatch injected embryos (mism.) produced 500 bp PCR products; *jag1aMO*-injected embryos display a reduction of the wt form and the presence of shorter product; sequence analysis of the shorter products reveals that the altered splicing forms of mRNA potentially produce premature truncated proteins. The expression of the homologous gene, *jag1b,* is unaffected in *jag1aMO*-injected embryos. *β-actin* was used as a reference gene. (C) *jag1b* gene structure, the squared boxes correspond to the exons, the blue lines correspond to the introns. *jag1b* splMO (*jag1bMO*) is targeted to the splice donor site between exon 3 and intron 3 (E3i3). The position of the primers used to analyze the altered splicing is indicated in green. (D) RT-PCR analysis of *jag1* genes expression in *jag1b*MO: *jag1bMO* alters the E3i3 splicing donor sites. Not injected and mismatch injected embryos (mism.) produced a 320 bp PCR produc*; jag1bMO*- injected embryos display a reduction of the wt form and the presence of shorter products; sequence analysis of the shorter products reveals a complete E3 skip; the shorter mRNA potentially produce premature truncated proteins. The expression of the homologous gene *jag1a* is unaffected in *jag1bMO*-injected embryos. *β-actin* was used as a reference gene.

Evaluation of the phenotype in jag1bMO-injected embryos

Considering the expression of *jag1b* in the early phase of thyroid primordium development, and the subsequent co-localization with *tg* expressing cells, we first analyzed into details the thyroid phenotype in *jag1bMO* embryos. For the initial phenotypic characterization of *jag1b*MO embryos, 3,2 ng of *jag1b*MO was injected into 1-cell stage zebrafish embryos. The embryos were then examined throughout early development (from 24 hpf to 120 hpf) in comparison to age-matched controls (morpholino mismatch injected embryos, mmMO).

All *jag1bMO*-injected embryos display small head and eyes, a feature visible from 24 hpf on, thin midbrain-hindbrain boundary, mild craniofacial abnormalities, and, in 40% of the cases, cardiac edema. At 120 hpf, *jag1bMO* larvae fail to inflate the swim bladder.

jag1bMO embryos were then classified into three graded phenotype classes (Class 1, Class 2 and Class 3), depending on the severity of defects in the body length and curvature (Fig. 3.14). Class 1: displays mildly affected phenotypes: moderately shortened body and slightly curved tail. Class 2: displays intermediate affected phenotypes: shortened body and notochord abnormalities. Class 3: displays severely affected phenotypes: shortened body, notochord defects and twisted or truncated tail.

We performed three independent experiments of *jag1bMO*-injection and we distributed *jag1bMO*-injected embryos in the three classes with the following frequency: Class 1: 13%; Class 2: 63%; Class 3: 15% (*jag1bMO*-injected embryos n= 180). The remaining embryos (9%) were similar to the mismatch counterpart.

Altogether, *jag1bMO* embryos belonging to the three classes exhibit craniofacial defects, clearly evident from 48 hpf.

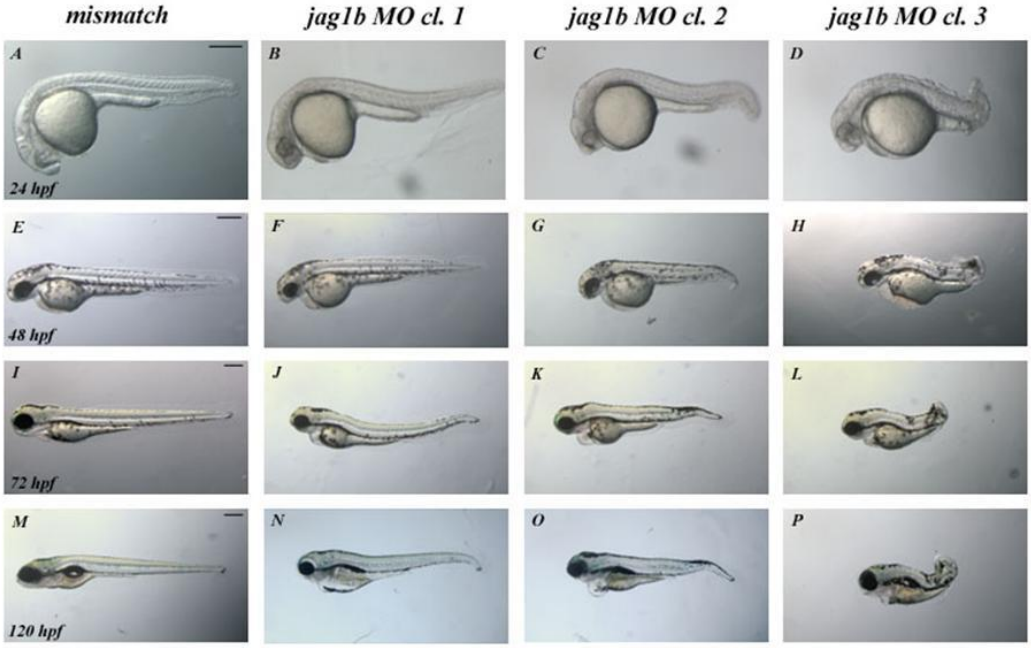

Figure 3.14: Morphological appearance of *jag1bMO*-injected embryos. *jag1bMO*-injected embryos were analyzed from 24 to 120 hpf and subdivided in three major classes, based on body length and curvature. (A, E, I, M) Control group: mmMO injected embryos; Class 1 (B, F, J, N): mild phenotype with slight curved tail; Class 2 (C, G, K, O) intermediate phenotype: shortened body, curved tail; Class 3 (D, H, L, P) severe phenotype: severely reduced body length, twisted tail. Altogether, *jag1bMO* embryos belonging to the three classes exhibit craniofacial defects, clearly evident from 48 hpf on; Stage: first column, bottom left. Scale bar: 250 µm.

Alcian Blue staining allows the visualization of cartilage structures. At 120 hpf, *jag1b*MO larvae have variable craniofacial abnormalities that range from mild to more striking short pharynx (Fig. 3.15). *Jag1* is strongly expressed in the first and second pharyngeal arches during mouse development and *jag1b* regulates skeletal identity in zebrafish face (Kamath et al., 2002; Zuniga et al., 2010). We observed that knockdown of zebrafish *jag1b* gene altered the size of facial cartilages that are derived from the first and second branchial arches (palatoquadrate, Meckel's and ceratohyal cartilages), with abnormalities in hyoid symplectic cartilage (Fig. 3.15). We considered the craniofacial defects of *jag1b*MO larvae to be compatible with a *jag1b* loss of function.

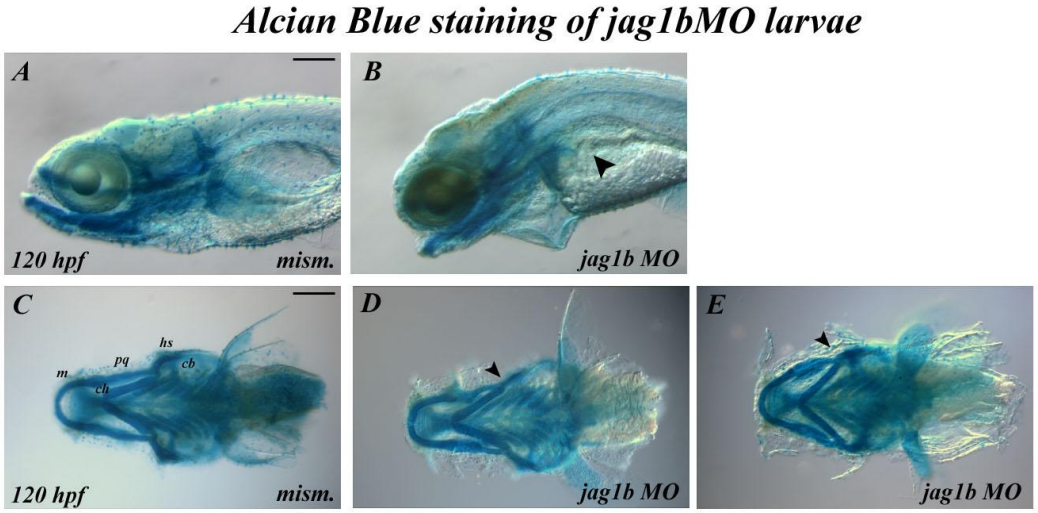

Figure 3.15: Alcian blue staining of *jag1b*MO larvae. (A-B) Alcian blue staining of mismatch (A) and *jag1b*MO (B) larvae, 120 hpf; lateral view (arrowhead: *jab1b*MO fails to inflate the swim bladder); (C-E) Craniofacial cartilages, ventral view, anterior to the left; (C) structure of the head cartilages in a mismatch injected larva; (D-E) structure of the head cartilages in two examples of *jag1b* morphants; the arrowheads indicate abnormalities in the hyoid symplectic (hs) cartilage; moreover the Merkel's (m), palatoquadrate (pq) and ceratohyal (ch) cartilages are smaller than in the mismatch larvae. Abbreviations: m, Meckel's cartilage; ch, ceratohyal; pq, palatoquadrate hs, hyosymplectic; cb, ceratobranchial. Scale bar: 200 µm.

To have a confirmation of the specific phenotype resulting from *jag1b* morpholino activity, we performed mRNA rescue experiments co-injecting *jag1b* splicing morpholino with human JAGGED1 mRNA. Considering that *jag1b*MO-injected embryos share, independently from the class they belong to, craniofacial abnormalities such as small head and eyes, we decided to look at the restoration of this specific trait, associated with normal or reduced/altered body length. We considered two major groups: class1: null/slight craniofacial defects and correct body length; class2: mild/severe craniofacial defects and reduced/altered body length. We analyzed embryos injected with 3.2 ng of *jag1b*MO in association with increasing doses of human JAGGED1 mRNA (from 0.75 pg to 5 pg/embryo) at 24 and 48 hpf. Both at 24 and 48 hpf we found a linear correlation between increasing doses of human JAGGED1 mRNA and reduction of class2 embryos (see graph in Figure 3.16). Of note, at high doses, the mRNA injection resulted in increased mortality of co-injected embryos. The embryos injected with the combination of 3.2 ng of *jag1b*MO + 2.5 pg of human JAGGED1 mRNA gave the best results, with an increase of 50% in embryos belonging to class 1 compared to the *jag1b*MO-only injected group (se graph and panel in Figure 3.16).

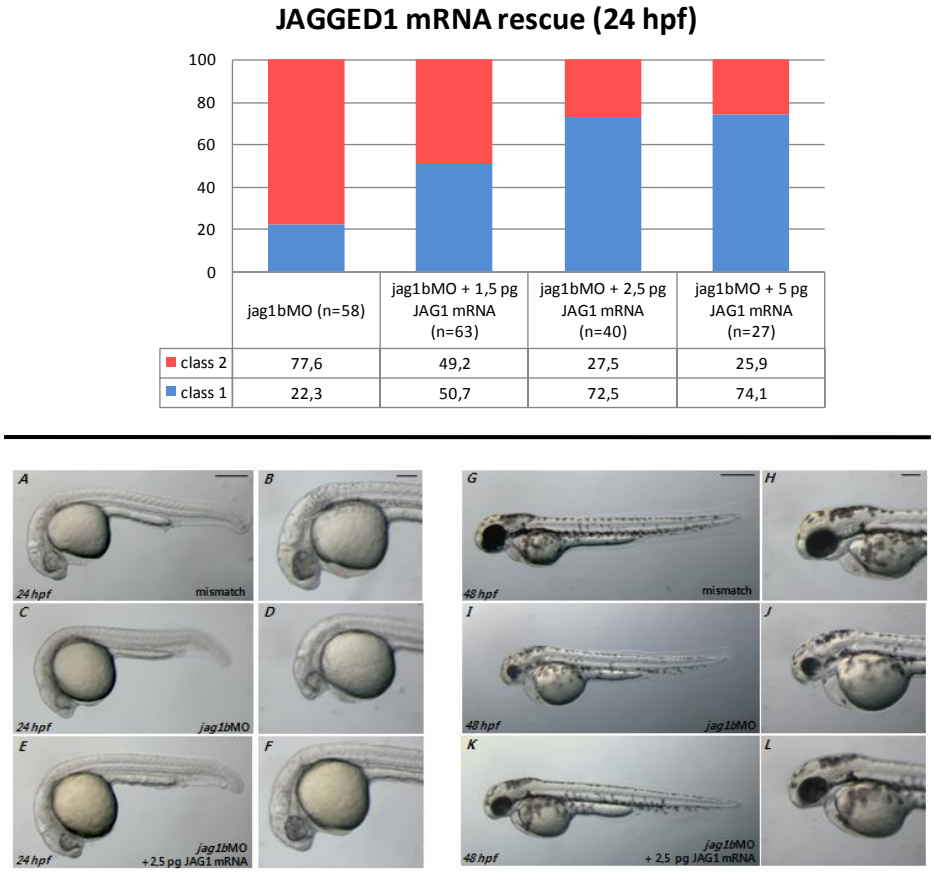

Figure 3.16: Rescue of zebrafish *jag1b*MO embryos defects with human JAGGED1 mRNA. Upper panel: percentage of embryos belonging to the phenotypic class 1 or 2, injected, respectively, with *jag1b*MO-only or jag1bMO plus increasing dose of human JAG1 mRNA; 24 hpf. The same percentages have been maintained at 48 hpf. Lower panel: (A-F) phenotypic comparison between a mismatch (A-B), *jag1b*MO-injected (C-F) and *jag1b*MO + human JAG1 co-injected (E-F) embryos at 24 hpf. The injection of human JAG1 mRNA partially rescues the smaller head/eyes and the body length. (G-L) Phenotypic comparison between a mismatch (G-H), *jag1b*MO-injected (I-J) and *jag1b*MO + human JAG1 co-injected (K-L) embryos at 48 hpf. The injection of human JAG1 mRNA partially rescues the smaller head/eyes and the body length. Stages, bottom left. Lateral views, anterior to the left. Scale bar (A,C,E,G,I,K): 250 µm, (B,D,F,H,J,L): 100 µm.

jag1b-mediated Notch signaling regulates thyroid development

Following the set up of *jag1b* gene knockdown and embryonic phenotype analysis, we performed whole mount *in situ* hybridization to analyze the effects of *jag1b* loss-of-function on zebrafish thyroid development.

To this purpose, we analyzed the expression of the transcription factor *nkx2.1a* and the differentiative markers *tg* and *slc5a5* at different time points (Fig. 3.17).

The analysis of *nkx2.1a* expression revealed that the thyroid primordium is correctly induced and specified at 24 hpf in *jag1b* morphants, and maintains a comparable level of expression of *nkx2.1a* at 48 and 72 hpf. Moreover, the thyroid cells are correctly localized along the midline (Fig. 3.17: A-C, I-K). At 48 hpf *tg* expression is comparable between *jag1bMO*-injected embryos and the mismatch counterpart, *tg* positive cells are organized in a compact globular group (Fig. 3.17: D, L). The time course analysis of the differentiative marker *tg* showed that the most prominent differences appeared at 72 and 120 hpf. At these stages the thyroid primordium of *jag1bMO*-injected embryos fails to elongate along the AP axis and results, in the end, in hypoplastic tissue with a lower number of *tg* positive cells at 72 and 120 hpf. The difference between the number of *tg* expressing cells in mismatch and *jag1bMO*-injected embryos was calculated by dividing the area of positive staining by the average area of a single cell. At 72 hpf, *jag1bMO*-injected embryos showed 30% of reduction in the number of *tg* expressing cells compared to that of mismatch embryo group (mism.: 84.79 ± 4.4, N=16; *jag1bMO*: 61.27 ± 2.1, N=18; difference between means: 23.51 ± 4.9, $P<0.003$, Student's t-test). At 120 hpf, *jag1bMO*-injected larvae showed 47% of reduction in the number of *tg* expressing cells compared to that of mismatch embryo group (mism.: 140.8 ± 8.8 N=19; *jag1bMO*: 75.41 ± 4.1 N=19; difference between means: 65.41 ± 9.7; $P<0,0001$, Student's t-test). The time course analysis of the differentiative marker *slc5a5* showed a pronounced reduced expression of the sodium-iodine symporter in *jag1bMO*-injected embryos (Figure 3.17: O-P). The drastically decreased expression of *slc5a5* could indicate that this gene is a more sensitive direct target of Jag1b-Notch signaling.

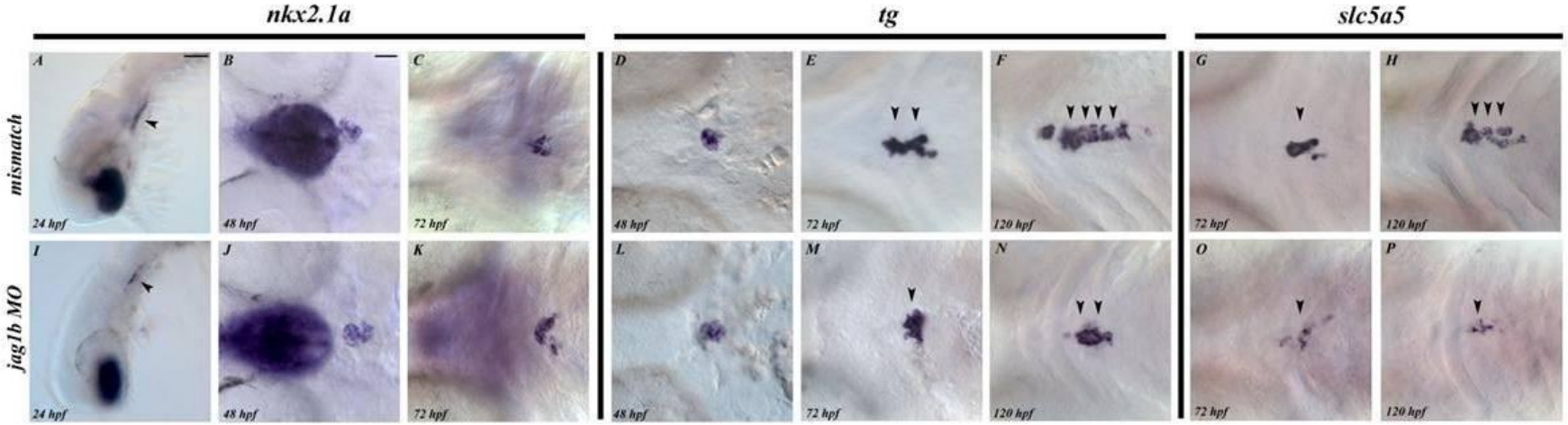

Figure 3.17: Effects of *jag1b* knockdown in thyroid cells. *jag1b* knockdown results in impaired thyroid development. (A-I) The thyroid primordium of *jag1bMO*-injected embryos is visible at 24 hpf, as a group of cells expressing *nkx2.1a* (arrowheads); (B-C, J-K) comparable *nkx2.1a* expression between *jag1bMO*-injected embryos and mismatch embryos; (D-F, L-N) at 48 hpf *tg* expressing cells are organized in a compact group both in morphant and mismatch embryos; subsequently the primordium fails to elongate and, in the end, results in hypoplastic tissue (arrowheads); (G-H, O-P) *slc5a5* expression is strongly reduced in *jag1b* morphants both at 72 and 120 hpf. Ventral views, anterior to the left. Stage: bottom left. Scale bar: 100 µm.

T4 production in jag1bMO and jag1bMUT larvae

T4 whole-mount antibody staining is a useful tool to assess the status of thyroid function in zebrafish. We used this method in order to visualize the thyroid gland in *jag1b*MO and *jag1b*MUT zebrafish larvae at 120 hpf.

In whole wild type larvae, a growing number of thyroid follicles was detectable in the pharyngeal area, dispersed along the ventral aorta (see Fig. 3.5, O). We decided to distribute the larvae in four main categories, according to the number of T4 positive follicles at 120 hpf: >6 follicles, 4-6 follicles, 2-3 follicles, 1 follicle. We analyzed T4 production in a total of 60 mismatch larvae, 74 *jag1b*MO larvae, and 12 *jag1b*MUT larvae. The mismatch group (n=60) is mainly distributed among the three highest categories (>6 follicles: 17.9% of the larvae; 4-6 follicles: 58.8%; 2-3 follicles: 23.3%; 1 follicle: 3.1%) (see graph in Fig. 3.18, A and B). In *jag1b*MO-injected larvae (n=71) we never found >6 follicles, and 84.5% of the larvae are distributed between the two lowest categories: 2-3 and 1 follicles; we found only 15.5% of *jag1b*MO-injected larvae into the 4-6 follicles group (Fig. 3.18, A and B). These results are consistent with the distribution of the *jag1b*MUT group of larvae (n=12) (Fig. 3.18, A and B). This is of particular interest considering that *jag1b* mutants display very mild craniofacial defects and result indistinguishable from the sibling counterpart. Genotyping of embryos allowed us to identify *jag1b*MUT larvae.

Overall we observed an impaired T4 production and thyroid function in *jag1b* loss-of-function conditions.

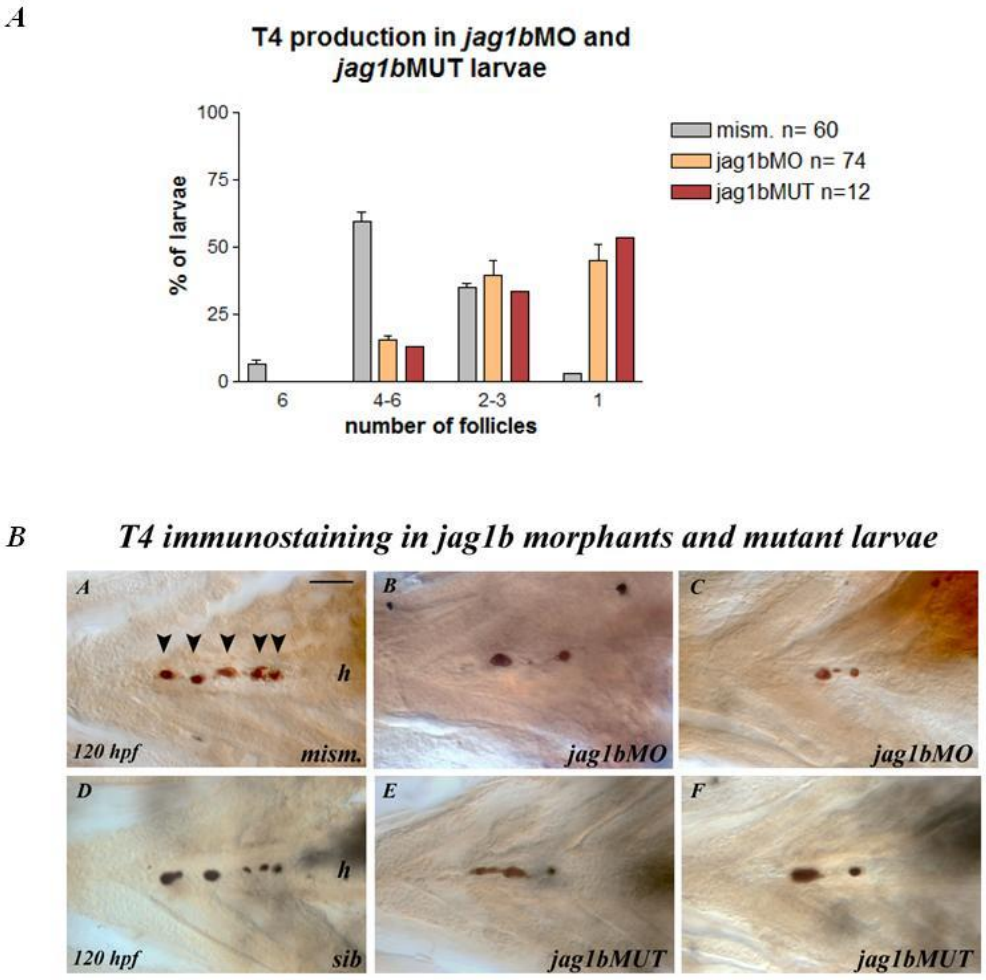

Figure 3.18: T4 production in *jag1b*MO and *jag1b*MUT larvae. (A) Distribution (%) of mismatch, *jag1b*MO and *jag1b*MUT larvae on the basis of the number of follicles producing T4. (B) Whole-mount T4 antibody staining: (A, D) distinct follicles (arrowheads) form a row along the anterior–posterior axis, at the pharyngeal midline, in mismatch and sibling larvae; (B-C) *jag1b*MOs have a reduced number of follicles producing T4; anyhow, the follicles maintain the correct position; (E-F) *jag1b*MUT have a reduced row of follicles. Abbreviations: h, heart. Stage: bottom left. Ventral views, anterior to the left. Scale bar: 100 µm.

Evaluation of the phenotype in jag1aMO-injected embryos

*jag1a*MO knockdown results in a homogeneous phenotype characterized by a peculiar curvature of the body axis. *jag1aMO*-injected embryos had smaller head and forebrain-midbrain delayed development; this characteristic became evident from 72 hpf. Most of *jag1a*MO injected embryos didn't inflate their swim bladder at 120 hpf (Fig. 3.19). The alcian blue staining allowed us to appreciate a moderate reduction in the dimension of the facial cartilage structures (Fig. 3.20). Additionally, *jag1aMO*-injected larvae exhibited a whirling movement when touched with a small plastic tip at 120 hpf.

This phenotype has been obtained using, separately, two different morpholinos (see Fig. 3.13, C): a translation blocking morpholino (*jag1a* atgMO; 0.25 ng/embryo) and a morpholino targeted to the splicing donor site E2i2 (*jag1a* splMO; 4 ng/embryo).

Figure 3.19: Morphological appearance of *jag1aMO*-injected embryos. *jag1aMO*-injected embryos were analyzed from 24 to 120 hpf; the major differences between mismatch and morphant embryos become evident at 48 hpf. Comparison between a mismatch embryo (left column) and an age-matched

jag1aMO-injected embryo (right column) at different stages of development. The curvature of the body is the most evident and peculiar characteristic of *jag1aMO*-injected embryos. Stages: bottom left.

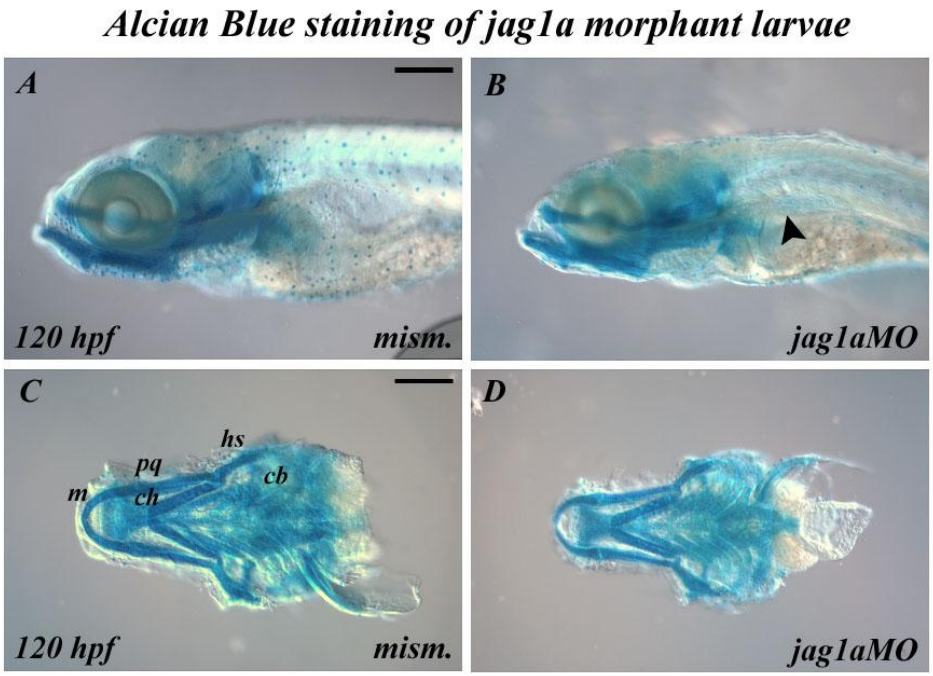

Figure 3.20: Alcian blue staining of *jag1a*MO larvae. (A-B) Alcian blue staining of mismatch (A) and *jag1a*MO (B) larvae, 120 hpf, lateral view (arrowhead: *jab1a*MO fails to inflate the swim bladder); (C-D) Craniofacial cartilages, ventral view, anterior to the left; (C) structure of the head cartilages in a mismatch injected larva; (D) structure of the head cartilages of a *jag1a* morphant larva; this staining shows that the Merkel's (m), palatoquadrate (pq) and ceratohyal (ch) cartilages are smaller than in the mismatch larva (C). Abbreviations: m, Meckel's cartilage; ch, ceratohyal; pq, palatoquadrate hs, hyosymplectic; cb, ceratobranchial. Scale bar: 200 µm.

jag1a-mediated Notch signaling is a minor regulator of thyroid development

We analyzed, by *in situ* hybridization, the thyroid development in *jag1a*-knockdown zebrafish embryos from 24 to 120 hpf. As done for *jag1b*MO-injected embryos, we evaluated the expression of the transcription factor *nkx2.1a* and the differentiative markers *tg* and *slc5a5* at different time points (Fig. 3.21). In *jag1a* loss of function embryos, the first group of cells expressing *nkx2.1a* was correctly specified in the pharyngeal endoderm by 24 hpf. The thyroid primordium of *jag1a* morphants maintains a comparable level of expression of *nkx2.1a* at 48 and 72 hpf. The thyroid cells are correctly localized at the midline and grow along the A-P axis starting from 72 hpf (Fig. 3.21, C, K, E-H, M-P). As regards *tg* expression, there are no differences between *jag1aMO*-injected embryos and the mismatch counterparts both at 48 and 72 hpf (quantification of *tg* expressing cells at 72 hpf: mism. 77.51 ± 4.182 N=23; *jag1a*MO 85.25 ± 5.485 N=20; the difference between means was not significant, P= 0.26 by Student's t-test) (Fig. 3.21: D-E, L-M). *tg* expressing cells are reduced in *jag1a*MO-injected larvae at 120 hpf (*tg* positive cells: mism. 130.0 ± 6.892 N=16; *jag1a*MO 95.70 ± 6.893 N=17; the difference between means was significant, 34.25 ± 9.757; P< 0.0014 by Student's t-test) (Fig. 3.21: F-N). Altogether, *jag1aMO*-injected larvae showed 26% of reduction in the number of *tg* expressing cells compared to that of mismatch larvae at 120 hpf. The time course analysis of the differentiative marker *slc5a5* showed a reduced expression of the sodium-iodine symporter in *jag1aMO*-injected larvae at 120 hpf, while at 72 hpf the staining is comparable. (Fig. 3.21: G-H, O-P). The decreased expression of *slc5a5* could indicate that this gene is a sensitive and direct target of Jag1a-Notch signaling.

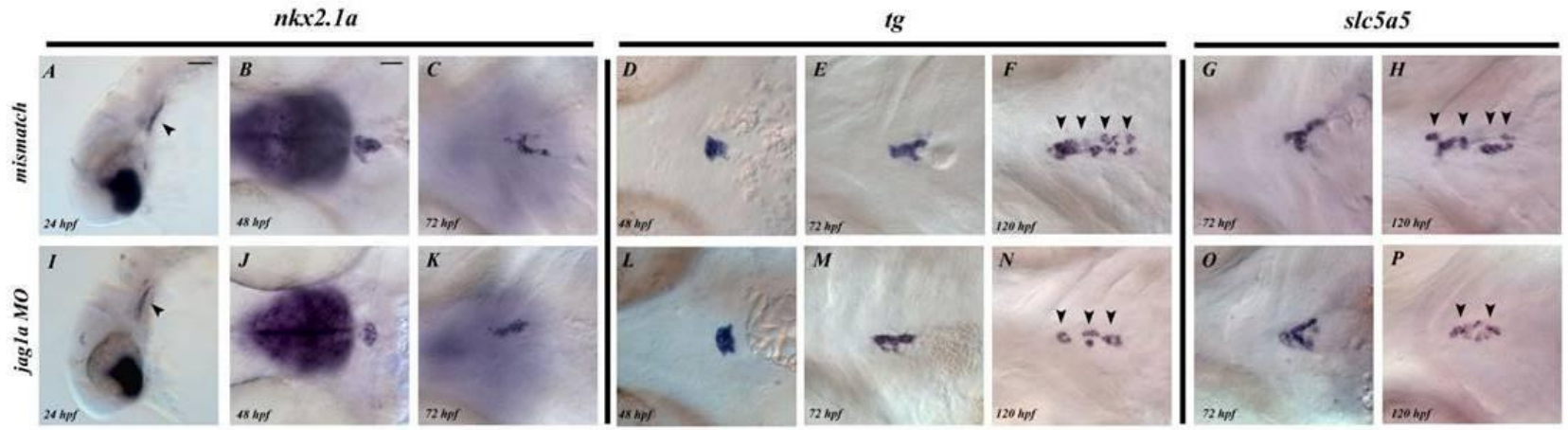

Figure 3.21: Effects of *jag1a* knockdown on thyroid development. *jag1*a knockdown results in mildly impaired thyroid development, evident at 120 hpf. (A-I) The thyroid primordium of *jag1aMO*-injected embryos is specified at 24 hpf, as a group of cells expressing *nkx2.1a* (arrowheads); (B-C, J-K) *nkx2.1a* expression is similar between *jag1aMO*-injected and mismatch embryos; (D-F, L-N) at 48 hpf *tg* expressing cells are organized in a compact group in both morphant and mismatch embryos; subsequently, the primordium elongates along the A-P axis; (F-N) the number of *tg* expressing cells is reduced in *jag1aMO*-injected embryos at 120 hpf (arrowheads); (G-H, O-P) *slc5a5* expression; *slc5a5* expression is reduced in *jag1a* morphants at 120 hpf (arrowheads). Ventral views, anterior to the left. Stage: bottom left. Scale bar: 100 µm.

T4 production in jag1aMO larvae

We performed T4 whole-mount antibody staining to assess the status of thyroid function in *jag1a*MO larvae at 120 hpf.

In mismatch larvae, a growing number of thyroid follicles was detectable in the pharyngeal area, spread in the pharyngeal jaw (see Fig. 3.5, O). As done for *jag1b* morphants and mutants, we divided the larvae in four main categories, according to the number of T4 positive follicles at 120 hpf: >6 follicles, 4-6 follicles, 2-3 follicles, 1 follicle. We analyzed T4 production in a total of 110 mismatch larvae and 120 *jag1a*MO. The mismatch group (n=110) is mainly distributed among three categories (>6 follicles: 19% of the larvae; 4-6 follicles: 56.2% of the larvae; 2-3 follicles: 24.8% of the larvae; 1 follicles: 2.3% of the larvae) (see graph in Fig. 3.22, A). In *jag1a*MO-injected larvae (n=120) we only found 4.1% of the larvae with >6 follicles, and more than half of the larvae (58.6 %) are distributed between the two lowest categories: 2-3 and 1 follicles; we found 37.3 % of *jag1a*MO-injected larvae in the 4-6 follicles group (see graph in Fig. 3.22, A).

Overall we observed a mild impaired T4 production and thyroid function in *jag1a* loss-of-function conditions.

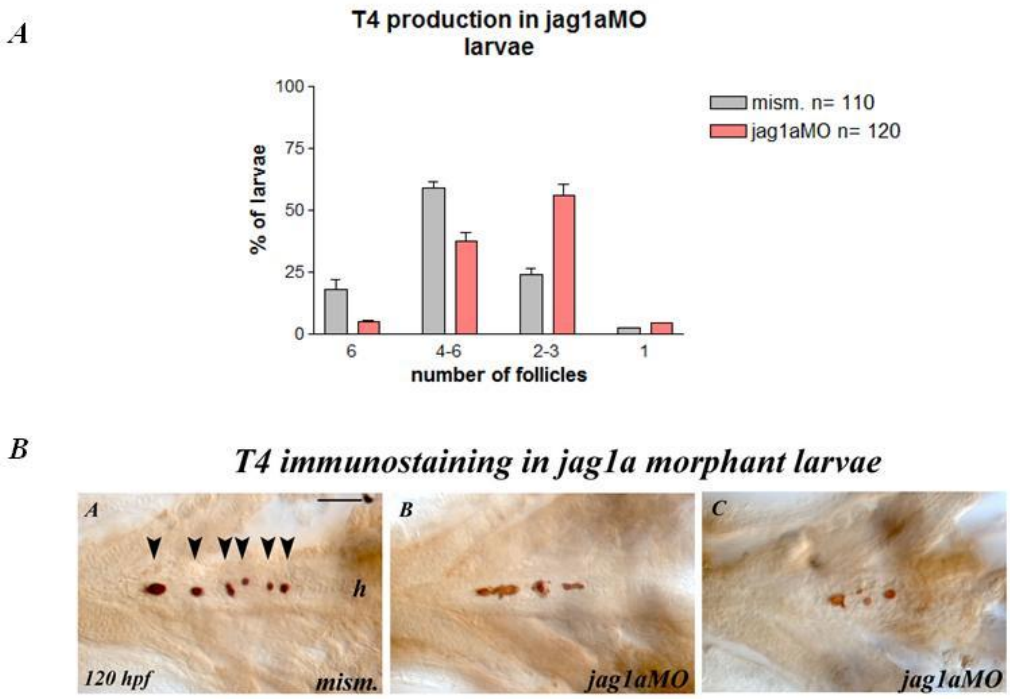

Figure 3.22: T4 production in *jag1a*MO larvae. (A) Distribution (%) of mismatch (grey) and *jag1a*MO (red) larvae, on the basis of the number of follicles producing T4. (B) Whole-mount T4 antibody staining: (A-D) distinct follicles (arrowheads) compose a row along the anterior–posterior axis at the pharyngeal midline in mismatch larvae; (B-C) *jag1a*MO larvae have a mildly reduced number of follicles producing T4; anyhow, the follicles maintain the correct position; Abbreviations: h, heart. Stage: bottom left. Ventral views, anterior to the left. Scale bar: 100 µm.

4.Discussion

In humans, congenital hypothyroidism (CH) is the most common congenital endocrine disorder and several evidences indicate its increased incidence which is, nowadays, of about 1:1500 newborns in the Italian population (Corbetta et al., 2009). Thyroid developmental defects, leading to thyroid dysgenesis (TD), account for 85% of the cases, comprising agenesis, hypoplasia and ectopic thyroid gland. The etiology of TD is still poorly understood. Most cases of CH with TD occur as a sporadic disease; however accumulating evidences indicate that genetic factors are involved in the pathogenesis of TD. The evidence that mutations in genes involved in thyroid development cause TD in animal models and that mutations in the same genes are associated with TD in humans confirms unequivocally that TD can be a genetic and inheritable condition (De Felice and Di Lauro, 2004; De Felice and Di Lauro, 2007). However, only few cases are associated with mutations of thyroidal transcription factors (NKX2-1; PAX8 or FOXE1), suggesting that other unknown genes play a role during thyroid organogenesis. Moreover, familial studies (Castanet et al., 2010; Leger et al., 2002), as well as animal models (Amendola et al., 2010), have brought evidence that CH may be a multigenic disease characterized by variable penetrance and expressivity. According to several reports, TD is associated with other major birth defects in 5–6% of cases (Devos et al., 1999; Olivieri et al., 2002; Roberts et al., 1997), and, among these, cardiac anomalies are particularly frequent. It is therefore possible to hypothesize that the genes involved in multi-organ development might also participate in thyroid development and in influencing the expression of CH.

In this study, we analyzed the role of Notch signaling and of short-range, cell-to-cell interactions, mediated by Jagged1-Notch, during thyroid development and differentiation in zebrafish.

Notch signaling in zebrafish thyroid development

In the first series of experiments, we have found that the over-expression of Notch results in the lack of thyroid cells expressing *nkx2.1a,* together with a significant reduction in the number of *tg* positive cells. Given the limited knowledge of master genes controlling the combined expression of the four main thyroidal transcription factors (*nkx2.1a*, *pax2a*, *hhex* and *pax8*), we were not able to establish whether the lack of *nkx2.1a*-expressing cells was associated with the persistent expression of upstream progenitor-related markers.

The model in which the Notch signaling is directly involved in the maintenance of precursors, limiting the number of committed cells that proceed to a specialized fate, has been already described during development of different organs and systems. With regard to the endocrine system, for instance, this process limits the number of differentiating pancreatic precursor cells and the initial differentiation of enteroendocrine cells (Dutta et al., 2008; Fukuda et al., 2006; Jensen et al., 2000; Zecchin et al., 2007).

According to the proposed role of the Notch signaling in thyroid development, we found that *mib* mutants, in which Notch signaling is impaired, exhibit an increased expression of *nkx2.1a*, *tg* and *slc5a5*. The number of *tg* positive cells was significantly higher in *mib* mutants compared to the *sib* counterpart. Consistently, the treatment with the gamma-secretase inhibitor DAPT gave very similar results.

The reduction or increase in the number of thyroid cells have been respectively obtained hyperactivating or blocking of the Notch signaling from about 20 hpf, just few hours before the onset of thyroid primordium. Given that the constitutive lack of Notch signaling (*mib* mutants) or its time-controlled inhibition at 20 hpf (DAPT-treated embryos) results in an indistinct thyroid phenotype, we can infer that Notch signaling has a major role in thyroid cell differentiation beginning from about 20 hpf. This hypothesis agrees with the finding that the

hyperactivation of Notch, immediately before the onset of thyroid primordium, is sufficient to prevent thyroid differentiation from the endodermal layer.

Moreover, this finding lead us to hypothesize that the gain- or loss- of Notch signaling function, in any preceding phases of embryonic development, has a minor influence on endoderm constitution and patterning. In many lower organisms, the canonical Notch signaling pathway, mediated by Delta- and Jagged-like Notch ligands, promotes the specification and patterning of endoderm, mesoderm, or ectoderm germ layers during gastrulation, but this function is not evolutionary conserved (Shi and Stanley, 2006). In sea urchins, activation of Notch signaling increases mesodermal precursors and reduces the number of presumptive endoderm cells, while opposite changes take place when Notch signaling is inhibited (Sherwood and McClay, 1999; Sherwood and McClay, 2001).

In zebrafish, the role of Notch signaling in endoderm layer specification is poorly defined, and it seems to be involved in the endoderm anterior-posterior patterning, by restricting the expression of the hairy enhancer of split-related gene her5 to a subpopulation of dorsal endodermal precursors (Bally-Cuif et al., 2000). Moreover, activating Notch signaling during early development results in a numerical reduction of endodermal cells, suggesting that Notch might play a role in the segregation of mesoderm from endoderm (Kikuchi et al., 2004). However, none of the strategies employed to block Notch signaling resulted in the opposite effects. With regard to mammals, this function is not conserved and the Notch signaling is not required for earliest cell fate specifications or for the constitution of the three germ layers (Shi et al., 2005; Shi and Stanley, 2006).

Our results show that a conserved Notch signaling is required for proper thyroid precursor cell differentiation. We propose therefore a model in which, at the time the thyroid primordium forms, Notch is necessary for endodermal precursors differentiation in thyrocytes, restricting the number of cells committed to a thyroid fate. We found that loss- or gain- of Notch function is sufficient to induce or prevent the development of thyroid cells. In conclusion, these results are consistent with a model of thyroid differentiation in which

Notch signaling mediates a specific feedback on precursors, thus limiting the number of committed cells, a mechanism known as lateral inhibition (Lai, 2004). In the lack of the correct feedback (*mib* mutants and DAPT treated embryos), too many cells proceed to a thyroid fate, while a constantly and highly maintained feedback mechanism (NICD over-expressing embryos) prevents the precursors from differentiation.

To our knowledge this is the first evidence of Notch signaling contribution to thyroid development. Thyroid organogenesis has never been investigated in other models, such as, for example, Notch signaling effectors *knock-out* mice.

Role of the Notch ligands, jag1a and jag1b, in zebrafish thyroid development

In this study, our main interest was to decipher *jagged1a (jag1a)* and *jagged1b (jag1b)* functions during thyroid development. *jag1a* and *jag1b* are orthologues of the single mammalian *Jagged1* gene. We firstly analyzed *jag1a* and *jag1b* thyroid specific expression patterns at different life stages.

We found *jag1a* positive cells confined in the most anterior portion of cells expressing *tg* at 72 hpf. This expression is of particular interest considering that Alt and colleagues have analyzed, with a transplantation of *Tar** mRNA injected cells, the way the thyroid follicles grow during zebrafish larval life (Alt et al., 2006b). Analyzing the bias of grafted cells contributing to the most anterior follicle in the mosaic experiment, the authors suggest this tissue being the first to form, assuming that further tissue is added caudally. Thus, the most anterior domain of this group corresponds to the remnant of the first differentiating follicle. In such a model, a proportion of cells would remain at the position of the first follicle during thyroid growth, and other cells would proliferate and add tissue caudally. The first follicle could be considered as a group of cells where *jag1a-Notch* signaling contributes to define the number of cells able to proliferate and move caudally to originate new follicles. This model is supported

by the finding that, in *jag1a* loss- of function zebrafish larvae, a lower number of follicles proceed to differentiate and produce T4, as a consequence of a minor number of *tg* and *slc5a5* positive cells.

We found *jag1b* expression in the thyroid at both 48 and 72 hpf and, in a more dispersed pattern, in a region corresponding to the pharyngeal endoderm expressing *nkx2.1a* at 24 hpf. Coherently, *jag1b* morphants display a severe reduction in the number of *tg* and *slc5a5* expressing cells. Moreover, both *jag1b* morphants and *jag1b* mutants larvae showed a mean of 1-2 follicles producing T4, compared to the 4-5 follicles in the control larvae.

In both *jag1a* and *jag1b* loss-of-function conditions, the onset of *nkx2.1a* expression and the budding of the thyroid primordium is unaffected. Thus, it is tempting to speculate that other Notch signaling ligands (belonging to Jagged or Delta families) could have a role during the early phases of thyroid primordium constitution. Notch signaling can function at several stages during the differentiation of a single organ and different ligands can play multiple roles within a given tissue. This process is well known, in zebrafish as in mammals, when different ligands or Notch receptors participate to the development of single organ subdomains (i.e. endocrine/exocrine pancreas, adenohypophysis) or when they contribute to orchestrate the multiple steps of a particular organ development (i.e. heart, notchocord) (Dutta et al., 2008; Golson et al., 2009; High and Epstein, 2008; Latimer and Appel, 2006; Yamamoto et al., 2010; Zecchin et al., 2007). Further analysis has to be conducted to define if other Notch ligands could participate to thyroid primordium development in zebrafish.

Moreover, the combined *jag1a*/*jag1b* loss of function condition could increase the severity of thyroid phenotype in zebrafish. Using zebrafish, it has been already demonstrated that specific combinations of *jagged*/*notch* gene knockdowns are able to perturb the biliary, kidney, pancreas and craniofacial development. Such defects are only partially evident when inhibiting one jagged or notch gene separately (Lorent et al., 2004). Noteworthy, these defects are

compatible with Alagille syndrome (ALGS), an inheritable autosomal dominant disorder, that affects multiple organ systems and is also characterized by highly variable intrafamilial expressivity (Li et al., 1997; Oda et al., 1997; Piccoli and Spinner, 2001). Studies in the mouse support the idea that multiple Notch pathway elements contribute to ALGS. Homozygous jagged1 mutant mice died at E9.5-10.5 from widespread hemorrhage (Xue et al., 1999). However heterozygous jagged1 mutant mice develop only mild ocular defects and only the compound jagged1/notch2 mutant condition results in cardiac and biliary defects typical of ALGS (McCright et al., 2002). Altogether, these data emphasize not only the well conserved role of the Notch signaling pathway, but also the fine sensitivity of this pathway to gene dosage, highlighting the importance of analyzing the combined *jag1a/jag1b* knockdown and the resulting thyroid phenotype. Finally, the phenotypes of our *jag1a* and *jag1b* morphants embryos (craniofacial defects, ventralization and, infrequently, cardiac edema) is very close to the ones described in other similar reports (Gwak et al., 2010; Lorent et al., 2004; Yamamoto et al., 2010; Zuniga et al., 2010). This leads us to assume that these features are specific.

The finding that *jag1a* and *jag1b* morphants exhibit a reduced number of *tg* positive cells could result from impaired proliferation of the cells that constitute the first follicles, from impaired ability to differentiate or to survive. Our results indicate that the thyroid primordium fails to elongate and differentiate from 72 hpf to 120 hpf, in *jag1* loss of function conditions. The hypothesis that *jag1* could contribute to thyroid cells proliferation, after the budding and positioning of the primordium along the midline, appears particularly fascinating. Data from the mouse model indicate that the proliferation rate varies considerably at different stages of thyroid development (Fagman et al., 2006). An unexpectedly low proliferation rate characterizes the early thyroid primordium in mouse embryos, as supported by the observation that both the placode and the emerging bud contain few BrdU positive cells as compared to the immediate neighboring endoderm and adjacent mesoderm (Fagman et al., 2006). This suggests that,

initially, the bud size expands by annexation of proliferating endoderm from outside the placode so that the central region of the bud consists of the first integrated progenitor cells that display a lower rate of proliferation. In the mouse model, the proliferation of the thyroid follicular cells takes place from E10.5 and proceeds onwards (Fagman et al., 2006). In zebrafish this proliferative phase is evident by 72 hpf (Elsalini et al., 2003). At this time we noticed a reduced number of *tg* positive cells in *jag1* loss of function condition. We can suppose that the characteristic proliferative phase, that allows the thyroid cells to elongate along the midline and to constitute scattered thyroid follicles, fails in absence of a functional *jag1-notch* signaling.

We can exclude that, at 120 hpf, the reduced number of follicles producing T4 is a consequence of an impaired TSH production by the thyrotrope cells in the anterior pituitary. The expression of *jag1a* or *jag1b* has never been documented in adenohypophysis of zebrafish even if, in the mouse, *Jag1* is expressed during the early phases of pituitary development and its role has not yet been functionally dissected (Zhu et al., 2006). Notably, both in mouse and in zebrafish the early thyroid growth and differentiation is proved to be TSH independent. As highlighted by genetic deletion experiments, TSH does not participate in mouse embryonic morphogenesis and in the growth of thyroid gland (Postiglione et al., 2002). Moreover, zebrafish *lia*^{t24149} mutants, lacking FGF3 signals, do not develop thyrotrope progenitors secreting TSH. In spite of that, it is possible to observe a row of normally sized distinct follicles producing T4 at 120 hpf (Alt et al., 2006b).

The combined expression of *Nkx2-1*, *Pax8*, *Foxe1* and *Hhex* is specific to the developing thyroid: these transcription factors are not individually required for thyroid cell specification or early budding, but their concerted action is fundamental in progenitor cell recruitment and survival, leading to enlargement and maintenance of the thyroid tissue both in mouse and zebrafish (Elsalini et al., 2003; Parlato et al., 2004; Wendl et al., 2002). In this work, we have analyzed the expression of *nkx2.1a*, that resulted unaffected in *jag1a* or *jag1b* morphants

embryos from 24 to 72 hpf. After this time, the expression of *nkx2.1a* physiologically decreases and becomes undetectable in zebrafish thyroid. Due to the conserved role of *pax2a*, *pax8* and *hhex* in zebrafish thyroid development, it will be interesting to analyze if, in the lack of *jag1a* or *jag1b* expression, one of these transcription factors is directly down-regulated. This could explain the inability of thyroid primordium to maintain its identity, due to an impaired cell grow and differentiation.

We found that the expression of *slc5a5* is strongly impaired in *jag1* loss of function conditions, especially in *jag1b* morphants. Tentatively, this could be the result of two different situations: an impaired expression of *pax2a*, *pax8* or *heex*, so that the correct thyroid differentiation is no more guaranteed, or a direct influence of Jag1-Notch signaling on *slc5a5* expression. Some evidence supports that this last hypothesis could be consistent. Ferretti et al. (2008) have recently demonstrated that both human and rat *slc5a5* promoter contains multiple Hes1 binding sites. The hyperactivation of Notch1 is able to induce the expression of a luciferase reporter construct with the regions of the rat *slc5a5* promoter comprising the Hes1-binding sites *in vitro* (Ferretti et al., 2008). Therefore we can suppose that the strongly reduced expression of *slc5a5* is, at least in part, a direct consequence of Jag1-Notch signaling down-regulation in zebrafish thyroid cells. However, the analysis of zebrafish *slc5a5* promoter sequence is necessary to confirm the presence and the conservation of hes1 binding motifs.

There is a strong relationship between thyroid and cardiovascular tree development. Several mouse and zebrafish mutants with defective cardiovascular development also present a thyroid phenotype that consists in a disorganized and misshaped primordium (Alt et al., 2006a; Fagman et al., 2006). We noticed a similar thyroid phenotype in *mib* mutants and DAPT-treated embryos. *mib* mutants have already been analyzed from a vascular point of view and, despite the proper expression of endothelial markers, they exhibit circulatory shunts and defective remodeling of the major vessels (Lawson et al.,

2001). Since well organized pharyngeal vessel architecture is a fundamental physical guide in the positioning of the thyroid cells both in mouse and in zebrafish, a disturbed Notch signaling (*mib* mutants or DAPT-treated embryos) is consistent with major defects in the thyroid final shape. We have demonstrated that, in *mib* mutants, the thyroid looses the contact with the major pharyngeal vessels and fails to grow along the AP axis.

If a suitable contact of the thyroid with the pharyngeal vessel is fundamental for thyroid morphogenesis, there are experimental indications that thyroid development, at least in zebrafish, is independent from signals emanating from the endothelial cells (Alt et al., 2006a). These considerations led us to conclude that the misshapen thyroid primordium, observed in *mib* mutants and DAPT-treated embryos at 72 hpf, is the result of disorganized pharyngeal vessel architecture. Even so, the increased number of *tg* expressing cells appears as a consequence of the lack of the Notch signaling pathway in the thyroid region and this agrees with the lateral inhibition model mentioned above. Following this model, it is also possible to assume that a premature differentiation of the thyroid precursor cells, in the lack of Notch signaling, gives rise to a depletion of the defined pool of precursors able to sustain the later phase of thyroid proliferation and growth and this results, in the end, in a lower number of cells able to organize and produce T4.

The thyroid follicular cells are correctly organized along the midline in both *jag1a* and *jag1b* loss-of-function conditions. This is an indirect indication of the correct positioning of the pharyngeal vessels. At 120 hpf, *jag1a and jag1b* morphants and *jag1b* mutant larvae have variable facial defects that ranged from a mildly reduced to a more striking shorter pharynx, with defects in the craniofacial cartilage elements, confirming the alterations documented in previous studies (Lorent et al., 2004; Zuniga et al., 2010). In a shorter pharynx, it is reasonable to think that the follicular cells have less space to organize themselves and constitute 4-6 follicles producing T4 at 120 hpf. We have also noticed that other described mutants, such as the *lia*^{t24149} mutants, display a shorter pharynx, but at

least 4 thyroid follicles are present at the midline. The authors defined those follicles normally shaped, but more compactly organized and less interspersed in the jaw (Alt et al., 2006b). In our condition we found a slightly reduce number of T4 producing follicles in *jag1a* morphants, but a more significant reduction in both *jag1b* morphants and mutants: this thyroid phenotype is a consequence of *jag1* deficiency that could be unrelated to the reduced pharynx length.

The analysis of thyroid development, in *jag1* loss of function conditions, cannot exempt from taking into account heart development. Considering the close spatial relationship between heart and thyroid development, it could be hypothesized the existence of common patterning traits in the early morphogenesis of both tissues.

Several evidences indicate concomitant cardiac and thyroid defects both in TD affected patients and in experimental models (Casanova et al., 2000; Dentice et al., 2006; Fagman et al., 2007; Olivieri et al., 2002; Westerlund et al., 2008). Interestingly, some transcription factors, such as Nkx2.5 and Isl1, are expressed in both cardiac and thyroid precursors. Nkx2.5 and Isl1 knockout mice exhibit a rudimentary or smaller thyroid along with severely disturbed heart development (Biben et al., 2002; Cai et al., 2003; Dentice et al., 2006; Westerlund et al., 2008).

Studies from human and mouse embryos revealed that Jagged1 is strongly expressed both in the outflow tract of the heart and in the pharyngeal endoderm and mesenchyme (Crosnier et al., 2000; High et al., 2009). The results of this study confirm, for the first time in zebrafish, the expression of *jag1b* in scattered cells of the pharyngeal endoderm: these cells have a pattern similar to those expressing *nkx2.1a* at 24 hpf. Moreover, *jag1a* and *jag1b* are later expressed in *tg* positive cells.

It has been recently demonstrated that the activity of Jagged1 in the second heart field sustains the expression of *Fgf8* and *Bmp4*, critical factors involved in the outflow tract development (High et al., 2009). Studies in zebrafish and mice firmly establish that FGF-signaling is crucial to early thyroid development and

that the cardiac mesoderm is a probable source of inductive and permissive signals (Lania et al., 2009; Wendl et al., 2007). We can suppose *jag1* as an upstream actor in these signaling processes.

The role of *jag1* in promoting the expression of FGF from zebrafish heart has never been investigated. At the moment there is neither evidence that *jag1a* and/or *jag1b* could have a similar role in orchestrating FGFs or BMPs expression in zebrafish, nor that these ligands could be expressed or contribute to the different phases of zebrafish heart development. We can conclude that the thyroid phenotype in *jag1* loss- of function conditions is, fist of all, the result of a cell-autonomous role of *jag1* in thyroid cells. We cannot totally exclude a non cell-autonomous influence of *jag1* expressed by the heart, trough FGF signals, in contributing to thyroid development. This role has still to be confirmed both in zebrafish and in mammals.

Presumptive cardiac defects result, in zebrafish, from the compound *jag1a/jag2* and *jag1b/jag2* knockdowns (Lorent et al., 2004). We observed some cardiac defects in less than 40% of *jag1bMO* embryos. The alterations consist in the lack of the characteristic heart curvatures of the ventricle and the atrium (unlooped heart tube), and they have a relatively late onset (from 72 to 120 hpf). Of note, we have never observed a cardiac phenotype in *jag1b* mutant embryos.

Considering that the reduction in the number of thyroid follicles is a little more severe in *jag1b* mutants than in *jag1b* morphants, and the first ones have no evident heart dysfunctions, we have a further evidence supporting the cell-autonomous role of *jag1b* in the thyroid. Further studies are needed to clarify the origin of heart phenotypes in *jag1b* morphants and to explain the discrepancy between *jag1b* morphants and mutants.

Our *in vivo* studies allow us to suggest that *jag1a* and, even more, *jag1b* affect, in a cell-autonomous manner, the proliferation and/or survival of thyroid follicular cells, sustaining their differentiation process during development. However, in the early phases of thyroid primordium induction and budding, the activity of

jag1 ligands is dispensable. Instead, *jag1* activity appears crucial in further steps of thyroid cell maintenance/proliferation and function (see the model in Fig. 4.1).

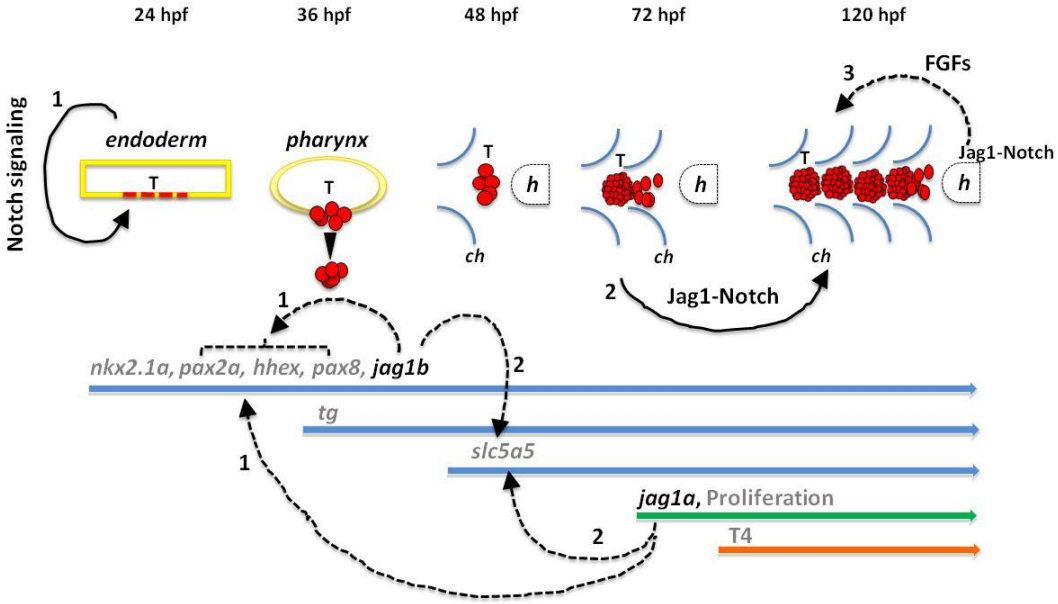

Figure 4.1: Model describing the role of Notch signaling and Jag1-Notch interaction in zebrafish thyroid differentiation. The thyroid primordium originates from the pharyngeal endoderm by 24 hpf: the role of Notch signaling is fundamental in limiting the number of thyroidal differentiating precursors (black arrow,1, left side of the panel). The combined expression of *nkx2.1a*, *pax2a*, *hhex* and *pax8* is distinctive of the thyroid follicular cells. *jag1b* is expressed from 24 to 72 hpf in the thyroid*; jag1a* is expressed at 72 hpf, in the most anterior portion of the first thyroid follicle. By 72 hpf, the thyroid cells start to proliferate and to produce T4. Jag1-Notch signaling sustains, in a cell-autonomous manner, the proliferation and the maintenance of thyroid cells (black arrow, 2). *Jag1* loss of function conditions give rise to an impaired thyroid growth and differentiation. This could be the result of different mechanisms, not mutually exclusive (broken arrows, 1-3): impaired expression of *pax2a*, *hhex* or *pax8* in absence of *Jag1* (broken arrows, 1); a direct down-regulation of *slc5a5* in absence of *Jag1* (broken arrows, 2). Moreover, *Jag1* could act in a non cell-autonomous manner during thyroid differentiation (broken arrow, 3, close to the heart). In mouse, Jag1 in the second heart field orchestrates FGFs expression. FGFs signals from the cardiac mesoderm are known to be important for proper thyroid development. Abbreviations: T, thyroid; ch, ceratohyal; h, heart. Stages: upper part of the panel. 24 hpf and 36 hpf: transversal views; from 48 to 120 hpf: ventral views.

Expression of Jagged1 in differentiated thyroid tissue

In a second series of experiments, we have documented the expression of *Jagged1* in FRTL5, a well-differentiated rat thyroid cell line, and in murine thyroid tissues. The expression of Jagged1 in human thyroid tissue has been documented only by Li and colleagues in 1998 and it was never reported in other studies (Li et al., 1998). Moreover, the biological role of Jagged1 in the adult thyroid gland has never been defined. We found that the expression of Jagged1, together with other components of the Notch signaling pathway, is down-regulated upon TSH stimulation in FRTL5. TSH promotes thyroid cell proliferation and differentiation both *in vitro* and *in vivo.* The down-regulation of some Notch signaling components upon TSH stimulation led us to hypothesize that the Notch pathway can contribute to the maintenance of the homeostasis of the thyroid cells: when these cells are required to proliferate and differentiate, the Notch pathway is down-regulated. Considering the important role of Notch in preserving stem cell pools in other tissues, the above described findings raise the exciting possibility that undifferentiated thyroid precursor cells may rely on Notch for cell renewal and for possible cell expansion. There are examples of down-regulation of the Notch signaling pathway as stem cells differentiate, suggesting that Notch helps to maintain this particular subset in an undifferentiated state (Duncan et al., 2005). However, the existence of thyroid stem cells is still and active matter of debate. Adult stem cells of the human thyroid gland were first postulated in 1992, then suspected in 2003 by the demonstration of p63 expression in solid cell nests of the thyroid, and finally proven in 2006 by the Oct-4, Gata-4, HNF4α, and Pax8 expression in cultured cells derived from goiters (Dumont et al., 1992; Reis-Filho et al., 2003; Thomas et al., 2006). Rapidly accumulating evidence indicates the presence of adult thyroid stem cells (Chen et al., 2009; Fierabracci et al., 2008; Hoshi et al., 2007; Lan et al., 2007). However, the presence or activity of Notch signaling pathway has never been analyzed in these populations of cells.

In addition, we found that the mouse thyroid follicles are positive for the expression of all four Notch receptors, even if the receptors are in different states of activation (membrane bound or present both at the plasma membrane and into the nucleus as NICD). Ferretti and colleagues have already documented that different Notch receptors (Notch1, 2 and 3) are expressed during the development of murine thyrocytes, and their expression levels parallel those of thyroid differentiation markers: the expression of Notch receptors in FRTL5 and human thyroid tissue is up-regulated by TSH (Ferretti et al., 2008). This result seems to depict a situation opposite to our data, but we have to take into account that, of the three Notch receptors found to be expressed by Ferretti, only Notch1 and Notch3 are up-regulated upon TSH stimulation, whereas Notch2, even if present, is insensitive to TSH action. This is a further demonstration that more than one Notch receptor (and probably more than one Notch ligand) is expressed by thyroid tissue, and that different ligand-receptor combinations can play multiple roles within a given tissue. The role of Notch signaling in adult thyroid tissue has to be investigated in more details.

In conclusion, to our knowledge this study documented, for the first time, the involvement of the Notch signaling pathway during thyroid development using zebrafish. Moreover, we demonstrated that, when the Notch ligand Jagged1 is lacking, the thyroid primordium exhibits an impaired differentiation, enlisting *Jagged1* as a novel gene whose variations might be involved in the pathogenesis of congenital hypothyroidism.

5.References

Aggarwal, V. S., Liao, J., Bondarev, A., Schimmang, T., Lewandoski, M., Locker, J., Shanske, A., Campione, M. and Morrow, B. E. (2006). Dissection of Tbx1 and Fgf interactions in mouse models of 22q11DS suggests functional redundancy. *Hum Mol Genet* **15**, 3219-28.

Alexander, J., Rothenberg, M., Henry, G. L. and Stainier, D. Y. (1999). casanova plays an early and essential role in endoderm formation in zebrafish. *Dev Biol* **215**, 343-57.

Alt, B., Elsalini, O. A., Schrumpf, P., Haufs, N., Lawson, N. D., Schwabe, G. C., Mundlos, S., Gruters, A., Krude, H. and Rohr, K. B. (2006a). Arteries define the position of the thyroid gland during its developmental relocalisation. *Development* **133**, 3797-804.

Alt, B., Reibe, S., Feitosa, N. M., Elsalini, O. A., Wendl, T. and Rohr, K. B. (2006b). Analysis of origin and growth of the thyroid gland in zebrafish. *Dev Dyn* **235**, 1872-83.

Amendola, E., De Luca, P., Macchia, P. E., Terracciano, D., Rosica, A., Chiappetta, G., Kimura, S., Mansouri, A., Affuso, A., Arra, C. et al. (2005). A mouse model demonstrates a multigenic origin of congenital hypothyroidism. *Endocrinology* **146**, 5038-47.

Amendola, E., Sanges, R., Galvan, A., Dathan, N., Manenti, G., Ferrandino, G., Alvino, F. M., Di Palma, T., Scarfo, M., Zannini, M. et al. (2010). A locus on mouse chromosome 2 is involved in susceptibility to congenital hypothyroidism and contains an essential gene expressed in thyroid. *Endocrinology* **151**, 1948-58.

Aoki, T. O., Mathieu, J., Saint-Etienne, L., Rebagliati, M. R., Peyrieras, N. and Rosa, F. M. (2002). Regulation of nodal signalling and mesendoderm formation by TARAM-A, a TGFbeta-related type I receptor. *Dev Biol* **241**, 273-88.

Apelqvist, A., Li, H., Sommer, L., Beatus, P., Anderson, D. J., Honjo, T., Hrabe de Angelis, M., Lendahl, U. and Edlund, H. (1999). Notch signalling controls pancreatic cell differentiation. *Nature* **400**, 877-81.

Artavanis-Tsakonas, S., Rand, M. D. and Lake, R. J. (1999). Notch signaling: cell fate control and signal integration in development. *Science* **284**, 770-6.

Ascano, J. M., Beverly, L. J. and Capobianco, A. J. (2003). The C-terminal PDZ-ligand of JAGGED1 is essential for cellular transformation. *J Biol Chem* **278**, 8771-9.

Bally-Cuif, L., Goutel, C., Wassef, M., Wurst, W. and Rosa, F. (2000). Coregulation of anterior and posterior mesendodermal development by a hairy-related transcriptional repressor. *Genes Dev* **14**, 1664-77.

Bamforth, J. S., Hughes, I. A., Lazarus, J. H., Weaver, C. M. and Harper, P. S. (1989). Congenital hypothyroidism, spiky hair, and cleft palate. *J Med Genet* **26**, 49-51.

Baris, I., Arisoy, A. E., Smith, A., Agostini, M., Mitchell, C. S., Park, S. M., Halefoglu, A. M., Zengin, E., Chatterjee, V. K. and Battaloglu, E. (2006). A novel missense mutation in human TTF-2 (FKHL15) gene associated with congenital hypothyroidism but not athyreosis. *J Clin Endocrinol Metab* **91**, 4183-7.

Bassett, A. S., Chow, E. W., Husted, J., Weksberg, R., Caluseriu, O., Webb, G. D. and Gatzoulis, M. A. (2005). Clinical features of 78 adults with 22q11 Deletion Syndrome. *Am J Med Genet A* **138**, 307-13.

Biben, C., Wang, C. C. and Harvey, R. P. (2002). NK-2 class homeobox genes and pharyngeal/oral patterning: Nkx2-3 is required for salivary gland and tooth morphogenesis. *Int J Dev Biol* **46**, 415-22.

Bogue, C. W., Ganea, G. R., Sturm, E., Ianucci, R. and Jacobs, H. C. (2000). Hex expression suggests a role in the development and function of organs derived from foregut endoderm. *Dev Dyn* **219**, 84-9.

Bolos, V., Grego-Bessa, J. and de la Pompa, J. L. (2007). Notch signaling in development and cancer. *Endocr Rev* **28**, 339-63.

Bray, S. J. (2006). Notch signalling: a simple pathway becomes complex. *Nat Rev Mol Cell Biol* **7**, 678-89.
Cabrera, C. V. (1990). Lateral inhibition and cell fate during neurogenesis in Drosophila: the interactions between scute, Notch and Delta. *Development* **110**, 733-42.
Cai, C. L., Liang, X., Shi, Y., Chu, P. H., Pfaff, S. L., Chen, J. and Evans, S. (2003). Isl1 identifies a cardiac progenitor population that proliferates prior to differentiation and contributes a majority of cells to the heart. *Dev Cell* **5**, 877-89.
Calebiro, D., de Filippis, T., Lucchi, S., Martinez, F., Porazzi, P., Trivellato, R., Locati, M., Beck-Peccoz, P. and Persani, L. (2006). Selective modulation of protein kinase A I and II reveals distinct roles in thyroid cell gene expression and growth. *Mol Endocrinol* **20**, 3196-211.
Carre, A., Castanet, M., Sura-Trueba, S., Szinnai, G., Van Vliet, G., Trochet, D., Amiel, J., Leger, J., Czernichow, P., Scotet, V. et al. (2007). Polymorphic length of FOXE1 alanine stretch: evidence for genetic susceptibility to thyroid dysgenesis. *Hum Genet* **122**, 467-76.
Casanova, J. B., Daly, R. C., Edwards, B. S., Tazelaar, H. D. and Thompson, G. B. (2000). Intracardiac ectopic thyroid. *Ann Thorac Surg* **70**, 1694-6.
Castanet, M., Marinovic, D., Polak, M. and Leger, J. (2010). Epidemiology of thyroid dysgenesis: the familial component. *Horm Res Paediatr* **73**, 231-7.
Castanet, M., Park, S. M., Smith, A., Bost, M., Leger, J., Lyonnet, S., Pelet, A., Czernichow, P., Chatterjee, K. and Polak, M. (2002). A novel loss-of-function mutation in TTF-2 is associated with congenital hypothyroidism, thyroid agenesis and cleft palate. *Hum Mol Genet* **11**, 2051-9.
Castanet, M., Sura-Trueba, S., Chauty, A., Carre, A., de Roux, N., Heath, S., Leger, J., Lyonnet, S., Czernichow, P. and Polak, M. (2005). Linkage and mutational analysis of familial thyroid dysgenesis demonstrate genetic heterogeneity implicating novel genes. *Eur J Hum Genet* **13**, 232-9.
Chen, C. Y., Kimura, H., Landek-Salgado, M. A., Hagedorn, J., Kimura, M., Suzuki, K., Westra, W., Rose, N. R. and Caturegli, P. (2009). Regenerative potentials of the murine thyroid in experimental autoimmune thyroiditis: role of CD24. *Endocrinology* **150**, 492-9.
Chitnis, A. (2006). Why is delta endocytosis required for effective activation of notch? *Dev Dyn* **235**, 886-94.
Congdon, T., Nguyen, L. Q., Nogueira, C. R., Habiby, R. L., Medeiros-Neto, G. and Kopp, P. (2001). A novel mutation (Q40P) in PAX8 associated with congenital hypothyroidism and thyroid hypoplasia: evidence for phenotypic variability in mother and child. *J Clin Endocrinol Metab* **86**, 3962-7.
Corbetta, C., Weber, G., Cortinovis, F., Calebiro, D., Passoni, A., Vigone, M. C., Beck-Peccoz, P., Chiumello, G. and Persani, L. (2009). A 7-year experience with low blood TSH cutoff levels for neonatal screening reveals an unsuspected frequency of congenital hypothyroidism (CH). *Clin Endocrinol (Oxf)* **71**, 739-45.
Covassin, L. D., Villefranc, J. A., Kacergis, M. C., Weinstein, B. M. and Lawson, N. D. (2006). Distinct genetic interactions between multiple Vegf receptors are required for development of different blood vessel types in zebrafish. *Proc Natl Acad Sci U S A* **103**, 6554-9.
Crosnier, C., Attie-Bitach, T., Encha-Razavi, F., Audollent, S., Soudy, F., Hadchouel, M., Meunier-Rotival, M. and Vekemans, M. (2000). JAGGED1 gene expression during human embryogenesis elucidates the wide phenotypic spectrum of Alagille syndrome. *Hepatology* **32**, 574-81.
De Felice, M. and Di Lauro, R. (2004). Thyroid development and its disorders: genetics and molecular mechanisms. *Endocr Rev* **25**, 722-46.

De Felice, M. and Di Lauro, R. (2007). Murine models for the study of thyroid gland development. *Endocr Dev* **10**, 1-14.
De Felice, M., Ovitt, C., Biffali, E., Rodriguez-Mallon, A., Arra, C., Anastassiadis, K., Macchia, P. E., Mattei, M. G., Mariano, A., Scholer, H. et al. (1998). A mouse model for hereditary thyroid dysgenesis and cleft palate. *Nat Genet* **19**, 395-8.
Dentice, M., Cordeddu, V., Rosica, A., Ferrara, A. M., Santarpia, L., Salvatore, D., Chiovato, L., Perri, A., Moschini, L., Fazzini, C. et al. (2006). Missense mutation in the transcription factor NKX2-5: a novel molecular event in the pathogenesis of thyroid dysgenesis. *J Clin Endocrinol Metab* **91**, 1428-33.
Devos, H., Rodd, C., Gagne, N., Laframboise, R. and Van Vliet, G. (1999). A search for the possible molecular mechanisms of thyroid dysgenesis: sex ratios and associated malformations. *J Clin Endocrinol Metab* **84**, 2502-6.
Dick, A., Mayr, T., Bauer, H., Meier, A. and Hammerschmidt, M. (2000). Cloning and characterization of zebrafish smad2, smad3 and smad4. *Gene* **246**, 69-80.
Draper, B. W., Morcos, P. A. and Kimmel, C. B. (2001). Inhibition of zebrafish fgf8 pre-mRNA splicing with morpholino oligos: a quantifiable method for gene knockdown. *Genesis* **30**, 154-6.
Dufour, J. F. and Pratt, D. S. (2001). Alagille syndrome with colonic polyposis. *Am J Gastroenterol* **96**, 2775-7.
Dumont, J. E., Lamy, F., Roger, P. and Maenhaut, C. (1992). Physiological and pathological regulation of thyroid cell proliferation and differentiation by thyrotropin and other factors. *Physiol Rev* **72**, 667-97.
Duncan, A. W., Rattis, F. M., DiMascio, L. N., Congdon, K. L., Pazianos, G., Zhao, C., Yoon, K., Cook, J. M., Willert, K., Gaiano, N. et al. (2005). Integration of Notch and Wnt signaling in hematopoietic stem cell maintenance. *Nat Immunol* **6**, 314-22.
Dutta, S., Dietrich, J. E., Westerfield, M. and Varga, Z. M. (2008). Notch signaling regulates endocrine cell specification in the zebrafish anterior pituitary. *Dev Biol* **319**, 248-57.
Eldadah, Z. A., Hamosh, A., Biery, N. J., Montgomery, R. A., Duke, M., Elkins, R. and Dietz, H. C. (2001). Familial Tetralogy of Fallot caused by mutation in the jagged1 gene. *Hum Mol Genet* **10**, 163-9.
Elsalini, O. A. and Rohr, K. B. (2003). Phenylthiourea disrupts thyroid function in developing zebrafish. *Dev Genes Evol* **212**, 593-8.
Elsalini, O. A., von Gartzen, J., Cramer, M. and Rohr, K. B. (2003). Zebrafish hhex, nk2.1a, and pax2.1 regulate thyroid growth and differentiation downstream of Nodal-dependent transcription factors. *Dev Biol* **263**, 67-80.
Esperante, S. A., Rivolta, C. M., Miravalle, L., Herzovich, V., Iorcansky, S., Baralle, M. and Targovnik, H. M. (2008). Identification and characterization of four PAX8 rare sequence variants (p.T225M, p.L233L, p.G336S and p.A439A) in patients with congenital hypothyroidism and dysgenetic thyroid glands. *Clin Endocrinol (Oxf)* **68**, 828-35.
Fagman, H., Andersson, L. and Nilsson, M. (2006). The developing mouse thyroid: embryonic vessel contacts and parenchymal growth pattern during specification, budding, migration, and lobulation. *Dev Dyn* **235**, 444-55.
Fagman, H., Liao, J., Westerlund, J., Andersson, L., Morrow, B. E. and Nilsson, M. (2007). The 22q11 deletion syndrome candidate gene Tbx1 determines thyroid size and positioning. *Hum Mol Genet* **16**, 276-85.
Fagman, H. and Nilsson, M. (2009). Morphogenesis of the thyroid gland. *Mol Cell Endocrinol* **323**, 35-54.
Feldman, B., Gates, M. A., Egan, E. S., Dougan, S. T., Rennebeck, G., Sirotkin, H. I., Schier, A. F. and Talbot, W. S. (1998). Zebrafish organizer development and germ-layer formation require nodal-related signals. *Nature* **395**, 181-5.

Ferretti, E., Tosi, E., Po, A., Scipioni, A., Morisi, R., Espinola, M. S., Russo, D., Durante, C., Schlumberger, M., Screpanti, I. et al. (2008). Notch signaling is involved in expression of thyrocyte differentiation markers and is down-regulated in thyroid tumors. *J Clin Endocrinol Metab* **93**, 4080-7.
Fierabracci, A., Puglisi, M. A., Giuliani, L., Mattarocci, S. and Gallinella-Muzi, M. (2008). Identification of an adult stem/progenitor cell-like population in the human thyroid. *J Endocrinol* **198**, 471-87.
Fiuza, U. M. and Arias, A. M. (2007). Cell and molecular biology of Notch. *J Endocrinol* **194**, 459-74.
Friedrichsen, S., Christ, S., Heuer, H., Schafer, M. K., Parlow, A. F., Visser, T. J. and Bauer, K. (2004). Expression of pituitary hormones in the Pax8-/- mouse model of congenital hypothyroidism. *Endocrinology* **145**, 1276-83.
Fukuda, A., Kawaguchi, Y., Furuyama, K., Kodama, S., Horiguchi, M., Kuhara, T., Koizumi, M., Boyer, D. F., Fujimoto, K., Doi, R. et al. (2006). Ectopic pancreas formation in Hes1 -knockout mice reveals plasticity of endodermal progenitors of the gut, bile duct, and pancreas. *J Clin Invest* **116**, 1484-93.
Gasser, R. F. (2006). Evidence that some events of mammalian embryogenesis can result from differential growth, making migration unnecessary. *Anat Rec B New Anat* **289**, 53-63.
Geling, A., Steiner, H., Willem, M., Bally-Cuif, L. and Haass, C. (2002). A gamma-secretase inhibitor blocks Notch signaling in vivo and causes a severe neurogenic phenotype in zebrafish. *EMBO Rep* **3**, 688-94.
Gillam, M. P. and Kopp, P. (2001). Genetic regulation of thyroid development. *Curr Opin Pediatr* **13**, 358-63.
Golson, M. L., Le Lay, J., Gao, N., Bramswig, N., Loomes, K. M., Oakey, R., May, C. L., White, P. and Kaestner, K. H. (2009). Jagged1 is a competitive inhibitor of Notch signaling in the embryonic pancreas. *Mech Dev* **126**, 687-99.
Greenway, S. C., Pereira, A. C., Lin, J. C., DePalma, S. R., Israel, S. J., Mesquita, S. M., Ergul, E., Conta, J. H., Korn, J. M., McCarroll, S. A. et al. (2009). De novo copy number variants identify new genes and loci in isolated sporadic tetralogy of Fallot. *Nat Genet* **41**, 931-5.
Gruters, A. and Krude, H. (2007). Update on the management of congenital hypothyroidism. *Horm Res* **68 Suppl 5**, 107-11.
Gruters, A., Krude, H. and Biebermann, H. (2004). Molecular genetic defects in congenital hypothyroidism. *Eur J Endocrinol* **151 Suppl 3**, U39-44.
Gualdi, R., Bossard, P., Zheng, M., Hamada, Y., Coleman, J. R. and Zaret, K. S. (1996). Hepatic specification of the gut endoderm in vitro: cell signaling and transcriptional control. *Genes Dev* **10**, 1670-82.
Gwak, J. W., Kong, H. J., Bae, Y. K., Kim, M. J., Lee, J., Park, J. H. and Yeo, S. Y. (2010). Proliferating neural progenitors in the developing CNS of zebrafish require Jagged2 and Jagged1b. *Mol Cells* **30**, 155-9.
Habeck, H., Odenthal, J., Walderich, B., Maischein, H. and Schulte-Merker, S. (2002). Analysis of a zebrafish VEGF receptor mutant reveals specific disruption of angiogenesis. *Curr Biol* **12**, 1405-12.
Hatta, K., Kimmel, C. B., Ho, R. K. and Walker, C. (1991). The cyclops mutation blocks specification of the floor plate of the zebrafish central nervous system. *Nature* **350**, 339-41.
High, F. A. and Epstein, J. A. (2008). The multifaceted role of Notch in cardiac development and disease. *Nat Rev Genet* **9**, 49-61.
High, F. A., Jain, R., Stoller, J. Z., Antonucci, N. B., Lu, M. M., Loomes, K. M., Kaestner, K. H., Pear, W. S. and Epstein, J. A. (2009). Murine Jagged1/Notch signaling in the

second heart field orchestrates Fgf8 expression and tissue-tissue interactions during outflow tract development. *J Clin Invest* **119**, 1986-96.
Hoffenberg, E. J., Narkewicz, M. R., Sondheimer, J. M., Smith, D. J., Silverman, A. and Sokol, R. J. (1995). Outcome of syndromic paucity of interlobular bile ducts (Alagille syndrome) with onset of cholestasis in infancy. *J Pediatr* **127**, 220-4.
Hoshi, N., Kusakabe, T., Taylor, B. J. and Kimura, S. (2007). Side population cells in the mouse thyroid exhibit stem/progenitor cell-like characteristics. *Endocrinology* **148**, 4251-8.
Iso, T., Kedes, L. and Hamamori, Y. (2003). HES and HERP families: multiple effectors of the Notch signaling pathway. *J Cell Physiol* **194**, 237-55.
Itoh, M., Kim, C. H., Palardy, G., Oda, T., Jiang, Y. J., Maust, D., Yeo, S. Y., Lorick, K., Wright, G. J., Ariza-McNaughton, L. et al. (2003). Mind bomb is a ubiquitin ligase that is essential for efficient activation of Notch signaling by Delta. *Dev Cell* **4**, 67-82.
Jensen, J., Pedersen, E. E., Galante, P., Hald, J., Heller, R. S., Ishibashi, M., Kageyama, R., Guillemot, F., Serup, P. and Madsen, O. D. (2000). Control of endodermal endocrine development by Hes-1. *Nat Genet* **24**, 36-44.
Jung, J., Zheng, M., Goldfarb, M. and Zaret, K. S. (1999). Initiation of mammalian liver development from endoderm by fibroblast growth factors. *Science* **284**, 1998-2003.
Kamath, B. M., Loomes, K. M., Oakey, R. J., Emerick, K. E., Conversano, T., Spinner, N. B., Piccoli, D. A. and Krantz, I. D. (2002). Facial features in Alagille syndrome: specific or cholestasis facies? *Am J Med Genet* **112**, 163-70.
Kameda, Y., Ito, M., Nishimaki, T. and Gotoh, N. (2009). FRS2alpha is required for the separation, migration, and survival of pharyngeal-endoderm derived organs including thyroid, ultimobranchial body, parathyroid, and thymus. *Dev Dyn* **238**, 503-13.
Kameda, Y., Nishimaki, T., Miura, M., Jiang, S. X. and Guillemot, F. (2007). Mash1 regulates the development of C cells in mouse thyroid glands. *Dev Dyn* **236**, 262-70.
Kikuchi, Y., Trinh, L. A., Reiter, J. F., Alexander, J., Yelon, D. and Stainier, D. Y. (2000). The zebrafish bonnie and clyde gene encodes a Mix family homeodomain protein that regulates the generation of endodermal precursors. *Genes Dev* **14**, 1279-89.
Kikuchi, Y., Verkade, H., Reiter, J. F., Kim, C. H., Chitnis, A. B., Kuroiwa, A. and Stainier, D. Y. (2004). Notch signaling can regulate endoderm formation in zebrafish. *Dev Dyn* **229**, 756-62.
Kimmel, C. B., Ballard, W. W., Kimmel, S. R., Ullmann, B. and Schilling, T. F. (1995). Stages of embryonic development of the zebrafish. *Dev Dyn* **203**, 253-310.
Kimura, S., Hara, Y., Pineau, T., Fernandez-Salguero, P., Fox, C. H., Ward, J. M. and Gonzalez, F. J. (1996). The T/ebp null mouse: thyroid-specific enhancer-binding protein is essential for the organogenesis of the thyroid, lung, ventral forebrain, and pituitary. *Genes Dev* **10**, 60-9.
Kimura, S., Ward, J. M. and Minoo, P. (1999). Thyroid-specific enhancer-binding protein/thyroid transcription factor 1 is not required for the initial specification of the thyroid and lung primordia. *Biochimie* **81**, 321-7.
Krantz, I. D., Smith, R., Colliton, R. P., Tinkel, H., Zackai, E. H., Piccoli, D. A., Goldmuntz, E. and Spinner, N. B. (1999). Jagged1 mutations in patients ascertained with isolated congenital heart defects. *Am J Med Genet* **84**, 56-60.
Krude, H., Schutz, B., Biebermann, H., von Moers, A., Schnabel, D., Neitzel, H., Tonnies, H., Weise, D., Lafferty, A., Schwarz, S. et al. (2002). Choreoathetosis, hypothyroidism, and pulmonary alterations due to human NKX2-1 haploinsufficiency. *J Clin Invest* **109**, 475-80.
Kumar, M., Jordan, N., Melton, D. and Grapin-Botton, A. (2003). Signals from lateral plate mesoderm instruct endoderm toward a pancreatic fate. *Dev Biol* **259**, 109-22.

Lai, E. C. (2002). Keeping a good pathway down: transcriptional repression of Notch pathway target genes by CSL proteins. *EMBO Rep* **3**, 840-5.
Lai, E. C. (2004). Notch signaling: control of cell communication and cell fate. *Development* **131**, 965-73.
Lammert, E., Cleaver, O. and Melton, D. (2001). Induction of pancreatic differentiation by signals from blood vessels. *Science* **294**, 564-7.
Lan, L., Cui, D., Nowka, K. and Derwahl, M. (2007). Stem cells derived from goiters in adults form spheres in response to intense growth stimulation and require thyrotropin for differentiation into thyrocytes. *J Clin Endocrinol Metab* **92**, 3681-8.
Lania, G., Zhang, Z., Huynh, T., Caprio, C., Moon, A. M., Vitelli, F. and Baldini, A. (2009). Early thyroid development requires a Tbx1-Fgf8 pathway. *Dev Biol* **328**, 109-17.
Lanigan, T. M., DeRaad, S. K. and Russo, A. F. (1998). Requirement of the MASH-1 transcription factor for neuroendocrine differentiation of thyroid C cells. *J Neurobiol* **34**, 126-34.
Latimer, A. J. and Appel, B. (2006). Notch signaling regulates midline cell specification and proliferation in zebrafish. *Dev Biol* **298**, 392-402.
Lawson, N. D., Scheer, N., Pham, V. N., Kim, C. H., Chitnis, A. B., Campos-Ortega, J. A. and Weinstein, B. M. (2001). Notch signaling is required for arterial-venous differentiation during embryonic vascular development. *Development* **128**, 3675-83.
Lazzaro, D., Price, M., de Felice, M. and Di Lauro, R. (1991). The transcription factor TTF-1 is expressed at the onset of thyroid and lung morphogenesis and in restricted regions of the foetal brain. *Development* **113**, 1093-104.
Le Borgne, R., Bardin, A. and Schweisguth, F. (2005). The roles of receptor and ligand endocytosis in regulating Notch signaling. *Development* **132**, 1751-62.
Le Borgne, R. and Schweisguth, F. (2003). Notch signaling: endocytosis makes delta signal better. *Curr Biol* **13**, R273-5.
Leger, J., Marinovic, D., Garel, C., Bonaiti-Pellie, C., Polak, M. and Czernichow, P. (2002). Thyroid developmental anomalies in first degree relatives of children with congenital hypothyroidism. *J Clin Endocrinol Metab* **87**, 575-80.
Li, L., Krantz, I. D., Deng, Y., Genin, A., Banta, A. B., Collins, C. C., Qi, M., Trask, B. J., Kuo, W. L., Cochran, J. et al. (1997). Alagille syndrome is caused by mutations in human Jagged1, which encodes a ligand for Notch1. *Nat Genet* **16**, 243-51.
Li, L., Milner, L. A., Deng, Y., Iwata, M., Banta, A., Graf, L., Marcovina, S., Friedman, C., Trask, B. J., Hood, L. et al. (1998). The human homolog of rat Jagged1 expressed by marrow stroma inhibits differentiation of 32D cells through interaction with Notch1. *Immunity* **8**, 43-55.
Liao, W., Ho, C. Y., Yan, Y. L., Postlethwait, J. and Stainier, D. Y. (2000). Hhex and scl function in parallel to regulate early endothelial and blood differentiation in zebrafish. *Development* **127**, 4303-13.
Lindsay, E. A., Vitelli, F., Su, H., Morishima, M., Huynh, T., Pramparo, T., Jurecic, V., Ogunrinu, G., Sutherland, H. F., Scambler, P. J. et al. (2001). Tbx1 haploinsufficieny in the DiGeorge syndrome region causes aortic arch defects in mice. *Nature* **410**, 97-101.
Lints, T. J., Parsons, L. M., Hartley, L., Lyons, I. and Harvey, R. P. (1993). Nkx-2.5: a novel murine homeobox gene expressed in early heart progenitor cells and their myogenic descendants. *Development* **119**, 419-31.
Lorent, K., Yeo, S. Y., Oda, T., Chandrasekharappa, S., Chitnis, A., Matthews, R. P. and Pack, M. (2004). Inhibition of Jagged-mediated Notch signaling disrupts zebrafish biliary development and generates multi-organ defects compatible with an Alagille syndrome phenocopy. *Development* **131**, 5753-66.
Macchia, P. E. (2000). Recent advances in understanding the molecular basis of primary congenital hypothyroidism. *Mol Med Today* **6**, 36-42.

Macchia, P. E., Lapi, P., Krude, H., Pirro, M. T., Missero, C., Chiovato, L., Souabni, A., Baserga, M., Tassi, V., Pinchera, A. et al. (1998). PAX8 mutations associated with congenital hypothyroidism caused by thyroid dysgenesis. *Nat Genet* **19**, 83-6.

Manfroid, I., Delporte, F., Baudhuin, A., Motte, P., Neumann, C. J., Voz, M. L., Martial, J. A. and Peers, B. (2007). Reciprocal endoderm-mesoderm interactions mediated by fgf24 and fgf10 govern pancreas development. *Development* **134**, 4011-21.

Mansouri, A., Chowdhury, K. and Gruss, P. (1998). Follicular cells of the thyroid gland require Pax8 gene function. *Nat Genet* **19**, 87-90.

Martinez Barbera, J. P., Clements, M., Thomas, P., Rodriguez, T., Meloy, D., Kioussis, D. and Beddington, R. S. (2000). The homeobox gene Hex is required in definitive endodermal tissues for normal forebrain, liver and thyroid formation. *Development* **127**, 2433-45.

Matsumoto, K., Yoshitomi, H., Rossant, J. and Zaret, K. S. (2001). Liver organogenesis promoted by endothelial cells prior to vascular function. *Science* **294**, 559-63.

McCright, B., Lozier, J. and Gridley, T. (2002). A mouse model of Alagille syndrome: Notch2 as a genetic modifier of Jag1 haploinsufficiency. *Development* **129**, 1075-82.

McDaniell, R., Warthen, D. M., Sanchez-Lara, P. A., Pai, A., Krantz, I. D., Piccoli, D. A. and Spinner, N. B. (2006). NOTCH2 mutations cause Alagille syndrome, a heterogeneous disorder of the notch signaling pathway. *Am J Hum Genet* **79**, 169-73.

McElhinney, D. B., Krantz, I. D., Bason, L., Piccoli, D. A., Emerick, K. M., Spinner, N. B. and Goldmuntz, E. (2002). Analysis of cardiovascular phenotype and genotype-phenotype correlation in individuals with a JAG1 mutation and/or Alagille syndrome. *Circulation* **106**, 2567-74.

Meno, C., Takeuchi, J., Sakuma, R., Koshiba-Takeuchi, K., Ohishi, S., Saijoh, Y., Miyazaki, J., ten Dijke, P., Ogura, T. and Hamada, H. (2001). Diffusion of nodal signaling activity in the absence of the feedback inhibitor Lefty2. *Dev Cell* **1**, 127-38.

Merscher, S., Funke, B., Epstein, J. A., Heyer, J., Puech, A., Lu, M. M., Xavier, R. J., Demay, M. B., Russell, R. G., Factor, S. et al. (2001). TBX1 is responsible for cardiovascular defects in velo-cardio-facial/DiGeorge syndrome. *Cell* **104**, 619-29.

Montanelli, L. and Tonacchera, M. (2010). Genetics and phenomics of hypothyroidism and thyroid dys- and agenesis due to PAX8 and TTF1 mutations. *Mol Cell Endocrinol* **322**, 64-71.

Muller, F., Blader, P., Rastegar, S., Fischer, N., Knochel, W. and Strahle, U. (1999). Characterization of zebrafish smad1, smad2 and smad5: the amino-terminus of smad1 and smad5 is required for specific function in the embryo. *Mech Dev* **88**, 73-88.

Murtaugh, L. C., Stanger, B. Z., Kwan, K. M. and Melton, D. A. (2003). Notch signaling controls multiple steps of pancreatic differentiation. *Proc Natl Acad Sci U S A* **100**, 14920-5.

Muzza, M., Persani, L., de Filippis, T., Gastaldi, R., Vigone, M. C., Sala, D., Weber, G., Lorini, R., Beck-Peccoz, P. and Fugazzola, L. (2008). Absence of sonic hedgehog (Shh) germline mutations in patients with thyroid dysgenesis. *Clin Endocrinol (Oxf)* **69**, 828-9.

Nakada, C., Iida, A., Tabata, Y. and Watanabe, S. (2009). Forkhead transcription factor foxe1 regulates chondrogenesis in zebrafish. *J Exp Zool B Mol Dev Evol* **312**, 827-40.

Nasevicius, A. and Ekker, S. C. (2000). Effective targeted gene 'knockdown' in zebrafish. *Nat Genet* **26**, 216-20.

Nowotschin, S., Liao, J., Gage, P. J., Epstein, J. A., Campione, M. and Morrow, B. E. (2006). Tbx1 affects asymmetric cardiac morphogenesis by regulating Pitx2 in the secondary heart field. *Development* **133**, 1565-73.

Nusslein-Volhard, C. and Dahm, R. (2002). Zebrafish : a practical approach. Oxford: Oxford University Press.

Oda, T., Elkahloun, A. G., Pike, B. L., Okajima, K., Krantz, I. D., Genin, A., Piccoli, D. A., Meltzer, P. S., Spinner, N. B., Collins, F. S. et al. (1997). Mutations in the human Jagged1 gene are responsible for Alagille syndrome. *Nat Genet* **16**, 235-42.

Ohuchi, H., Hori, Y., Yamasaki, M., Harada, H., Sekine, K., Kato, S. and Itoh, N. (2000). FGF10 acts as a major ligand for FGF receptor 2 IIIb in mouse multi-organ development. *Biochem Biophys Res Commun* **277**, 643-9.

Olivieri, A., Stazi, M. A., Mastroiacovo, P., Fazzini, C., Medda, E., Spagnolo, A., De Angelis, S., Grandolfo, M. E., Taruscio, D., Cordeddu, V. et al. (2002). A population-based study on the frequency of additional congenital malformations in infants with congenital hypothyroidism: data from the Italian Registry for Congenital Hypothyroidism (1991-1998). *J Clin Endocrinol Metab* **87**, 557-62.

Parlato, R., Rosica, A., Rodriguez-Mallon, A., Affuso, A., Postiglione, M. P., Arra, C., Mansouri, A., Kimura, S., Di Lauro, R. and De Felice, M. (2004). An integrated regulatory network controlling survival and migration in thyroid organogenesis. *Dev Biol* **276**, 464-75.

Perry, R., Heinrichs, C., Bourdoux, P., Khoury, K., Szots, F., Dussault, J. H., Vassart, G. and Van Vliet, G. (2002). Discordance of monozygotic twins for thyroid dysgenesis: implications for screening and for molecular pathophysiology. *J Clin Endocrinol Metab* **87**, 4072-7.

Piccoli, D. A. and Spinner, N. B. (2001). Alagille syndrome and the Jagged1 gene. *Semin Liver Dis* **21**, 525-34.

Plachov, D., Chowdhury, K., Walther, C., Simon, D., Guenet, J. L. and Gruss, P. (1990). Pax8, a murine paired box gene expressed in the developing excretory system and thyroid gland. *Development* **110**, 643-51.

Pohlenz, J., Dumitrescu, A., Zundel, D., Martine, U., Schonberger, W., Koo, E., Weiss, R. E., Cohen, R. N., Kimura, S. and Refetoff, S. (2002). Partial deficiency of thyroid transcription factor 1 produces predominantly neurological defects in humans and mice. *J Clin Invest* **109**, 469-73.

Porazzi, P., Calebiro, D., Benato, F., Tiso, N. and Persani, L. (2009). Thyroid gland development and function in the zebrafish model. *Mol Cell Endocrinol* **312**, 14-23.

Postiglione, M. P., Parlato, R., Rodriguez-Mallon, A., Rosica, A., Mithbaokar, P., Maresca, M., Marians, R. C., Davies, T. F., Zannini, M. S., De Felice, M. et al. (2002). Role of the thyroid-stimulating hormone receptor signaling in development and differentiation of the thyroid gland. *Proc Natl Acad Sci U S A* **99**, 15462-7.

Poulain, M. and Lepage, T. (2002). Mezzo, a paired-like homeobox protein is an immediate target of Nodal signalling and regulates endoderm specification in zebrafish. *Development* **129**, 4901-14.

Reifers, F., Walsh, E. C., Leger, S., Stainier, D. Y. and Brand, M. (2000). Induction and differentiation of the zebrafish heart requires fibroblast growth factor 8 (fgf8/acerebellar). *Development* **127**, 225-35.

Reis-Filho, J. S., Preto, A., Soares, P., Ricardo, S., Cameselle-Teijeiro, J. and Sobrinho-Simoes, M. (2003). p63 expression in solid cell nests of the thyroid: further evidence for a stem cell origin. *Mod Pathol* **16**, 43-8.

Reiter, J. F., Kikuchi, Y. and Stainier, D. Y. (2001). Multiple roles for Gata5 in zebrafish endoderm formation. *Development* **128**, 125-35.

Roberts, H. E., Moore, C. A., Fernhoff, P. M., Brown, A. L. and Khoury, M. J. (1997). Population study of congenital hypothyroidism and associated birth defects, Atlanta, 1979-1992. *Am J Med Genet* **71**, 29-32.

Robson, E. J., He, S. J. and Eccles, M. R. (2006). A PANorama of PAX genes in cancer and development. *Nat Rev Cancer* **6**, 52-62.

Rodaway, A., Takeda, H., Koshida, S., Broadbent, J., Price, B., Smith, J. C., Patient, R. and Holder, N. (1999). Induction of the mesendoderm in the zebrafish germ ring by yolk cell-derived TGF-beta family signals and discrimination of mesoderm and endoderm by FGF. *Development* **126**, 3067-78.
Rohr, K. B. and Concha, M. L. (2000). Expression of nk2.1a during early development of the thyroid gland in zebrafish. *Mech Dev* **95**, 267-70.
Scheer, N. and Campos-Ortega, J. A. (1999). Use of the Gal4-UAS technique for targeted gene expression in the zebrafish. *Mech Dev* **80**, 153-8.
Schier, A. F. (2001). Axis formation and patterning in zebrafish. *Curr Opin Genet Dev* **11**, 393-404.
Schier, A. F. (2009). Nodal morphogens. *Cold Spring Harb Perspect Biol* **1**, a003459.
Serls, A. E., Doherty, S., Parvatiyar, P., Wells, J. M. and Deutsch, G. H. (2005). Different thresholds of fibroblast growth factors pattern the ventral foregut into liver and lung. *Development* **132**, 35-47.
Sherwood, D. R. and McClay, D. R. (1999). LvNotch signaling mediates secondary mesenchyme specification in the sea urchin embryo. *Development* **126**, 1703-13.
Sherwood, D. R. and McClay, D. R. (2001). LvNotch signaling plays a dual role in regulating the position of the ectoderm-endoderm boundary in the sea urchin embryo. *Development* **128**, 2221-32.
Shi, S., Stahl, M., Lu, L. and Stanley, P. (2005). Canonical Notch signaling is dispensable for early cell fate specifications in mammals. *Mol Cell Biol* **25**, 9503-8.
Shi, S. and Stanley, P. (2006). Evolutionary origins of Notch signaling in early development. *Cell Cycle* **5**, 274-8.
Sirotkin, H. I., Gates, M. A., Kelly, P. D., Schier, A. F. and Talbot, W. S. (2000). Fast1 is required for the development of dorsal axial structures in zebrafish. *Curr Biol* **10**, 1051-4.
Thiery, J. P., Acloque, H., Huang, R. Y. and Nieto, M. A. (2009). Epithelial-mesenchymal transitions in development and disease. *Cell* **139**, 871-90.
Thisse, B., Wright, C. V. and Thisse, C. (2000). Activin- and Nodal-related factors control antero-posterior patterning of the zebrafish embryo. *Nature* **403**, 425-8.
Thomas, P. Q., Brown, A. and Beddington, R. S. (1998). Hex: a homeobox gene revealing peri-implantation asymmetry in the mouse embryo and an early transient marker of endothelial cell precursors. *Development* **125**, 85-94.
Thomas, T., Nowka, K., Lan, L. and Derwahl, M. (2006). Expression of endoderm stem cell markers: evidence for the presence of adult stem cells in human thyroid glands. *Thyroid* **16**, 537-44.
Tonacchera, M., Banco, M. E., Montanelli, L., Di Cosmo, C., Agretti, P., De Marco, G., Ferrarini, E., Ordookhani, A., Perri, A., Chiovato, L. et al. (2007). Genetic analysis of the PAX8 gene in children with congenital hypothyroidism and dysgenetic or eutopic thyroid glands: identification of a novel sequence variant. *Clin Endocrinol (Oxf)* **67**, 34-40.
Tremblay, K. D. and Zaret, K. S. (2005). Distinct populations of endoderm cells converge to generate the embryonic liver bud and ventral foregut tissues. *Dev Biol* **280**, 87-99.
Varga, I., Pospisilova, V., Gmitterova, K., Galfiova, P., Polak, S. and Galbavy, S. (2008). The phylogenesis and ontogenesis of the human pharyngeal region focused on the thymus, parathyroid, and thyroid glands. *Neuro Endocrinol Lett* **29**, 837-45.
Vassart, G. and Dumont, J. E. (2005). Thyroid dysgenesis: multigenic or epigenetic ... or both? *Endocrinology* **146**, 5035-7.
Vilain, C., Rydlewski, C., Duprez, L., Heinrichs, C., Abramowicz, M., Malvaux, P., Renneboog, B., Parma, J., Costagliola, S. and Vassart, G. (2001). Autosomal dominant transmission of congenital thyroid hypoplasia due to loss-of-function mutation of PAX8. *J Clin Endocrinol Metab* **86**, 234-8.

Vogelstein, B. and Gillespie, D. (1979). Preparative and analytical purification of DNA from agarose. *Proc Natl Acad Sci U S A* **76**, 615-9.
Warga, R. M. and Nusslein-Volhard, C. (1999). Origin and development of the zebrafish endoderm. *Development* **126**, 827-38.
Weinmaster, G. (2000). Notch signal transduction: a real rip and more. *Curr Opin Genet Dev* **10**, 363-9.
Wells, J. M. and Melton, D. A. (2000). Early mouse endoderm is patterned by soluble factors from adjacent germ layers. *Development* **127**, 1563-72.
Wendl, T., Adzic, D., Schoenebeck, J. J., Scholpp, S., Brand, M., Yelon, D. and Rohr, K. B. (2007). Early developmental specification of the thyroid gland depends on han-expressing surrounding tissue and on FGF signals. *Development* **134**, 2871-9.
Wendl, T., Lun, K., Mione, M., Favor, J., Brand, M., Wilson, S. W. and Rohr, K. B. (2002). Pax2.1 is required for the development of thyroid follicles in zebrafish. *Development* **129**, 3751-60.
Westerfield, M. (1995). The zebrafish book : a guide for the laboratory use of zebrafish (danio rerio). Eugene, Or.: [M. Westerfield?].
Westerlund, J., Andersson, L., Carlsson, T., Zoppoli, P., Fagman, H. and Nilsson, M. (2008). Expression of Islet1 in thyroid development related to budding, migration, and fusion of primordia. *Dev Dyn* **237**, 3820-9.
Whitman, M. (2001). Nodal signaling in early vertebrate embryos: themes and variations. *Dev Cell* **1**, 605-17.
Xue, Y., Gao, X., Lindsell, C. E., Norton, C. R., Chang, B., Hicks, C., Gendron-Maguire, M., Rand, E. B., Weinmaster, G. and Gridley, T. (1999). Embryonic lethality and vascular defects in mice lacking the Notch ligand Jagged1. *Hum Mol Genet* **8**, 723-30.
Yamamoto, M., Morita, R., Mizoguchi, T., Matsuo, H., Isoda, M., Ishitani, T., Chitnis, A. B., Matsumoto, K., Crump, J. G., Hozumi, K. et al. (2010). Mib-Jag1-Notch signalling regulates patterning and structural roles of the notochord by controlling cell-fate decisions. *Development* **137**, 2527-37.
Yelon, D., Ticho, B., Halpern, M. E., Ruvinsky, I., Ho, R. K., Silver, L. M. and Stainier, D. Y. (2000). The bHLH transcription factor hand2 plays parallel roles in zebrafish heart and pectoral fin development. *Development* **127**, 2573-82.
Zannini, M., Acebron, A., De Felice, M., Arnone, M. I., Martin-Perez, J., Santisteban, P. and Di Lauro, R. (1996). Mapping and functional role of phosphorylation sites in the thyroid transcription factor-1 (TTF-1). *J Biol Chem* **271**, 2249-54.
Zannini, M., Avantaggiato, V., Biffali, E., Arnone, M. I., Sato, K., Pischetola, M., Taylor, B. A., Phillips, S. J., Simeone, A. and Di Lauro, R. (1997). TTF-2, a new forkhead protein, shows a temporal expression in the developing thyroid which is consistent with a role in controlling the onset of differentiation. *EMBO J* **16**, 3185-97.
Zecchin, E., Conigliaro, A., Tiso, N., Argenton, F. and Bortolussi, M. (2005). Expression analysis of jagged genes in zebrafish embryos. *Dev Dyn* **233**, 638-45.
Zecchin, E., Filippi, A., Biemar, F., Tiso, N., Pauls, S., Ellertsdottir, E., Gnugge, L., Bortolussi, M., Driever, W. and Argenton, F. (2007). Distinct delta and jagged genes control sequential segregation of pancreatic cell types from precursor pools in zebrafish. *Dev Biol* **301**, 192-204.
Zhou, X., Sasaki, H., Lowe, L., Hogan, B. L. and Kuehn, M. R. (1993). Nodal is a novel TGF-beta-like gene expressed in the mouse node during gastrulation. *Nature* **361**, 543-7.
Zhu, X., Zhang, J., Tollkuhn, J., Ohsawa, R., Bresnick, E. H., Guillemot, F., Kageyama, R. and Rosenfeld, M. G. (2006). Sustained Notch signaling in progenitors is required for sequential emergence of distinct cell lineages during organogenesis. *Genes Dev* **20**, 2739-53.

Zorn, A. M. and Wells, J. M. (2009). Vertebrate endoderm development and organ formation. *Annu Rev Cell Dev Biol* **25**, 221-51.
Zuniga, E., Stellabotte, F. and Crump, J. G. (2010). Jagged-Notch signaling ensures dorsal skeletal identity in the vertebrate face. *Development* **137**, 1843-52.

ACKNOWLEDGMENTS

It is a great pleasure to thank my supervisor, Luca Persani, who gave me the opportunity of working on an exciting research project, that after three (largely enjoyable) years, finally culminated in this thesis.

This thesis own a lot to Natascia Tiso and Francesco Argenton, who provided the indispensable ingredients of this project: zebrafish! I truly appreciated the amount of time and energy that they invested in guiding me throughout this work and their constant support.

Throughout the last three years I had many opportunities of scientific interactions, which often resulted in ideas, suggestions and marvelous friendships. Alice, thank you! You shared with me the alternating fortunes of the PhD student life and of my new "Paduan life"! I am especially grateful to Enrico M., for his continuous support and encouragements, for his enthusiasm in sharing his vast knowledge. Thank you Benni, you were my first fish-teacher!

I would like to thank my parents, for giving me the opportunity to achieve my goal: keep researching and studying. Last but not least, I especially thank my sister, for her precious advices and for her continuous efforts for encouraging me…. thank you for believing that I could get through this.